Hemoglobin Catabolism in Human Macrophages and Inflammation

Dissertation

zur

Erlangung der naturwissenschaftlichen Doktorwürde

(Dr.sc.nat.)

vorgelegt der

Mathematisch-naturwissenschaftlichen Fakultät

der

Universität Zürich

von

Theresa Kämpfer

aus Deutschland

Promotionskomitee

Prof. Dr. Adriano Fontana (Vorsitz)

Prof. Dr. Gabriele Schoedon

PD Dr. Dominik Schaer

Prof. Dr. Burkhard Becher

Zürich, 2010

I. Preface

This thesis was performed at the Inflammation Research Unit, Department of Internal Medicine, University Hospital of Zurich, Zurich, Switzerland. It is an account of the results of projects supported by Fonds zur Föderung des Akademischen Nachwuchses (FAN) of the University of Zurich, and partially project No. 31-120658 of the Swiss National Science Foundation.

The aim of this work was to study the hemoglobin induced catabolism in human macrophages and the resulting global and characteristic impact on the transcriptome and proteome in order to define a novel phenotype of hemoglobin clearing macrophages in wounded tissues and inflammation.

The data is presented in form of manuscripts submitted or prepared for publication (chapters 2, 3, and 4). In chapter 1, an introduction in the biology of macrophages with emphasis on their role in hemoglobin clearance and catabolism, and an outline of the thesis are given.

An overall picture of the findings presented in this work and the conclusions drawn are given in chapter 5.

Parts of the work have been conducted in cooperation with the Functional Genomics Center Zurich, University of Zurich and ETH Zurich.

Table of contents

II. Abbreviations

ACN	Acetonitrile
ARE	Antioxidant response element
CID	Collision-induced dissociation
CIITA	Class II transactivator
DMEM	Dulbecco’s modified eagle medium
FCS	Fetal calf serum
FDR	False discovery rate
FTH	Ferritin heavy chain
FTL	Ferritin light chain
GSH	Reduced glutathione
Hb	Hemoglobin
HCD	Higher-energy collisional dissociation
HLA	Human leukocyte antigen
HO-1	Heme oxygenase 1
Hp	Haptoglobin
iTRAQ	Isobaric tag for relative and absolute quantitation
LPS	Lipopolysaccharide
LTQ	Linear trap quadrupole
MALDI	Matrix assisted laser desorption ionisation
MS	Mass spectrometry
Nano-LC	Nano liquid chromatography
NF-κB	Nuclear factor 'kappa-light-chain-enhancer' of activated B-cells
Nrf-2	Nuclear Factor E2-related factor 2
PAI-2	Plasminogen activator inhibitor type 2
ROS	Reactive oxygen species
SOD	Superoxide dismutase
SPR	Surface plasmon resonance
SRCR	Scavenger receptor cysteine rich
TCA	Trichloroacetic acid
TFA	Trifluoroacetic acid
TOF	Time-of-flight

III. Zusammenfassung

Das sauerstofftransportierende Protein Hämoglobin (Hb) ist anfällig für oxidative Schädigungen aufgrund seiner reaktiven Hämgruppe. Allein die Abschirmung durch die Erythrozytenmembran ermöglicht, dass Hämoglobin den Körper ausreichend mit Sauerstoff versorgen kann.

Zellfreies Hb tritt in verschiedenen Mengen während der Zerstörung von Erythrozyten, Gewebeverletzungen, Sichelzellanämie und Malaria auf. Das Freiwerden von sehr grossen Hämoglobinmengen in der Zirkulation hat verschiedenste klinische Konsequenzen, wobei man zwischen Kurz -und Langzeitkonsequenzen unterscheidet. Kurzzeitkonsequenzen sind unter anderem die oxidative Denaturierung von Hämoglobin, das verminderte Vorhandensein von vasoaktivem NO, Proteinschädigungen und Nierenversagen. Auf längere Sicht können Entzündungen, Bluthochdruck oder intraplaque Blutungen in fortgeschrittenen atherosklerotischen Läsionen auftreten. Haptoglobin (Hp) ist der primäre Hämoglobinfänger, der sofort und effektiv die verschiedenen toxischen Effekte von Hämoglobin durch die Bildung von stabilen Hb-Hp Komplexen minimiert und die Beseitigung der Komplexe durch den Makrophagen Rezeptor CD163 einleitet.

Aufgrund der wichtigen Funktion von CD163, gibt die vorliegende Doktorarbeit Aufschluss über die Rolle von verschiedenen CD163 Domänen bei der Bindung und Aufnahme von Hb-Hp Komplexen. Es konnte gezeigt werden, dass zusätzlich zu den bislang bekannten kritischen Domänen 3-6 auch Domäne 8 entscheidend für die Endozytose von Hb-Hp ist. Dies wird wahrscheinlich durch eine bisher unbekannte Rolle von Domäne 8 bei der Bildung oder Aufrechterhaltung der notwenigen 3D-Struktur des Rezeptors für die Ligandenaufnahme bewirkt.

Des Weiteren war es das Ziel dieser Doktorarbeit, die globale Langzeitantwort von Makrophagen auf die intensive Exposition mit Hb-Hp Komplexen, besonders im Hinblick auf die exklusive Rolle der Makrophagen bei der Hb- Beseitigung während der Hämolyse, zu untersuchen. Mit Hilfe von Genexpressionsanalysen und proteomischer Methoden gelang es, grosse Teile des umfangreichen Proteomes zu identifizieren und somit neue signifikante Eigenschaften von Wundheilungsmakrophagen zu definieren.

In dieser Dissertation konnte gezeigt werden, dass die Hb-Hp Exposition, welche das Freiwerden von Hb nach Gewebsverletzungen simuliert, eine supprimierte Expression von HLA Klasse 2 Molekülen auf Makrophagen hervorruft. Vermutlich verhindert dies die Präsentation von Autoantigenen gegenüber dem Immunsystem. Des Weiteren zeigten diese Makrophagen eine adaptive Antwort auf erhöhtes Hb durch verstärkte Expression von CD163 und Plasminogen Aktivator Inhibitor-2 (PAI-2) mit einhergehenden zellschützenden und antioxidativen Mechanismen, die unter anderem durch induzierte Hämoxygenase (HO-1) und erhöhtes reduziertes Glutathion mit dem Ziel des Wiederherstellens der zellulären Homeostase gekennzeichnet waren. Interessanterweise haben die Makrophagen unter diesen experimentellen Bedingungen in hohem Masse chemoattraktiv wirkendes IL-8 abgegeben, was vermutlich besonders Neutrophile zu den verletzten Geweben leiten soll. Die IL-8 Sekretion ist eine spezifische Antwort, welche explizit nicht im Rahmen einer gezielten Entzündungsreaktion steht. Im Einklang damit konnte das Fehlen von typischen NF-κB-abhängigen pro-inflammatorischen Mediatoren, wie TNF-α und IL-1β, im Kulturmedium dieser Makrophagen nachgewiesen werden.

Zusammenfassend definieren die vorliegenden Ergebnisse einen neuen nicht-inflammatorischen Makrophagenphänotypen mit einer hoher Hämoglobinaufnahme- und Beseitigungskapazität sowie anti-oxidativem Nutzen bei Entzündung und Wundheilung.

IV. Summary

The oxygen carrier protein hemoglobin (Hb) is vulnerable to oxidative injury due to its reactive heme group. Only sequestration by the erythrocyte membrane enables the Hb to facilitate efficient oxygen delivery throughout the body.

Cell-free Hb occurs in diverse quantities during e.g. erythrocyte destruction, tissue damage, sickle cell anemia and malaria. There are multiple clinical consequences following the release of massive amounts of free Hb in the circulation, among those are short-time observations such as oxidative denaturation of Hb, nitric oxide (NO) depletion, protein damage and renal failure. Long-term effects range from inflammation and hypertension to intraplaque hemorrhage in advanced atherosclerotic lesions. The primary Hb scavenger haptoglobin (Hp) instantly and effectively minimizes the multiple toxic effects of Hb by generating stable Hb-Hp complexes and triggering their clearance from the circulation by the macrophage CD163 receptor pathway.

Given the important function of CD163 this thesis sheds light on the role of CD163 receptor domains in Hb-Hp binding and uptake. In addition to the commonly known domains 3-6 that are sufficient for ligand uptake domain 8 was found to be essential for Hb-Hp endocytosis by CD163 suggesting this domain plays a role in the yet unknown 3D structure of CD163 crucial for Hb-Hp endocytosis.

Further, this thesis aimed to investigate the long-term global response of macrophages extensively exposed to Hb-Hp with regard to the exclusive role of macrophages in Hb - clearance during e.g. tissue injury and hemolysis. By gene expression profiling and *state-of-the-art* proteomic approaches in order to discover the comprehensive macrophage proteome new significant characteristics of macrophages with a crucial role in wound healing could be identified.

It could be shown that Hb-Hp exposure in order to mimic the Hb release in wounded tissues, profoundly suppressed HLA class 2 expression putatively avoiding auto-antigen presentation to the immune system. Further, these macrophages displayed an adaptive response to wounding by increased expression of CD163 and plasminogen activator inhibitor 2 (PAI-2) with subsequent cell-protective and anti-oxidative mechanisms characterized by e.g. induced heme oxygenase 1 (HO-1) and increased glutathione in order to recover the cellular homeostasis. Moreover, increased ferritin levels were observed indicating enhanced iron recycling activity in

these macrophages. Interestingly, the macrophages in these experimental setup released high amounts of the chemoattractant IL-8 putatively recruiting neutrophils to the wounded tissue sites. The majority of the detected genes characteristic for this macrophage phenotype is regulated by Nrf-2, a conserved oxidative transcription factor, indicating anti-oxidative potency of the stimulated macrophages. IL-8 secretion is a specific response that is not in the context of a directed inflammatory response. This is in accordance with the absence of typical NF-κB-driven cytokines, such as TNF-α and IL-1β, as it was confirmed in the culture supernatants of these macrophages.

In summary, the results presented herein define a new non-inflammatory macrophage phenotype with a high Hb-clearing capacity and anti-oxidative benefits in inflammation and wound healing.

1. General Introduction

1.1. Hemoglobin and Hemolysis

Hemoglobin (Hb) is one of the most abundant proteins in mammals and facilitates oxygen delivery from the lungs to the tissues. A single Hb-molecule is a tetramer that contains four heme-groups, each composed of protoporphyrin IX with a central iron atom. The iron exists in several redox states within the heme: the ferrous (Fe^{2+}), ferric (Fe^{3+}) and the ferryl (Fe^{4+}) forms of iron. Only the ferrous state is able to reversibly bind oxygen, whereas the higher oxidation forms of iron, namely ferric and ferryl state are non-functional for oxygen transport as illustrated in **Figure 1**. Free Hb exerts toxic and inflammatory effects arising from oxidative processes involving the reactive heme group [1]. The reducing environment within the erythrocytes prevents the deleterious activity of Hb [2].

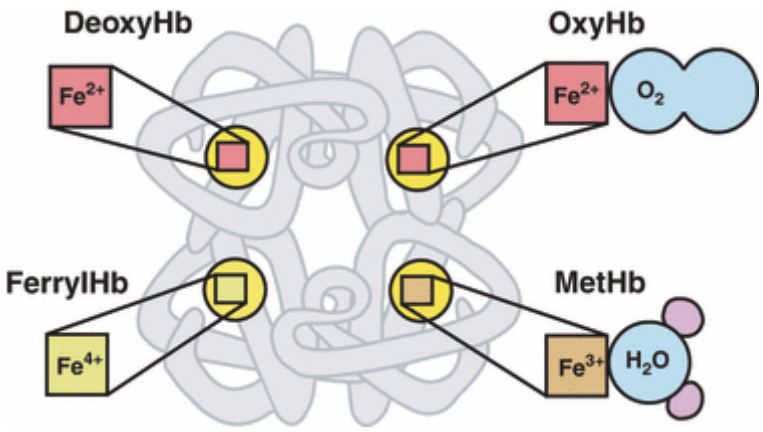

Figure 1 – Schematic illustration of the different oxidative states of heme iron. *Each Hb molecule consists of four globin chains with a central iron atom. Hb oxidation results in changes of the iron's oxidative state. The ferrous state (Fe^{2+}) allows oxygen binding to deoxygenated Hb (deoxy Hb) at physiological conditions. The resulting oxygenated Hb (oxy Hb) can undergo autoxidation to methemoglobin (metHb) with a heme iron in the ferric state (Fe^{3+}) and binds water instead of oxygen. Hydrogen peroxide can react with metHb to form ferrylheamoglobin (ferrylHb, Fe^{4+}) (adapted from [3]).*

When Hb tetramers are released from erythrocytes they dissociate spontaneously into Hb dimers that are easily oxidized into methemoglobin (Fe^{3+}) which readily liberates its heme moiety [4]. This leads, due to the hydrophobic nature of heme, to intercalation and passage of heme through cell membranes [3]. The cellular uptake of heme provokes oxidative damage of plasma proteins by intracellular generation of reactive oxygen species (ROS), such as superoxide anion (O_2^-) and hydrogen peroxide (H_2O_2). In erythrocytes, specific mechanisms protect against ROS damage.

Cytosolic enzymes such as catalase (CAT) and superoxide dismutase (SOD) detoxify ROS, whereas membrane antioxidants, namely vitamin A and E, protect against ROS-induced lipid peroxidation [5]. Several studies demonstrated that cell-free Hb intensifies the toxicity and lethality of LPS by enhancing the biological activity of LPS with subsequent augmented TNF-α production [6-7]. In 2004, D'Agnillo [8] could show that redox active Hb (Fe^{4+}) exacerbates LPS-induced apoptosis. In contrast, LPS binding to globin (Hb minus heme) attenuates LPS effects [9]. Free Hb has an established pathophysiological role in hemolytic anemias such as sickle cell disease and malaria [10]. Also, atherosclerosis with intraplaque hemorrhage and autoimmune hemolysis has very distinct links to cell-free Hb and heme reactivities [11-12]. In summary, all Hb-related disorders share typical characteristics, such as oxidative denaturation of Hb, membrane lipid and protein oxidation, hemolysis and the release of Hb into the circulation [13-14]. Taken together, the multiple toxic effects of Hb mandate an efficient physiologic Hb scavenge- and clearance system.

Figure 2 summarizes the hemoglobin toxicity, involved scavenger proteins, and detoxification pathways which are described in detail below.

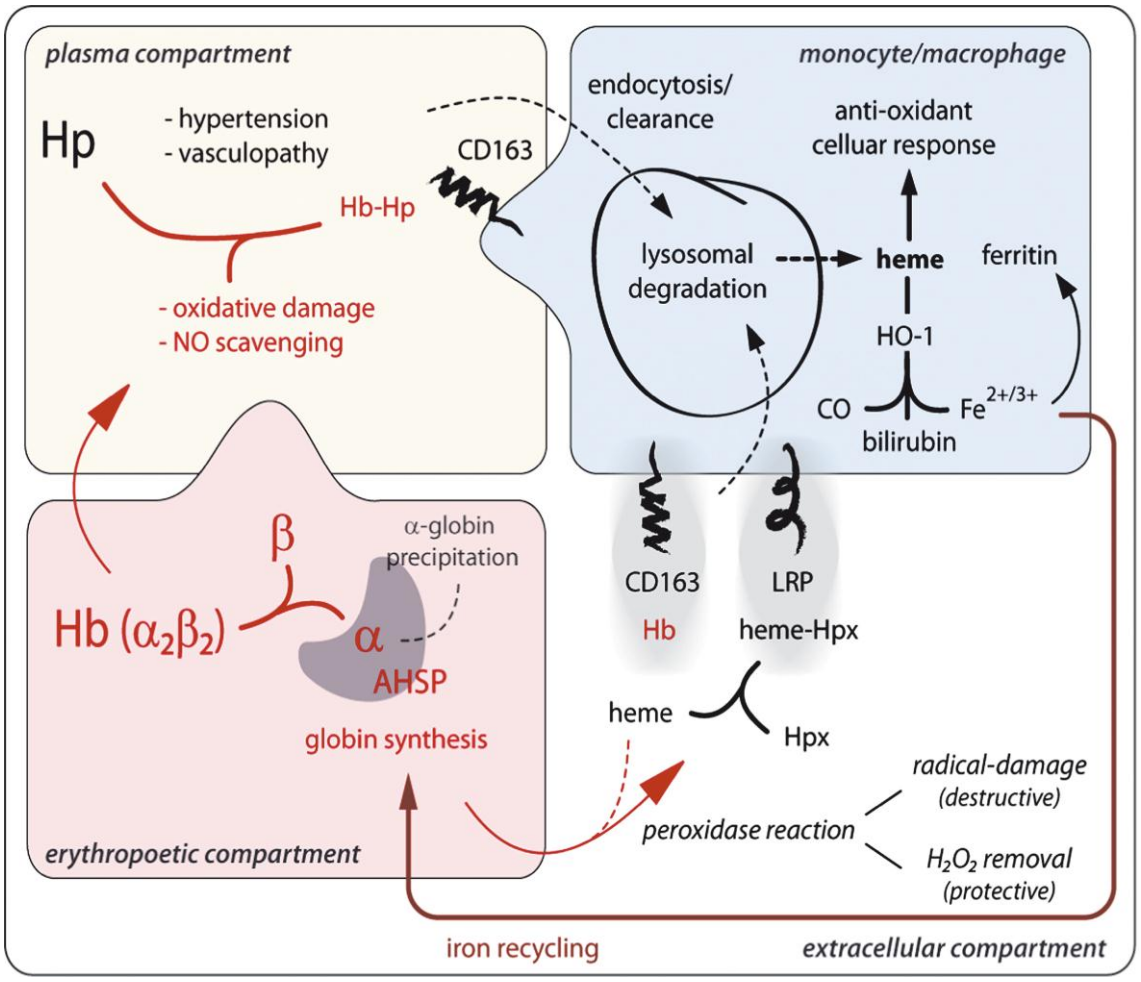

Figure 2 - Scheme of compartmentalized hemoglobin toxicity, scavenger proteins, and detoxification pathways. *Free Hb can be released from the erythropoietic compartment and accumulates in the plasma and extracellular compartments during hemolysis or after tissue injury. In the extracellular compartment, Hb can react with peroxides (H_2O_2 and lipidperoxides) and promotes oxidative tissue damage. In the plasma compartment, extracellular Hb is sequestered in the Hb-Hp complex. Complex formation prevents Hb-induced hypertensive and oxidative reactions. The Hb-Hp complex is subsequently endocytosed by the macrophage Hb scavenger receptor CD163. Within the macrophage, heme is released from globin and degraded by HO-1 into the antioxidant and anti-inflammatory products bilirubin and carbonmonoxide (CO). The released iron induces ferritin synthesis. Iron can either be exported for iron recycling to the bone marrow or it can be stored in a ferritin complex. Additionally, the hemopexin (Hpx)-heme complex receptor (LDL receptor related protein, LRP) pathway can detoxify free heme that is released from oxidized Hb (adapted from [15]).*

1.1.1. Erythropoietic compartment

The bottom left box (red) illustrates the erythropoetic compartment where the late stage of erythroid development takes place. It is mainly characterized by the production of the major oxygen carrier adult Hb A, a tetramer consisting of two pairs of α-globin and β-globin protein subunits. Each subunit is bound to a heme moiety and they remain unstable and cytotoxic till final assembly to the tetrameric ($\alpha_2\beta_2$)

hemoglobin [16]. In detail, monomeric α-chains generate ROS that damage cellular proteins, lipids, and nucleid acids. In addition, they are easily denaturated upon oxidation causing deleterious accumulation of precipitated α-globin polypeptides, free heme, porphyrins and iron in cytoplasm and cell membrane [17]. To prevent precipitation of premature Hb A subunits before assembly the chaperon α-hemoglobin-stabilization protein (AHSP) captures newly synthesized Hb α-globin chains forming the AHSP complex. Subsequently, AHSP slowly and safely releases α-globin chains into the higher-affinity αβ-globin interaction.

1.1.2. Plasma compartment

When free Hb occurs during intravascular hemolysis (upper left box), it is immediately captured by the acute phase protein haptoglobin (Hp) forming a non-covalent and stable complex with an extremely high affinity (1 x 10^{-15} mol L^{-1}) that can be considered irreversible [18-19]. The physiological importance of Hb-Hp formation lies mainly in the prevention of heme iron-driven oxidative damage and inflammation. Also, Hp-complexed Hb is not eliminated by glomerular filtration and prevents renal damage [20-21]. Furthermore, extracellular Hb can rapidly react with NO [22]. In sickle cell disease or malaria chronic hemolysis with high levels of cell free Hb is associated with diminished NO bioavailability leading to hypertension and other vascular outcomes. Once formed, Hb-Hp complexes are quickly removed from the circulation in the spleen (90%) and by circulating monocytes/macrophages (10%).

Hp is mainly produced by hepatic cells [23] and occurs in the plasma of all mammals. In bony fish, there is a Hp-like protein (32-34% identical to human Hp), whereas neither in chicken nor frog a gene coding for a protein similar to human Hp was found [24]. In humans, Hp is characterized by a genetic polymorphism with three structurally different major phenotypes (Hp 1-1, Hp 2-1 and Hp 2-2) which arise from the polymorphic Hp locus (*Hp1* and *Hp2*). Hp 1-1 is a smaller, more abundant dimer (86 kDa), whereas Hp 2-1 is characterized by heteropolymers (86–300 kDa), and Hp 2-2 forms large macromolecular complexes (170–1000 kDa) [21]. The hepatic "clearance" of free Hb in plasma appears to be less efficient for Hp 2-2 than for the other Hp phenotypes [20]. Also, the Hp2-2 phenotype has been associated with increased iron accumulation in hemochromatosis suggesting an influence of Hp phenotypes in iron homeostasis (reviewed in [21]).

The protective antioxidative effect of Hp was recently investigated by Boretti and co-workers [25] showing that Hp binding to Hb prevents the generation of oxidant species from cell free Hb mediating hypertension perhaps by capturing Hb as high-molecular weight complexes that cannot extravasate into the sub-endothelial sites. Nevertheless, Hp has also been reported to be involved in modulating immune responses, autoimmune diseases and inflammatory disorders [26-28]

1.1.3. Cellular compartment – The Hb/CD163/HO-1 pathway in macrophages

First, it was thought that the clearance of Hb-Hp complexes exclusively occurs in both liver and spleen. Kristiansen and co-workers [29] identified the scavenger receptor CD163 as the only high-affinity receptor for Hb-Hp during search of the endocytotic receptor for Hb-Hp within the liver. The upper right box (blue) illustrates how the formed Hb-Hp complex is immediately cleared by high affinity binding to CD163, exclusively expressed on monocytes and tissue macrophages, leading to endocytosis and degradation of the complex [30]. Moreover, in case of Hp-depletion as it appears during severe hemolysis, non Hp-complexed Hb is also scavenged through a low-affinity pathway by CD163. By means of competitive uptake experiments it could be shown that Hb binding to CD163 also inhibits Hb-Hp uptake suggesting that both Hb and Hb-Hp have a common binding site within the CD163 molecule [31-32]

Once the Hb-Hp complex or free Hb is endocytosed, Hb-derived heme is degraded and transported through an endosomal/lysosomal pathway towards the cytoplasm while the globin is undergoing proteolysis. There, heme oxygenase 1 (HO-1), the inducible isoform of HO, catalyzes the heme by oxidation to biliverdin, which is further converted to bilirubin, CO and free ferrous iron, which is immediately sequestered by ferritin [33]. All three byproducts (ferritin, bilirubin and CO) are known to have antioxidant properties and can protect the cell from oxidative damage and cell death [34-35].

Upon inflammatory stimulus, including bacterial endotoxins and activation of the Toll-like receptors TLR2, TLR4 or TLR5, the ectodomain is shed from the cell surface by a metalloproteinase-dependent mechanism [36-38] releasing soluble CD163 (sCD163). High levels of sCD163 are detected upon experimental endotoxin administration [37] and during macrophage activation syndrome [38]. Unlike LPS, free Hb has no effect on

CD163 cell surface expression on macrophages. This is in agreement with the common opinion that the receptor is not degraded after endocytosis but, instead recycles back to the cell surface after delivering the cargo to early endosomes **(Figure 3)**.

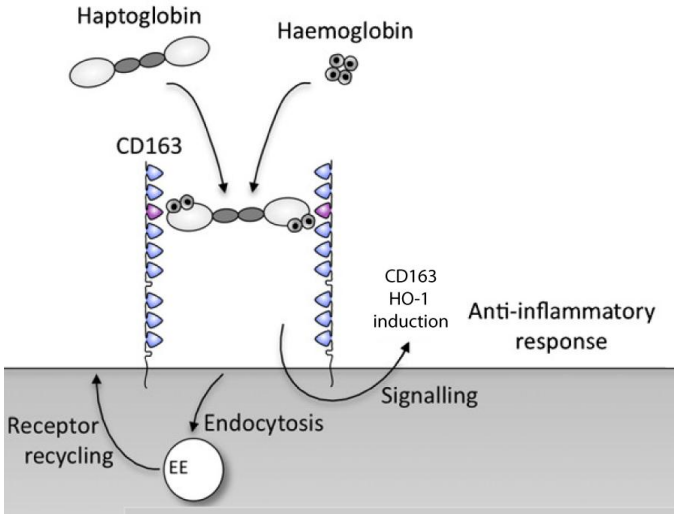

Figure 3 - CD163 functions as a scavenger receptor for Hb-Hp complexes or Hb alone. *Hb-Hp uptake induces CD163 and HO-1 expression and a subsequent anti-inflammatory response. After internalization CD163 recycles back to the surface (adapted from [39]).*

Furthermore, Fabriek and co-workers [40] could show that CD163 directly supports interactions with erythroblasts and identified a motif in the second SRCR domain responsible for mediating the binding of CD163 to erythroblasts. They also suggest that CD163 on liver and spleen macrophages could have dual function, namely the clearance of Hb and promoting erythropoiesis that could provide the recycled iron to developing erythroblasts.

About a year later, Fabriek and co-workers [41] could identify another function of CD163. Starting from the point that cross-linking of CD163 with monoclonal antibodies directed against CD163 triggered the production of inflammatory mediators, such as NO, TNF-α, IL-1β and IL-6, indicated a role of CD163 in immunity and host defense [42-43]. They could provide evidence that CD163 functions as a receptor for bacteria, including gram-negative and gram-positive species. Interestingly, motifs in the second and to a lesser extend in the third domain of CD163 were observed to be the bacteria binding site.

1.2. Monocytes/Macrophages

Leukocytes are a diverse group of cell types that have critical roles in the immune response of the body. They circulate through the blood and the lymphatic system and are recruited to sites of tissue damage and infection. Leukocytes have a common origin in hematopoietic stem cells and develop along distinct differentiation pathways in response to internal and external signals into different subsets bearing distinct functional and physical characteristics [44].

Monocytes in the steady state do not proliferate but circulate in the blood and reside in the bone marrow and in organs such as spleen and liver [45]. **Table 1** illustrates the two major subsets of human blood monocytes that vary in chemokine receptor (CCR) and adhesion molecule expression, as well as in migratory and differentiation properties [46]. Classical monocytes ($CD14^{++}$, $CD16^{-}$) are more likely to become macrophages, while non-classical monocytes ($CD14^{+}$, $CD16^{+}$) in turn could develop to dendritic cells (DCs) [47].

Table 1: *Characteristics of classical and non-classical monoycte subsets described in humans.*

Classical Monocytes	Non-classical Monocytes
$CD14^{++}$, $CD16^{-}$	$CD14^{+}$, $CD16^{+}$
$CCR2^{+}$, $CD64^{+}$, $CD62L^{+}$	$CCR2^{-}$, $CD64^{-}$, $CD62L^{-}$
$MHCII^{+}$	$MHCII^{++}$

Monocytes themselves are already effector cells and once activated they become macrophages and produce inflammatory cytokines, ingest cells and toxic molecules with a half-life in blood of about 3 days [48] They are also highly involved in antigen-presenting and T- and B-cell cooperation. Migration of monocytes to tissues and differentiation to DCs or macrophages is dependent on the microenvironment within the tissue sites [49].

Macrophages polarize towards distinct morphological and functional characteristics **(Figure 4)** depending on the cytokines and microbial products in the microenvironment.

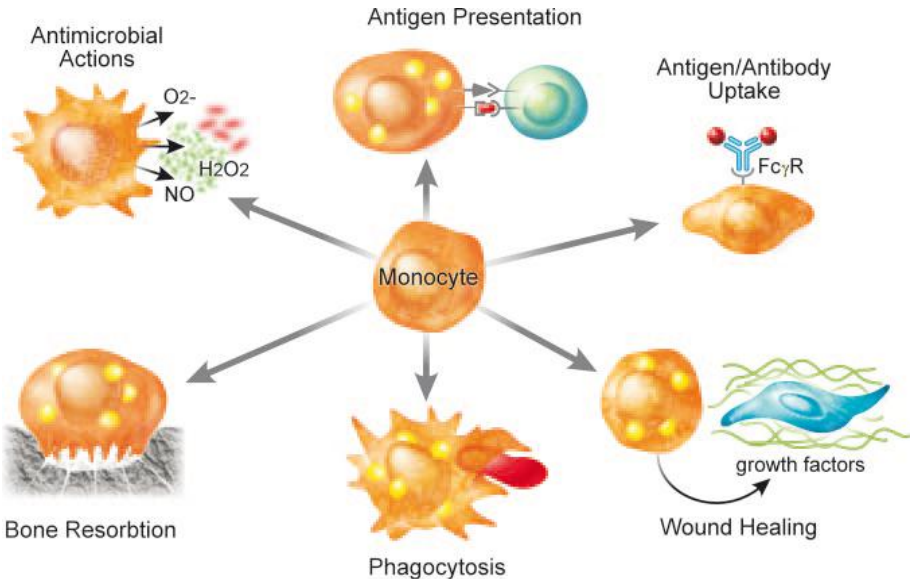

Figure 4 – Resident macrophages display a variety of functions. *Clockwise from upper left: Macrophages are key players of innate defense against pathogens by generating an inflammatory and respiratory burst; they initiate antigen- presentation to activate adaptive immune response; macrophages clear immune complexes by uptake; they promote wound healing by release of growth factors; red pulp macrophages in the spleen are highly specialized for clearance of aged red blood cells; another subset of macrophages located in the bone so-called osteoclasts and is critical for remodelling of bone (adapted from [50]).*

Mature macrophages can be classified into classically activated macrophages (M1) and alternatively activated macrophages (M2). Further, the more heterogeneous M2 macrophage population can be divided into sub-phenotypes: M2a, M2b and M2c [51]. While M2a macrophages are activated upon T helper 2 (T_H2) cytokines IL-4 and IL-13, the M2b sub-phenotype is induced by immune complexes or toll-like receptors and has a role in tissue repair during wound healing. M2c macrophages are induced in response to IL-10 or glucocorticoids resulting in decreased antigen presentation and increased immunosuppression [52] **(Figure 5)**.

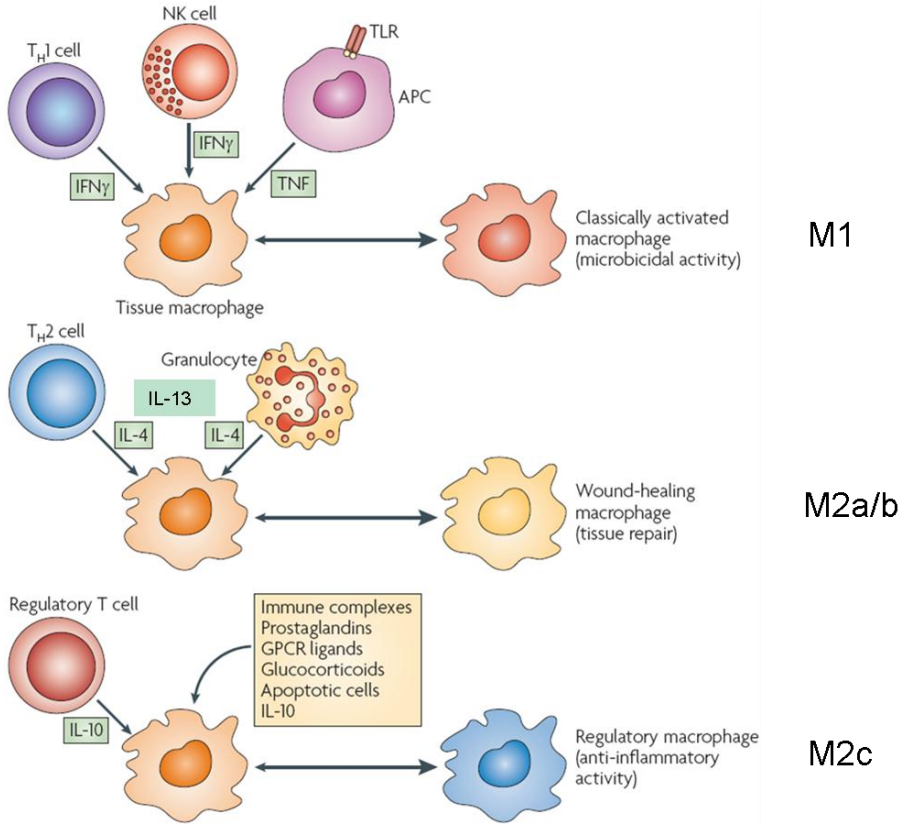

Figure 5 – Different macrophage subsets are induced dependent on a distinct cytokine environment. *APC, antigen presenting cell. TLR, Toll-like receptor (adapted from [53]).*

Classically activated macrophages arise in response to the cytokine IFN-γ produced by T helper 1 (T_H1) cells or natural killer (NK) cells. This activation can be mediated by IFN-γ alone or in combination with microbial products (e.g. LPS) or cytokines (e.g. TNF) which further leads to shedding of CD163 (sCD163). Additionally, those macrophages have a high capacity in antigen presentation [54]. In contrast, the synthesis of CD163 in macrophages is potently induced by anti-inflammatory signals such as IL-10 or glucocorticoids [55]. However, T helper 2 (T_H2) cell cytokines (IL-4/ IL-13) completely down-regulate CD163 expression and polarize macrophages into another alternatively activated phenotype. Of note, mature tissue macrophages, such as Kuppfer cells in the liver, red pulp macrophages in the spleen and cortical macrophages in the thymus, show a significantly higher expression of CD163 than peripheral blood monocytes indicating that CD163 expression may also increase along the macrophage differentiation [56-57]. CD163 positive macrophages are found during the healing phase of acute inflammation, in chronic inflammation and in wound healing tissue [58-59]. So far, it seems reasonable that macrophages high in CD163 expression refer more to an anti-inflammatory phenotyp. Moreover, the phenotype of

macrophages remains adaptable allowing the switch between sub-populations in response to present stimuli in the microenvironment [53].

1.2.1. A novel macrophage phenotype in wounding

Monocytes are among the first cells to arrive in injured tissue where they differentiate into macrophages and ingest apoptotic cells to avoid secondary necrosis and thus inflammation. In case of RBC extravasation and *in situ* lysis, macrophages scavenge Hb-Hp by CD163 and degrade heme via induced HO-1. Boyle and colleagues [12] could show that Hb-Hp uptake of macrophages during intraplaque hemorrhages in atherosclerotic lesions provoked the selective secretion of anti-inflammatory IL-10 and down-regulation of HLA class 2 molecules. HLA class 2 molecules are key players in induction and regulation of adaptive immunity to pathogens and exhibit constitutively low level expression on macrophages until induction by IFN-γ. Both, constitutive and regulated HLA class 2 expression is controlled by the activity of the transcriptional transactivator CIITA [61]. It has been shown *in vitro* that IL-10 is both, a potent inducer of CD163 and an inhibitor of HLA class 2 expression on macrophages. Diminished expression of HLA class 2 leads to subsequent impaired antigen presentation and activation of T_H1 cells [62-63].

In summary, the plasticity of macrophages is challenging and assigning specific biochemical markers to each population is difficult. Little attention has been paid to the hypothesis that extracellular Hb itself could be a modulator of macrophage phenotype polarization in wounded tissues. Therefore, we present a specialized macrophage phenotype with a distinct *in vivo* function in wound healing and atherosclerosis in this thesis.

1.3. Outline of the thesis

Macrophages play a crucial role in wound healing processes and control of inflammation after tissue damage. Moreover, macrophages have the unique ability to clear and detoxify extracellular Hb through the macrophage-specific scavenger receptor CD163 during pathological events such as hemolysis and intraplaque hemorrhage. Nevertheless, not much is known about this highly specialized Hb clearing macrophage phenotype.

Therefore, the specific aims of the research projects of this PhD thesis were:

- 1. To characterize the CD163 receptor SRCR domains in Hb-Hp binding and uptake outlined in chapter 2.

- 2. To characterize the macrophage proteome after long-term Hb-Hp exposure and to describe the generated phenotype outlined as a submitted manuscript in chapter 3.

- 3. To determine and characterize the impact of the Hb-Hp clearance pathway on the transcriptome of tissue macrophages outlined as a prepared manuscript in chapter 4.

1.4. References

1. Reeder BJ, Sharpe MA, Kay AD, Kerr M, Moore K, Wilson MT. Toxicity of myoglobin and hemoglobin: oxidative stress in patients with rhabdomyolysis and subarachnoid haemorrhage. Biochem Soc Trans. 2002;30:745-748.

2. Kapralov A, Vlasova II, Feng W, et al. Peroxidase activity of hemoglobin-haptoglobin complexes: covalent aggregation and oxidative stress in plasma and macrophages. J Biol Chem. 2009;284:30395-30407.

3. Kanias T, Acker JP. Biopreservation of red blood cells--the struggle with hemoglobin oxidation. FEBS J. 2010;277:343-356.

4. Umbreit J. Methemoglobin--it's not just blue: a concise review. Am J Hematol. 2007;82:134-144.

5. Clemens MR, Waller HD. Lipid peroxidation in erythrocytes. Chem Phys Lipids. 1987;45:251-268.

6. Bloom O, Wang H, Ivanova S, Vishnubhakat JM, Ombrellino M, Tracey KJ. Hypophysectomy, high tumor necrosis factor levels, and hemoglobinemia in lethal endotoxemic shock. Shock. 1998;10:395-400.

7. Su D, Roth RI, Levin J. Hemoglobin infusion augments the tumor necrosis factor response to bacterial endotoxin (lipopolysaccharide) in mice. Crit Care Med. 1999;27:771-778.

8. D'Agnillo F. Redox active hemoglobin enhances lipopolysaccharide-induced injury to cultured bovine endothelial cells. Am J Physiol Heart Circ Physiol. 2004;287:H1875-1882.

9. Yang H, Wang H, Bernik TR, et al. Globin attenuates the innate immune response to endotoxin. Shock. 2002;17:485-490.

10. Pamplona A, Hanscheid T, Epiphanio S, Mota MM, Vigario AM. Cerebral malaria and the hemolysis/methemoglobin/heme hypothesis: shedding new light on an old disease. Int J Biochem Cell Biol. 2009;41:711-716.

11. Gehrs BC, Friedberg RC. Autoimmune hemolytic anemia. Am J Hematol. 2002;69:258-271.

12. Boyle JJ, Harrington HA, Piper E, et al. Coronary intraplaque hemorrhage evokes a novel atheroprotective macrophage phenotype. Am J Pathol. 2009;174:1097-1108.

13. Scott MD, van den Berg JJ, Repka T, et al. Effect of excess alpha-hemoglobin chains on cellular and membrane oxidation in model beta-thalassemic erythrocytes. J Clin Invest. 1993;91:1706-1712.

14. Chaves MA, Leonart MS, do Nascimento AJ. Oxidative process in erythrocytes of individuals with hemoglobin S. Hematology. 2008;13:187-192.

15. Schaer DJ, Alayash AI. Clearance and control mechanisms of hemoglobin from cradle to grave. Antioxid Redox Signal. 2010;12:181-184.

16. Kong Y, Zhou S, Kihm AJ, et al. Loss of alpha-hemoglobin-stabilizing protein impairs erythropoiesis and exacerbates beta-thalassemia. J Clin Invest. 2004;114:1457-1466.

17. Shinar E, Rachmilewitz EA. Oxidative denaturation of red blood cells in thalassemia. Semin Hematol. 1990;27:70-82.

18. Okazaki T, Nagai T. Difference in hemoglobin-binding ability of polymers among haptoglobin phenotypes. Clin Chem. 1997;43:2012-2013.

19. Wicher KB, Fries E. Evolutionary aspects of hemoglobin scavengers. Antioxid Redox Signal. 2010;12:249-259.

20. Langlois MR, Delanghe JR. Biological and clinical significance of haptoglobin polymorphism in humans. Clin Chem. 1996;42:1589-1600.

21. Van Vlierberghe H, Langlois M, Delanghe J. Haptoglobin polymorphisms and iron homeostasis in health and in disease. Clin Chim Acta. 2004;345:35-42.

22. Olson JS, Foley EW, Rogge C, Tsai AL, Doyle MP, Lemon DD. No scavenging and the hypertensive effect of hemoglobin-based blood substitutes. Free Radic Biol Med. 2004;36:685-697.

23. Yang F, Brune JL, Baldwin WD, Barnett DR, Bowman BH. Identification and characterization of human haptoglobin cDNA. Proc Natl Acad Sci U S A. 1983;80:5875-5879.

24. Wicher KB, Fries E. Haptoglobin, a hemoglobin-binding plasma protein, is present in bony fish and mammals but not in frog and chicken. Proc Natl Acad Sci U S A. 2006;103:4168-4173.

25. Boretti FS, Buehler PW, D'Agnillo F, et al. Sequestration of extracellular hemoglobin within a haptoglobin complex decreases its hypertensive and oxidative effects in dogs and guinea pigs. J Clin Invest. 2009;119:2271-2280.

26. Delanghe J, Langlois M, Duprez D, De Buyzere M, Clement D. Haptoglobin polymorphism and peripheral arterial occlusive disease. Atherosclerosis. 1999;145:287-292.

27. Levy AP. Genetics of diabetic cardiovascular disease: identification of a major susceptibility gene. Acta Diabetol. 2003;40 Suppl 2:S330-333.

28. Quaye IK, Ababio G, Amoah AG. Haptoglobin 2-2 phenotype is a risk factor for type 2 diabetes in Ghana. J Atheroscler Thromb. 2006;13:90-94.

29. Kristiansen M, Graversen JH, Jacobsen C, et al. Identification of the hemoglobin scavenger receptor. Nature. 2001;409:198-201.

30. Nielsen MJ, Petersen SV, Jacobsen C, et al. A unique loop extension in the serine protease domain of haptoglobin is essential for CD163 recognition of the haptoglobin-hemoglobin complex. J Biol Chem. 2007;282:1072-1079.

31. Schaer DJ, Schaer CA, Buehler PW, et al. CD163 is the macrophage scavenger receptor for native and chemically modified hemoglobins in the absence of haptoglobin. Blood. 2006;107:373-380.

32. Schaer CA, Schoedon G, Imhof A, Kurrer MO, Schaer DJ. Constitutive endocytosis of CD163 mediates hemoglobin-heme uptake and determines the noninflammatory and protective transcriptional response of macrophages to hemoglobin. Circ Res. 2006;99:943-950.

33. Schaer CA, Vallelian F, Imhof A, Schoedon G, Schaer DJ. Heme carrier protein (HCP-1) spatially interacts with the CD163 hemoglobin uptake pathway and is a target of inflammatory macrophage activation. J Leukoc Biol. 2008;83:325-333.

34. Otterbein LE, Soares MP, Yamashita K, Bach FH. Heme oxygenase-1: unleashing the protective properties of heme. Trends Immunol. 2003;24:449-455.

35. Orozco LD, Kapturczak MH, Barajas B, et al. Heme oxygenase-1 expression in macrophages plays a beneficial role in atherosclerosis. Circ Res. 2007;100:1703-1711.

36. Droste A, Sorg C, Hogger P. Shedding of CD163, a novel regulatory mechanism for a member of the scavenger receptor cysteine-rich family. Biochem Biophys Res Commun. 1999;256:110-113.

37. Hintz KA, Rassias AJ, Wardwell K, et al. Endotoxin induces rapid metalloproteinase-mediated shedding followed by up-regulation of the monocyte hemoglobin scavenger receptor CD163. J Leukoc Biol. 2002;72:711-717.

38. Schaer DJ, Schleiffenbaum B, Kurrer M, et al. Soluble hemoglobin-haptoglobin scavenger receptor CD163 as a lineage-specific marker in the reactive hemophagocytic syndrome. Eur J Haematol. 2005;74:6-10.

39. Van Gorp H, Delputte PL, Nauwynck HJ. Scavenger receptor CD163, a Jack-of-all-trades and potential target for cell-directed therapy. Mol Immunol. 2010;47:1650-1660.

40. Fabriek BO, Polfliet MM, Vloet RP, et al. The macrophage CD163 surface glycoprotein is an erythroblast adhesion receptor. Blood. 2007;109:5223-5229.

41. Fabriek BO, van Bruggen R, Deng DM, et al. The macrophage scavenger receptor CD163 functions as an innate immune sensor for bacteria. Blood. 2009;113:887-892.

42. Ritter M, Buechler C, Kapinsky M, Schmitz G. Interaction of CD163 with the regulatory subunit of casein kinase II (CKII) and dependence of CD163 signaling on CKII and protein kinase C. Eur J Immunol. 2001;31:999-1009.

43. Polfliet MM, Fabriek BO, Daniels WP, Dijkstra CD, van den Berg TK. The rat macrophage scavenger receptor CD163: expression, regulation and role in inflammatory mediator production. Immunobiology. 2006;211:419-425.

44. Geissmann F, Manz MG, Jung S, Sieweke MH, Merad M, Ley K. Development of monocytes, macrophages, and dendritic cells. Science. 2010;327:656-661.

45. Auffray C, Sieweke MH, Geissmann F. Blood monocytes: development, heterogeneity, and relationship with dendritic cells. Annu Rev Immunol. 2009;27:669-692.

46. Tacke F, Randolph GJ. Migratory fate and differentiation of blood monocyte subsets. Immunobiology. 2006;211:609-618.

47. Randolph GJ, Sanchez-Schmitz G, Liebman RM, Schakel K. The CD16(+) (FcgammaRIII(+)) subset of human monocytes preferentially becomes migratory dendritic cells in a model tissue setting. J Exp Med. 2002;196:517-527.

48. Whitelaw DM, Batho HF. The distribution of monocytes in the rat. Cell Tissue Kinet. 1972;5:215-225.

49. Serbina NV, Jia T, Hohl TM, Pamer EG. Monocyte-mediated defense against microbial pathogens. Annu Rev Immunol. 2008;26:421-452.

50. Chawla A. Control of macrophage activation and function by PPARs. Circ Res. 2010;106:1559-1569.

51. Mantovani A, Sica A, Sozzani S, Allavena P, Vecchi A, Locati M. The chemokine system in diverse forms of macrophage activation and polarization. Trends Immunol. 2004;25:677-686.

52. Gordon S. Alternative activation of macrophages. Nat Rev Immunol. 2003;3:23-35.

53. Mosser DM, Edwards JP. Exploring the full spectrum of macrophage activation. Nat Rev Immunol. 2008;8:958-969.

54. Fuentes-Duculan J, Suarez-Farinas M, Zaba LC, et al. A Subpopulation of CD163-Positive Macrophages Is Classically Activated in Psoriasis. J Invest Dermatol. 2010.

55. Hogger P, Erpenstein U, Rohdewald P, Sorg C. Biochemical characterization of a glucocorticoid-induced membrane protein (RM3/1) in human monocytes and its application as model system for ranking glucocorticoid potency. Pharm Res. 1998;15:296-302.

56. Chamorro S, Revilla C, Alvarez B, Alonso F, Ezquerra A, Dominguez J. Phenotypic and functional heterogeneity of porcine blood monocytes and its relation with maturation. Immunology. 2005;114:63-71.

57. Van den Heuvel MM, Tensen CP, van As JH, et al. Regulation of CD 163 on human macrophages: cross-linking of CD163 induces signaling and activation. J Leukoc Biol. 1999;66:858-866.

58. Verschure PJ, Van Noorden CJ, Dijkstra CD. Macrophages and dendritic cells during the early stages of antigen-induced arthritis in rats: immunohistochemical analysis of cryostat sections of the whole knee joint. Scand J Immunol. 1989;29:371-381.

59. Moestrup SK, Moller HJ. CD163: a regulated hemoglobin scavenger receptor with a role in the anti-inflammatory response. Ann Med. 2004;36:347-354.

60. Weis N, Weigert A, von Knethen A, Brune B. Heme oxygenase-1 contributes to an alternative macrophage activation profile induced by apoptotic cell supernatants. Mol Biol Cell. 2009;20:1280-1288.

61. Steimle V, Siegrist CA, Mottet A, Lisowska-Grospierre B, Mach B. Regulation of MHC class II expression by interferon-gamma mediated by the transactivator gene CIITA. Science. 1994;265:106-109.

62. Fiorentino DF, Zlotnik A, Vieira P, et al. IL-10 acts on the antigen-presenting cell to inhibit cytokine production by Th1 cells. J Immunol. 1991;146:3444-3451.

63. de Waal Malefyt R, Haanen J, Spits H, et al. Interleukin 10 (IL-10) and viral IL-10 strongly reduce antigen-specific human T cell proliferation by diminishing the antigen-presenting capacity of monocytes via downregulation of class II major histocompatibility complex expression. J Exp Med. 1991;174:915-924.

64. Hubner G, Brauchle M, Smola H, Madlener M, Fassler R, Werner S. Differential regulation of pro-inflammatory cytokines during wound healing in normal and glucocorticoid-treated mice. Cytokine. 1996;8:548-556.

2. Characterization of CD163 scavenger receptor cysteine rich (SRCR) domains critical in Hb-Hp binding and uptake

2.1. Abstract

Chapter 2 summarizes the efforts to design several truncated CD163 constructs (pseudo-receptors) and set up functional assays in order to identify the SRCR domains important for Hb-Hp binding, uptake and endocytosis. So far, it could be shown that SRCR domain 3 of CD163 is critically involved in the calcium-dependent binding of Hp-Hb. In contrast, proteolytic cleavage in domain 3 inactivates ligand binding. By means of uptake assays with fluorescent Hb-Hp complexes we could show that besides the critical role of the third domain, also domains 5, 6 and 7 are significant for endocytotic receptor function. Surprisingly, a truncated version lacking only the ninth domain was unable to take up the Hb-Hp complex indicating a critical role for domain 8. Therefore, we assume that the 8th domain might need the presence of domain 9 to achieve a to date unknown 3D structure of the receptor essential for Hb-Hp binding and uptake.

2.2. Introduction

CD163 belongs to the scavenger receptor cysteine-rich (SRCR) superfamily, a highly glycosylated sub group of receptors belonging to the class of pattern recognition receptors. SRCR domains define the extracellular part of these transmembrane glycoproteins which are well conserved across multiple species [1]. CD163 exists in two variants, class A and B that only differ in the spacing between the cysteines. While CD163 belongs to the variant B receptors, it bears several splicing variants within that subclass. The predominant splicing form of the human scavenger receptor CD163 is a 130kDa protein consisting of an ecto-, transmembrane- (22 amino acids) and cytoplasmic domain as indicated in **Figure 1**. The large extracellular domain contains a signal sequence of 41 amino acids and 9 scavenger receptor cysteine rich domains (1009 amino acids). The cytoplasmic region exists as a short variant (39 amino acids) or as two long variants (84 and 89 amino acids, respectively) [2-4]. All three isoforms exhibit a common sequence located after the trans-membrane domain for phosphorylation and signal transduction involving protein kinase K and caseine kinase II [5]. The significance of the intracellular domain during the entry of the PRRS Virus was recently investigated by Lee and co-workers [6] which described an increased virus susceptibility of cells transfected with a tailless CD163 suggesting an important but yet unknown function.

Besides its ability to bind several other ligands as discussed in the general introduction chapter, this chapter focuses on the exclusive function of CD163 to bind and endocytose Hb-Hp in order to clear toxic Hb from the circulation and recycle heme-iron. The binding of Hb-Hp to CD163 was previously investigated assuming a critical role of domain 3 in ligand binding [7]. Furthermore, ligand-receptor binding was shown to be calcium dependent [8]. In order to define structural and functional important domains in the CD163 molecule, Schaer and colleagues [1] characterized the mouse homologue of human CD163 by SRCR sequence alignment indicating a highly conserved region between the fourth and sixth domain within the receptor. The soluble chicken Hb-binding protein (Pit54), also a member of the scavenger receptor cystein-rich protein family [9], shows sequence similarity between domains 4-6 and the first domain supporting the critical role of domains 4-6 in ligand binding. Upon inflammatory stimulus the ectodomain is shed from the cell surface by a

metalloproteinase-dependent mechanism [10-12] releasing soluble CD163 (sCD163) that covers 94% of the total extra-cellular part. Surface plasmon resonance (SPR) measurements with immobilized recombinant sCD163 showed a high-affinity binding to Hb-Hp while sCD163 in solution only weakly competed for Hb-Hp uptake by CD163-expressing cells [13]. Based on these findings, Moeller and colleagues assumed that only membrane bound CD163 effectively binds Hb-Hp because of possible receptor cross-linkages.

Therefore, we chose to sub-clone 12 truncated versions of CD163 composed of the signal peptide, the transmembrane domain and the cytoplasmatic tail into an EmeraldGFP-containing vector. Sequence checked constructs were expressed in HEK cells and full length CD163 served as positive control for Hb-Hp uptake assays. We observed a subsequently increasing binding and uptake rate of the contructs 1-5, 1-6 and 1-7, while 1-8 failed to endocytose Hb-Hp. These pre-eliminary results give more insights of possible conformational requirements sufficient for Hb-Hp uptake adding domain 8 as another critical region for ligand binding.

2.3. Methods

2.3.1. CD163 pseudo-receptor plasmid construction

CD163 pseudo-receptors were amplified from a human CD163 cDNA clone (OriGene Technologies, Rockville, MD, USA) by two subsequent PCR's using AccuPrime Polymerase with the primers listed in **Table 1** according to the cloning strategy illustrated in **Figure 2**. PCR products were sub-cloned into the expression vector pcDNA6.2/C-EmGFP/YFP-GW/TOPO (Invitrogen, Basel, Switzerland), and vector integrity was verified by nucleotide sequencing. Plasmids were transformed using TOP10 One Shot chemically competent *E.coli* cells (Invitrogen) and plasmid DNA was isolated by S.N.A.P. MidiPrep Method (Invitrogen), sequenced and linearized with *Sca I* (Roche diagnostics, Rotkreuz, Switzerland) before transfection. The following twelve constructs designated according to their CD163 SRCR domains were sub-cloned and expressed [1]: CD163 1-3 (aa 1-366); CD163 1-4 (aa 1-469); CD163 1-5 (aa 1-574); CD163 1-6 (aa 1-681); CD163 1-7 (aa 1-815); CD163 1-8 (aa 1-920); CD163 1-9 (aa 1-1024); CD163 3-4 (aa 258-496), CD163 3-5 (aa 258–574); CD163 3-6 (aa 258-681); CD163 3-9 (aa 258-1024) and CD163 4-6 (aa 356-681).

2.3.2. Expression of recombinant CD163 pseudo-receptors

HEK293A cells were transfected using Lipofectamine 2000 reagent (Invitrogen) in OptiMEM I Reduced Serum Medium (Gibco, Basel, Switzerland) according to the manufacturer's instruction. Stable transfected HEK293A clones were established by subsequent selection with 6ug/ml Blasticidin (Invitrogen). To obtain an uniform population of cells expressing CD163 pseudo-receptors, GFP-positive cells were separated by fluorescence activated cell sorting (FACS, FACS Aria, Becton Dickinson, Basel, Switzerland). After sorting, cells were passaged at least 5 times before performing experiments. CD163 pseudo-receptor expression was confirmed by quantitative real-time reverse transcription (RT-PCR). Additionally, GFP expression was confirmed by western blot using a polyclonal antibody against GFP.

2.3.3. Hb-Hp complex uptake assay by HEK293A cells

Highly purified HbA_0 (Sigma) or Hp phenotype 2-2 (Sigma) were labelled with Alexa-633 protein labelling kit (Molecular probes, Eugene, OR) as described before [14]. To measure the uptake of the complex, cells were incubated with Hb-Hp (20ug/m) in an incubator at 37°C, 5% CO_2 and 95% humidity for 45 minutes. All uptake assays were performed in cell culture medium without serum. Hb-Hp complexes were generated at a 1:1 (wt/wt) ratio 5 minutes before experimentation. After incubation with the ligand cells were trypsinized and washed 3 times with cold phosphate-buffered saline (PBS) to remove non-ingested Hb-Hp complexes. Uptake of the fluorescent ligand was then measured by flow cytometry using a FACSCalibur (BD Sciences, Basel, Switzerland) at 530nm excitation/530nm emission (GFP) and at 661nm excitation/616nm emission (Alexa-633).

2.3.4. Immunfluorescence analysis of Hb-Hp complex uptake by HEK293A cells

Cells were cultured on endotoxin-free, sterile, round 12-mm glass coverslips (Hecht-Assistant, Germany), pretreated with 6.25 µg/cm^2 poly-D-Lysine Hydro-bromide (BD Biosciences, San Jose, CA, USA) in 24-cluster wells and incubated with fluorescent Hb-Hp (20ug/ml) complexes as described above. After incubation, cells were washed 3 times with PBS and fixed for 15 minutes in 2.5% Paraformaldehyde (Sigma, Deisenhofen, Germany). Cells were permeabilized for 1 minute with 0.1% Triton-X-100 and washed three times with PBS. After blocking of nonspecific binding sites for

1 hour with 10% goat serum in PBS and nuclear counterstain using 10 µg/ml 4,6-diamidino-2-phenylindole (DAPI; Sigma) coverslips were mounted onto a microcope slide using ProLong Gold Antifade (Invitrogen). Images were taken with the Axioskop 2 microscopy system, equipped with an AxioCam MRC digital camera (Carl Zeiss, Feldbach, Switzerland) and AxioVision software, version 4.6.3. (Carl Zeiss).

2.3.5. Surface Plasmon resonance (SPR) measurements

SPR analysis of Hb-Hp complex binding to CD163 was carried out on a ProteOn XPR36 instrument equipped with ProteOn Manager Software (Bio-Rad Laboratories; Reinach, Switzerland). The ProteOn GLM sensor chips (General Layer, Medium capacity, Bio-Rad) were pre-conditioned according to the manufactuer's protocol (Bio-Rad) and activated with a 1:1 mixture of 0.4 M 1-ethyl-3- (3-dimethylamino-propyl)carbodiimide hydrochloride and 0.1 M N-hydroxysulfosuchinimide in water. 10 ug of recombinant CD163 or purified Hp 1-1 (Sigma) was immobilized in 10 mM sodium acetate, pH 4.0 and remaining binding sites were blocked with 1M ethanolamine, pH 8.5. The flow buffer contained 150 mM NaCl, 2 mM $CaCl_2$ and 10 mM HEPES with a pH of 7.4. Sensorgrams were generated using Hb-Hp concentrations ranging from 250-4000 nM or Hb concentrations ranging from 12.5-200 nM in flow buffer. In case of immobilized CD163 the flow cells were regenerated with 1.6 M glycine –HCl, pH 3.0 for reruns.

2.4. Results and Discussion

2.4.1. Identification of SRCR domains in CD163 critical for Hb-Hp binding and uptake

A panel of CD163 pseudo-receptors was expressed and stably transfected in HEK293A cells. Stable and uniform expression was obtained by selection with blasticidin and routinely FACS sorting of GFP-expressing cells. **Figure 3** shows the quantitative assessment of fluorescent Hb-Hp complex uptake. Truncated CD163 1-5 and CD163 1-6 showed a moderate uptake of Hb-Hp compared to HEK293A cells without the receptor. To our surprise, approximately 80% **(Figure 4)** of the cells expressing CD163 1-7 and CD163 1-9 were positive for Hb-Hp uptake and could only be exceeded by positive control cells (HEK293A CD163) (97%). The right panel of **Figure 3** illustrates the inability of the indicated truncated CD163 receptors to take up Hb-Hp. CD163 1-3 and CD163 1-4 were negative for Hb-Hp uptake, only one domain longer, CD163 1-5 instead was already able to internalize the ligand supporting the

hypothesis that region 4-6 is critical for Hb-Hp binding. Moreover, truncated receptors lacking the first, second and also the third domain could not take up the ligand **(see Figure 3)**. Nevertheless, the most surprising finding was the inability of CD163 1-8 to internalize Hb-Hp equal to HEK293A CD163-negative control cells. We further proofed by western blot that CD163 pseudo-receptors bear GFP as illustrated in **Figure 5.**

The indicated characteristics of selected CD163 pseudo-receptor transfected cells were further verified by immunofluorescence **(Figure 6)** analysis of Hb-Hp uptake. HEK293A cells transfected with the full-length receptor showed strong uptake of fluorescent Hb-Hp complexes, while CD163 1-3 bearing cells did not endocytose the ligand. In contrast, CD163 1-5, 1-7 and 1-9 transfected cells were positive for Hb-Hp uptake and GFP-expression.

Finally, we used recombinant human CD163 encoding the extracellular domain to investigate Hb-Hp binding on the immobilized receptor. Madsen and colleagues could show that ligand receptor binding is calcium- and pH-dependent. In detail, calcium-concentrations lower than 0.2 mM and pH less than 6.5 increased dissociation of Hb-Hp from CD163. We chose to use a running buffer with a calcium concentration of 0.5 mM and a pH of 7.4. As shown in **Figure 7**, we applied different concentrations of Hb-Hp to the receptor. After a short association phase of 60 sec, the complex dissociates biphasic. We visually observed a relatively fast dissociation followed by a very low dissociation phase. These results are in agreement with studies of Kristiansen and colleagues [8] and Buehler and co-workers [15]. Nevertheless, the initial idea was to isolate and purify the truncated CD163 receptors in order to immobilize them on a sensor chip and investigate the binding capacity for Hb-Hp. Unfortunately, pseudo-receptor isolation with GFP beads returned too less sample for receptor coating. Receptor elution from GFP beads was performed with a non-denaturating solution using a pH shift according to the manufacturer's instructions (Miltenyi Biotech, Bergisch Gladbach, Germany). We assume that the elution process might have interfered with the receptor conformation. Also, the suspension was still enriched with too many perturbing proteins. Immobilized polyclonal anti-GFP antibodies on the chip seemed promising to "fish out" the pseudo-receptors but failed due to insufficient receptor concentrations in the cell suspension. We further

speculated that GFP tagged to the receptor could interfere with its binding ability. Today, vectors are available that enzymatically release their GFP tag and could allow immobilization of truncated receptors in order to get more insights into CD163-Hb-Hp binding and endocytosis. Further experiments could also investigate the impact of a variation of the buffer composition e.g. in pH or calcium concentration.

In conclusion, we successfully expressed twelve CD163 pseudoreceptors and subsequent investigated their Hb-Hp binding and endocytosis capacity. Further, by means of immunofluorescence and uptake assays, we could show that besides the critical domains 4-6, also the domain 8 plays a non-redundant role in ligand binding and uptake. Unfortunately, we were not yet able to isolate sufficient amounts of purified CD163 pseudoreceptors to perform SPR experiments. Nevertheless, to identify the crystallographic structure of CD163 and the CD163-Hb-Hp complex would give a lot more answers to the open questions in receptor conformation and may help to define the interplay between Hb subunits and the CD163 SRCR domains. We suggest that the established pseudo-receptors could serve as the basis of these investigations.

Table 1- *Oligonucleotides used for cloning*

Primer	5' – 3'
hCD163 $_{80\text{-}104}$ for	CTTTGGAATGAGCAAACTCAGAATG
CD163 3Dom* rev	ATAAAGGATGACTGACGGGAATCAGAACATGTCACGCCAG
CD163 4Dom* rev	ATAAAGGATGACTGACGGGAGGCTGAGCAGGTAATTTTGG
CD163 5Dom* rev	ATAAAGGATGACTGACGGGATCTTGAGCAGACTACTCCAACATC
CD163 6Dom* rev	ATAAAGGATGACTGACGGGACTGGTTTCCTGAGCAGATTACAGAGGCCAC
CD163 7Dom* rev	ATAAAGGATGACTGACGGGATTCTGAGCAGATAACTCCCGC
CD163 8Dom* rev	ATAAAGGATGACTGACGGGAACATGTGATCCAGGTCT
CD163 9Dom* rev	ATAAAGGATGACTGACGGGATG
CD163 3Dom* for	ACTTCTCAGTGCCTGTTTTGTCACCAGTTCTCTTGGAGATCTGAGCCTGAGACTGGTAG
CD163 4Dom* for	ACTTCTCAGTGCCTGTTTTGTCACCAGTTCTCTTGGAGATCTGGAGCTAAGACTTAGAGGTG
CD163-TM-CT (Synth EmMutPlus rev)	GTTCATCTCCCGGTATTGAATTCTCTGTCTTCGCTTTTTAGCCAAGAAGAATAATGCGACGAAAATGGCCAACAGAACAACCCCAAGGATCCCGACTGCAATAAAGGATGACTGACGGGA
CD163-SP (Synth 163SignPep for)	CGCCGGAATGAGCAAACTCAGAATGGTGCTACTTGAAGACTCTGGATCTGCTGACTTCAGAAGACATTTTGTCAACTTGAGTCCCTTCACCATTACTGTGGTCTTACTTCTCAGTGCCTGTTTTG

* *SRCR domain*

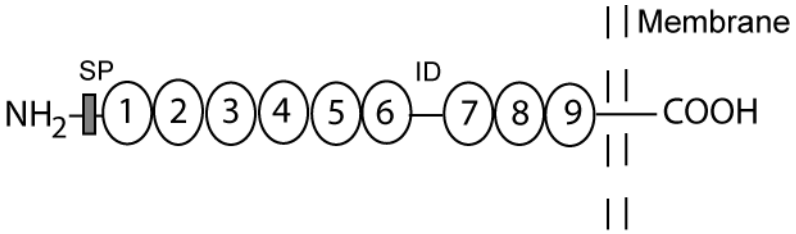

Figure 1 – Schematic representation of the CD163 receptor. *Shown are the SRCR domains and the indicated transmembrane domain (figure partly adapted from [2]). SP: signal peptide, ID: scavenger interspersed domain.*

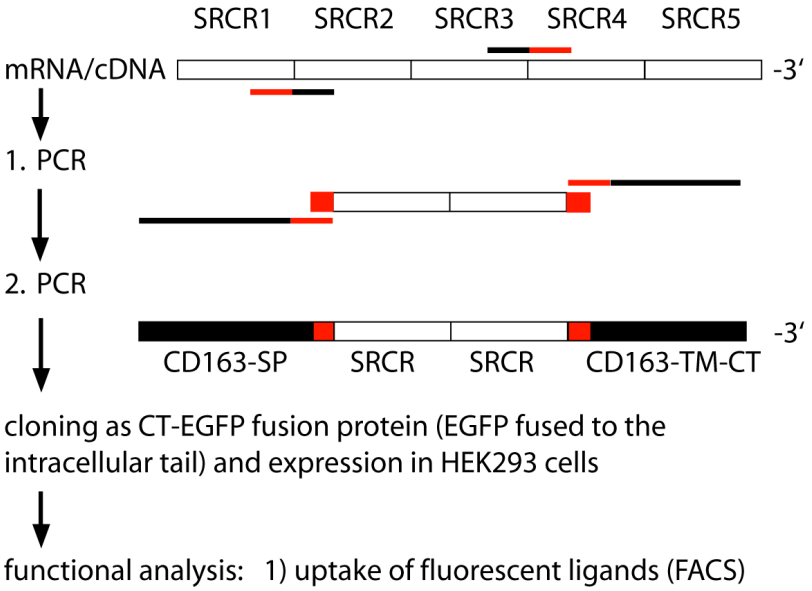

Figure 2 - Cloning strategy for the generation of CD163 SRCR domain pseudo-receptors. *Variable numbers of SRCR domains were amplified from SRCR domain cDNAs. The primers used for the generation of gene specific amplicons contain a consensus primer sequence (red) which was used in a second PCR for the fusion of the CD163 signal peptide (SP) to the 5' end of the SRCR domains as well as the CD163 transmembrane domain and a endocytosis mediating cytoplasmic tail (TM-CT) to the 3' end of the SRCR domains. This construct was then cloned as a fusion protein with enhanced GFP which allowed protein expression control in HEK293A cells.*

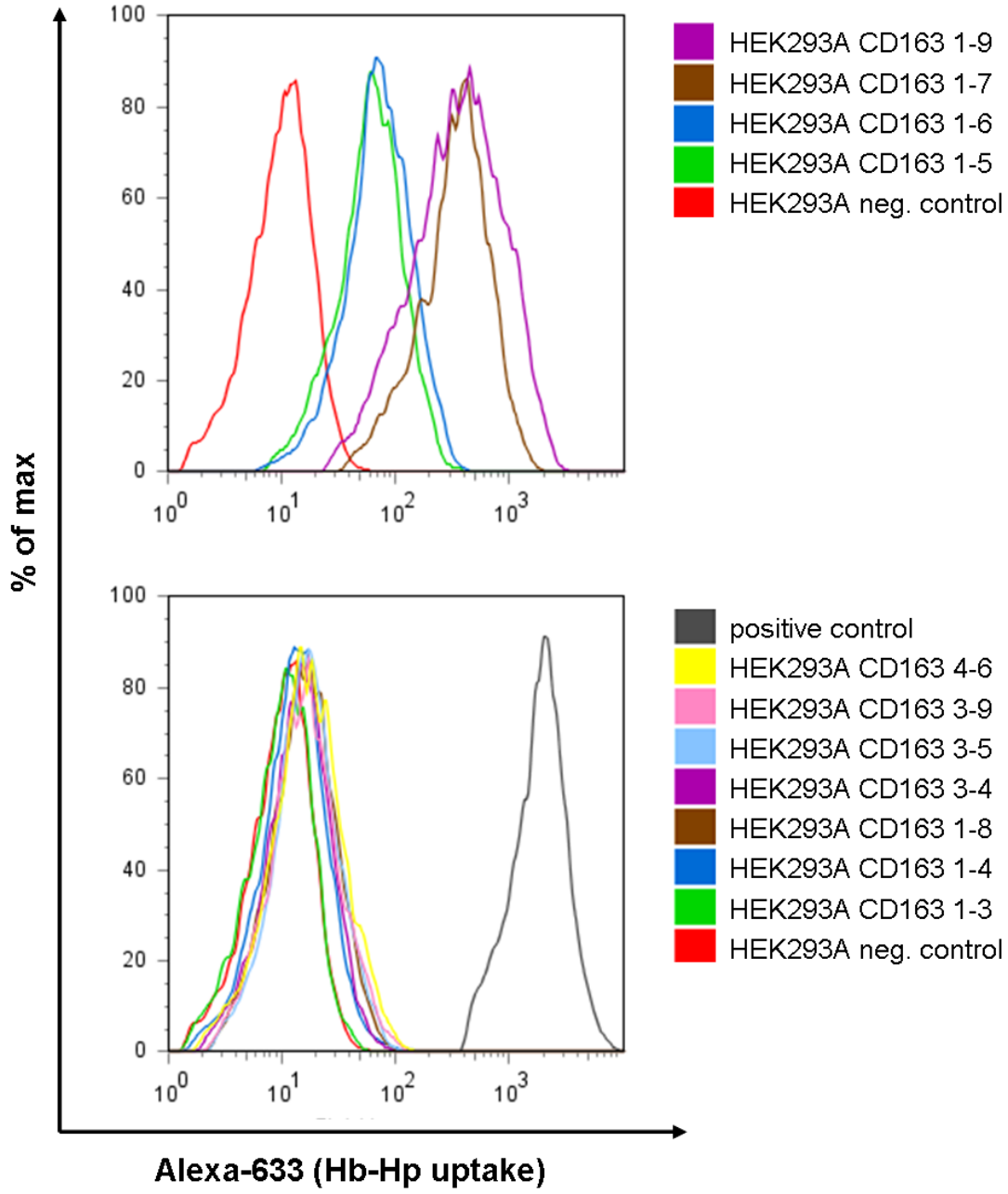

Figure 3 - Hb-Hp uptake levels of distinct CD163 pseudo-receptors*. Uptake was analyzed by flow cytometry. HEK293A cells served as negative control for uptake, while CD163 FL transfected HEK293A were the positive control for ligand uptake. Upper panel: pseudo-receptors positive for Hb-Hp uptake. Lower panel: pseudo-receptors negative for Hb-Hp uptake.*

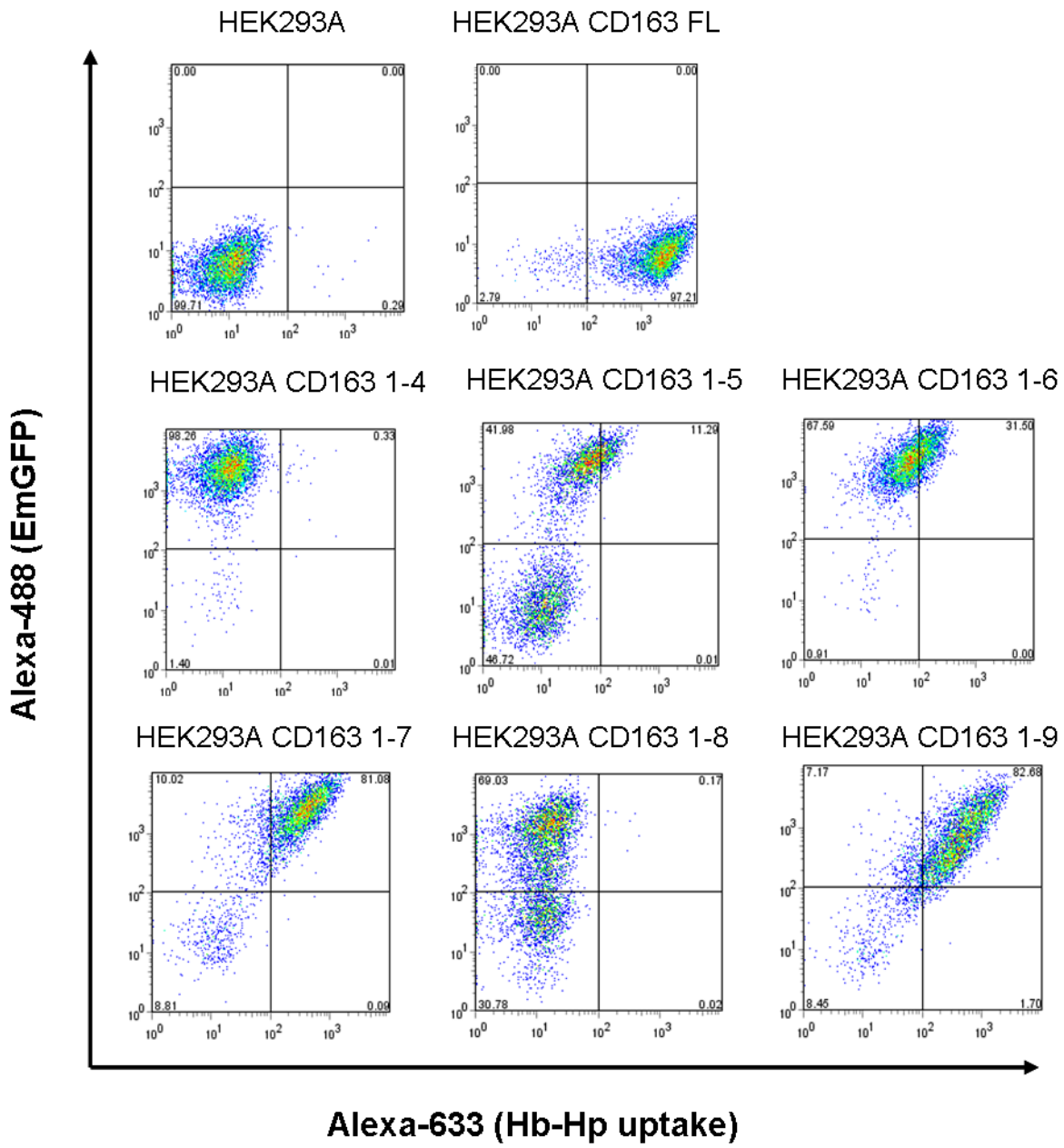

Figure 4 – FACS measurement *of GFP (Alexa 488) expression and quantitative assessment of fluorescent Hb-Hp uptake (Alexa 633) of several CD163 pseudo-receptors after 45 minutes of incubation with the ligand (Hb-Hp). HEK293A is referred as negative control while HEK293A CD163 FL served as positive control.*

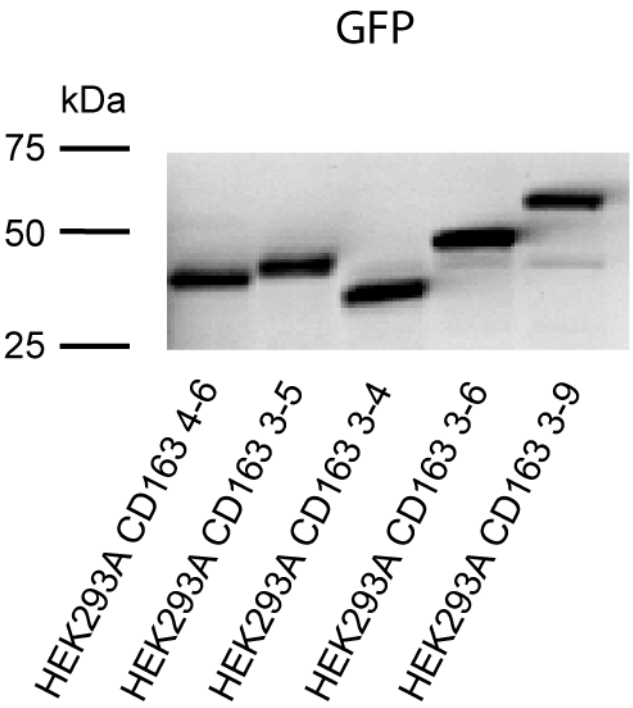

Figure 5 – Confirmation of GFP expression in CD163 pseudo-receptor transfected HEK293A cells using western blot analysis against recombinant GFP.

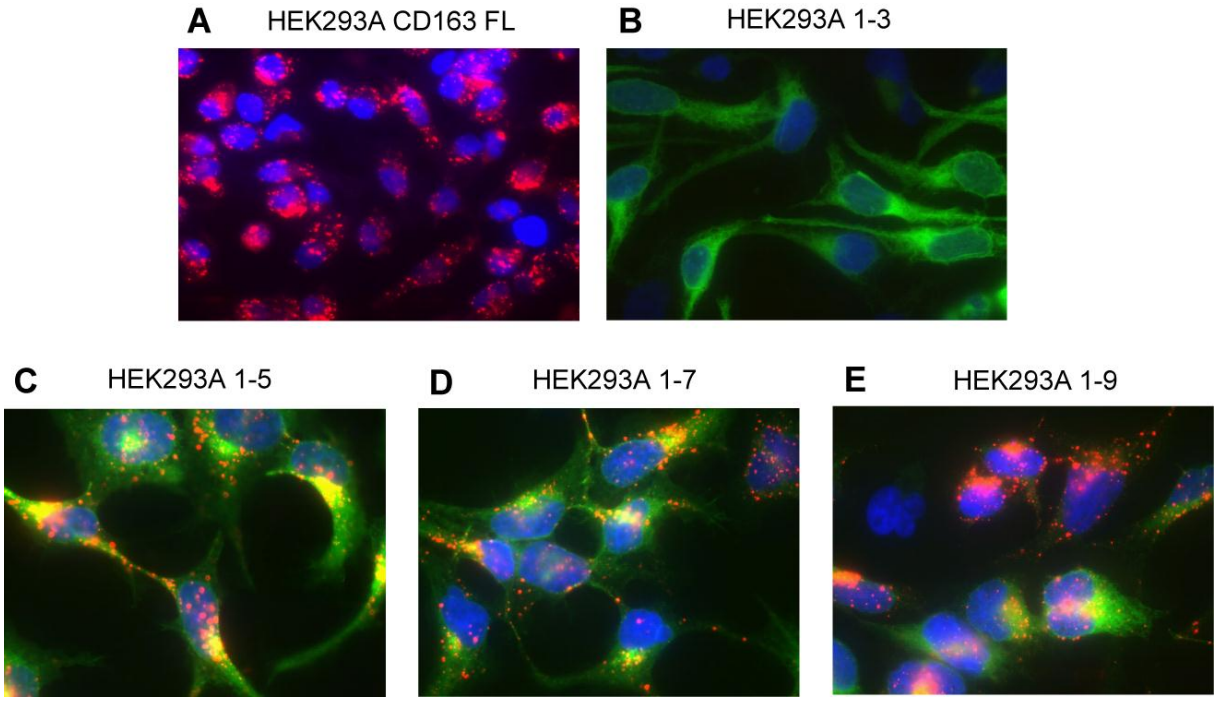

Figure 6 – Immunofluorescent assessment of Hb-Hp endocytosis *(red) and GFP expression (green) of transfected HEK293A cells.* ***(A)*** *HEK293A CD163 FL served as positive uptake control.* ***(B) – (E)*** *truncated pseudo-receptors transfected HEK293A cells. Nuclei (DAPI, blue).*

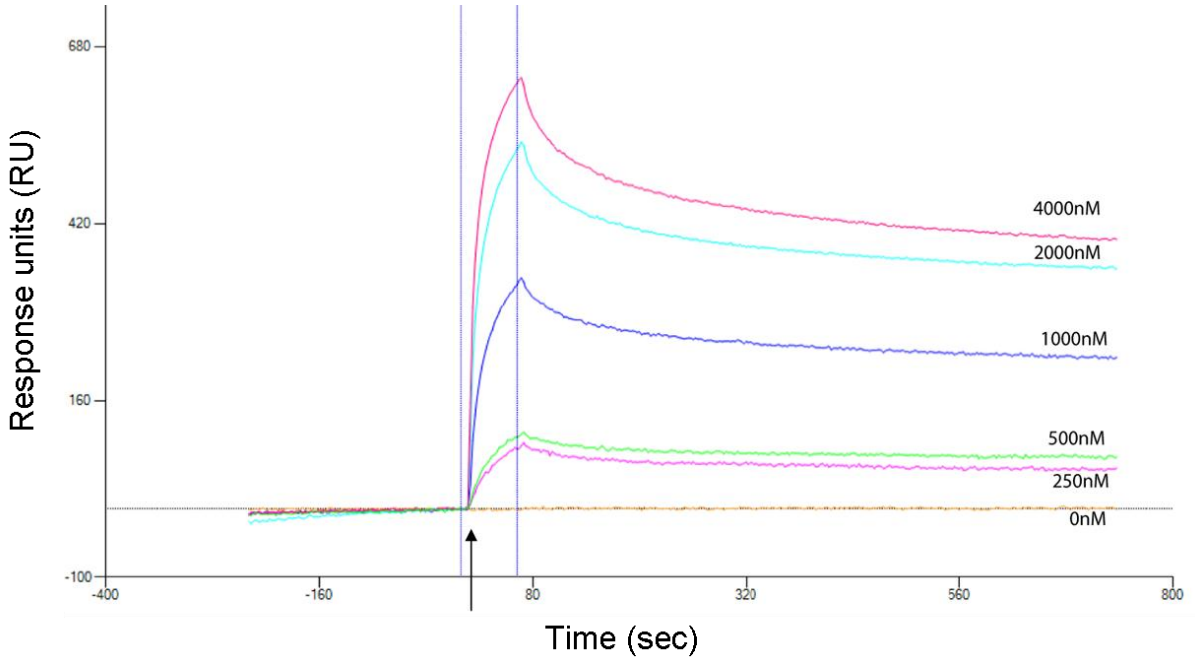

Figure 7 – SPR analysis of binding of Hb-Hp to immobilized recombinant human CD163 on a ProteOn sensor chip. *At time point 0 (indicated by black arrow), Hb-Hp complexes were applied to the immobilized ligand in a dose dependent manner. Binding and dissociation was recorded with 0.5 mM $CaCl_2$ in the flow buffer (pH 7.4).*

2.5. References

1. Schaer DJ, Boretti FS, Hongegger A, et al. Molecular cloning and characterization of the mouse CD163 homologue, a highly glucocorticoid-inducible member of the scavenger receptor cysteine-rich family. Immunogenetics. 2001;53:170-177.

2. Nielsen MJ, Petersen SV, Jacobsen C, et al. A unique loop extension in the serine protease domain of haptoglobin is essential for CD163 recognition of the haptoglobin-hemoglobin complex. J Biol Chem. 2007;282:1072-1079.

3. Ritter M, Buechler C, Langmann T, Orso E, Klucken J, Schmitz G. The scavenger receptor CD163: regulation, promoter structure and genomic organization. Pathobiology. 1999;67:257-261.

4. Law SK, Micklem KJ, Shaw JM, et al. A new macrophage differentiation antigen which is a member of the scavenger receptor superfamily. Eur J Immunol. 1993;23:2320-2325.

5. Ritter M, Buechler C, Kapinsky M, Schmitz G. Interaction of CD163 with the regulatory subunit of casein kinase II (CKII) and dependence of CD163 signaling on CKII and protein kinase C. Eur J Immunol. 2001;31:999-1009.

6. Lee YJ, Lee C. Deletion of the cytoplasmic domain of CD163 enhances porcine reproductive and respiratory syndrome virus replication. Arch Virol. 2010.

7. Madsen M, Moller HJ, Nielsen MJ, et al. Molecular characterization of the haptoglobin.hemoglobin receptor CD163. Ligand binding properties of the scavenger receptor cysteine-rich domain region. J Biol Chem. 2004;279:51561-51567.

8. Kristiansen M, Graversen JH, Jacobsen C, et al. Identification of the haemoglobin scavenger receptor. Nature. 2001;409:198-201.

9. Wicher KB, Fries E. Haptoglobin, a hemoglobin-binding plasma protein, is present in bony fish and mammals but not in frog and chicken. Proc Natl Acad Sci U S A. 2006;103:4168-4173.

10. Droste A, Sorg C, Hogger P. Shedding of CD163, a novel regulatory mechanism for a member of the scavenger receptor cysteine-rich family. Biochem Biophys Res Commun. 1999;256:110-113.

11. Hintz KA, Rassias AJ, Wardwell K, et al. Endotoxin induces rapid metalloproteinase-mediated shedding followed by up-regulation of the monocyte hemoglobin scavenger receptor CD163. J Leukoc Biol. 2002;72:711-717.

12. Schaer DJ, Schleiffenbaum B, Kurrer M, et al. Soluble hemoglobin-haptoglobin scavenger receptor CD163 as a lineage-specific marker in the reactive hemophagocytic syndrome. Eur J Haematol. 2005;74:6-10.

13. Moller HJ, Nielsen MJ, Maniecki MB, Madsen M, Moestrup SK. Soluble macrophage-derived CD163: a homogenous ectodomain protein with a dissociable haptoglobin-hemoglobin binding. Immunobiology. 2010;215:406-412.

14. Schaer CA, Vallelian F, Imhof A, Schoedon G, Schaer DJ. Heme carrier protein (HCP-1) spatially interacts with the CD163 hemoglobin uptake pathway and is a target of inflammatory macrophage activation. J Leukoc Biol. 2008;83:325-333.

15. Buehler PW, Abraham B, Vallelian F, et al. Haptoglobin preserves the CD163 hemoglobin scavenger pathway by shielding hemoglobin from peroxidative modification. Blood. 2009;113:2578-2586.

3. Hemoglobin polarizes the macrophage proteome towards high Hb clearance, enhanced anti-oxidant capacity and suppressed HLA class 2 expression

3.1. Abstract

Monocytes/macrophages are the key cell compartment of hemoglobin (Hb) clearance during hemolysis and wound healing. The rapid elimination of free extracellular Hb is crucial to limit its severe toxic effects due to the highly-reactive heme group of Hb. Free Hb avidly binds to the acute-phase serum protein haptoglobin (Hp) and is eliminated by macrophages that respond with anti-inflammatory and anti-oxidative properties. Quantitative mass spectrometry (MS) enables comprehensive identification and quantification of protein expression in complex cell samples, such as macrophages. We investigated the protein profile of macrophages after exposure to Hb-Hp complexes using Isobaric Tags for Relative and Absolute Quantification (iTRAQ)-based protein quantification followed by two different and highly complementary mass spectrometry platforms (MALDI-TOFTOF and LTQ Orbitrap). We identified a total of 3691 proteins obtained from three healthy donors with a considerable fraction of 848 significantly up- and down-regulated ($p < 0.005$) proteins by Hb-Hp treatment. Moreover, our data represent the so far most complete macrophage proteome. Beyond the identification of major Hb responsive pathways in macrophages, we could show that Hb-Hp exposure profoundly suppressed HLA class 2 expression putatively reducing antigen presentation to the immune system and therefore preventing specific immune responses. In summary, our data suggest that the Hb-Hp driven macrophage polarization represents a specialized macrophage phenotype with distinct *in vivo* functions in wound healing and atherosclerosis.

3.2. Introduction

Hemoglobin is released from red blood cells (RBCs) during hemolysis or when blood gets extravasated such as in wounded tissues, during hemorrhagic stroke or atherosclerotic intraplaque hemorrhage. As a result of heme's strong reactivity with physiologic oxidants such as hydrogen peroxide (H_2O_2) extracellular Hb can act as a pro-oxidant in extracellular environments [1-2]. Peroxidative tissue damage emanating from these reactions as well as pro-inflammatory effects exerted by heme and oxidatively damaged Hb protein aggregates has been reported [3-4]. Clearance of Hb from extracellular sites in concert with adaptive cellular responses tailored to attenuating the potentially damaging effects of Hb seem therefore essential.

Several potent mechanisms have evolved to protect against systemic or local Hb toxicity. Haptoglobin (Hp) is the primary Hb scavenger in plasma that binds free Hb in an irreversible complex [5-6]. When bound to Hp, Hb remains sequestered in the intravascular space and peroxidative processes are efficiently confined within the complex, thus shielding the environment from oxidative damage [7-8]. Much less knowledge exists about Hp's function in extracellular spaces such as in a wound where multiple cell types can express and secrete Hp upon stimulation [9]. However, it is known that Hp slows heme release, prevents formation of covalent protein crosslink products and protects the structural integrity of globin amino acids even during very severe oxidative impacts. The Hb-Hp complex is finally endocytosed by the CD163 scavenger receptor pathway that is strongly and exclusively expressed by circulating monocytes and macrophages [10-11]. It has been previously noticed that CD163 links extracellular Hb exposure to high heme oxygenase (HO-1) expression, enhanced heme and iron metabolisms and associated short-term anti-oxidative adaption [12].

Macrophages serve diverse functions during inflammation and wound healing. Circulating blood monocytes are attracted to injured tissue sites within short time of an inflammatory or mechanic impact and start to differentiate into mature tissue macrophages [13]. It is mainly the tissue environment (e.g. secreted cytokines) that directs polarization of the considerable differentiation plasticity of these cells into either pro-inflammatory phagocytes that fight invading pathogens or into a cell type

that mediates non-inflammatory removal of damaged tissue debris while promoting wound healing [14]. So far, little attention has been paid to the hypothesis that extracellular Hb itself could be a modulator of macrophage phenotype polarization in wounded tissues.

In this study we investigated how the differentiation of monocyte derived macrophages is modulated by extracellular Hb:Hb exposure. To get a comprehensive overview of the macrophage proteome in general and the quantitative changes in protein abundances resulting from Hb exposure we adopted a shotgun proteome exploration strategy. iTRAQ based protein quantification was combined with dual-analysis of identical samples by two different and highly complementary mass spectrometry platforms (MALDI-TOFTOF and LC-ESI MS/MS on a LTQ-Orbitrap). As a result of the high yield of unambiguous protein identifications we report here the so far most comprehensive macrophage proteome coverage. We found that continuous Hb exposure polarized the macrophage proteome towards a phenotype with high Hb clearance and anti-oxidative capacity that is uniquely characterized by profoundly suppressed HLA class 2 expression.

3.3. Materials and Methods

3.3.1. Cell culture and experimental conditions

Human monocytes were prepared from heparinized whole blood (100 U/ml) from different healthy volunteers by a Ficoll gradient separation (Ficoll-Paque^{TM} PLUS, Amersham Biosciences) and three washes with Mg^{2+}/Ca^{2+} -free phosphate buffered saline (PBS; GIBCO Europe). Cells were suspended in Iscove's modified Dulbecco's medium (IMDM; GIBCO Europe) supplemented with 10% autologous human serum to prevent activation and seeded at a density of 10^7 cells/ml in 6-well tissue culture plates (Falcon Oxnard, USA). During 2 h under standard cell culture conditions (37°C, 5% CO_2) in a SteriCult tissue culture incubator (Fisher Scientific, USA) monocytes adhered to the tissue culture plates. Afterwards, the cells were washed with Gey's balanced salt solution (Sigma, USA) to remove non-adherent cells and the remaining monocytes were stimulated with 2 mg/ml Hb/Hp or Hb. Endotoxin free Hb was obtained from Hemosol (Ontario, Canada). Hp (mixed phenotype) was from Sigma (Buchs, Switzerland). Macrophages derived from monocytes were kept in

IMDM containing 10% autologous human serum for 2 days and for 5 days for mRNA expression analysis, respectively. For protein expression analysis culture time was prolonged to 7 days.

3.3.2. Sample treatment for iTRAQ analyses

Human-blood derived monocytes were prepared from 3 healthy donors, as described before and cultured in IMDM (GIBCO, Europe), supplemented with 10% heat-inactivated, pooled human serum from 8 healthy donors. For each tested condition (media alone or 2 mg/ml Hb-Hp) samples were prepared in 3 biological replicates as mentioned above, whereas each replicate was divided into two portions for experimental replicates. At day 7 of culture total cellular protein was extracted from human-blood derived macrophages, grown in 24-well plates. Supernatant was removed and cells were harvested by scraping using 100 µl CelLytic-M reagent (Sigma) supplemented with Complete Mini Protease Inhibitor (Roche Diagnostics). After three freeze-thaw cycles and sonication with a Branson Sonifier 250, cellular debris was removed by centrifugation at 16’000 x g for 10 min. Protein concentration of each sample was determined using a protein Bradford assay (Bio-Rad, USA). Samples normalized to 60 µg of protein were precipitated by adding 1 volume of trichloroacetic acid (TCA) to 4 volumes of protein solution to a final concentration of 10-12% w/v TCA and incubated at 4°C for 10 min. After centrifugation at 16’000 x g supernatant was removed, pellets were washed three times with ice-cold acetone and dried in a heat block at 95°C for 10 min.

3.3.3. iTRAQ labeling

Pellets were reconstituted in 20 µl of dissolution buffer and 1 µl of denaturant according to the protocol of the iTRAQ manufacturer (Applied Biosystems, USA). Additionally, we added 4 µl of 6 M freshly prepared urea to the pellets. Disulfide bonds were reduced by adding 2 µl of reducing agent and blocked by treatment with 1 µl of cysteine blocking reagent. A total of 60 µg of protein was digested overnight at 37°C with trypsin (Promega, USA) in the ratio 1:10, trypsin to protein. Peptides were covalently modified for two hours with an isobaric tag reagent according to the following scheme: iTRAQ 114 (control macrophages), iTRAQ 115 (Hb-Hp treated macrophages), iTRAQ 116 (control macrophages) and iTRAQ 117 (Hb-Hp treated

macrophages) **(Figure 1)**. After combining the iTRAQ reagent labeled peptides, the reaction was stopped by adding 10 µl of phosphoric acid (pH 2-3).

3.3.4. SCX fractionation

The Labeled peptides were fractionated by strong cation exchange liquid chromatography (SCX) using a Polysulfoethyl A 2.1 mm x 200 mm, 5 µm, 300 Å column (PolyLC, USA). Solvent A was 10 mM potassium phosphate, 25% acetonitrile (ACN), pH 2.7, and solvent B was 10 mM potassium phosphate, 350 mM potassium chloride, 25% ACN, pH 2.7. The iTRAQ labeled peptides were diluted in a ratio 1:4 in solvent A and applied to the SCX column. Chromatography was performed at a flow rate of 0.3 ml/min according to the following gradient: 0-10 min 0% solvent B; 10-60 min 0-100% solvent B; 60-65 min 100% solvent B; 65-90 min 0-100% solvent A. For each HPLC run, 24 out of 27 fractions were collected and partially evaporated to remove ACN in a vacuum concentrator. The collected fractions were redissolved in 5% ACN, 0.1% trifluoroacetic acid (TFA), combined to 8 pools (each pool contained 3 fractions) and desalted with Sep Pak C_{18} cartridges (Waters, USA). The 8 labeled sample pools were dried in a vacuum concentrator and reconstituted in 10 µl of 3% (v/v) ACN /0.2% formic acid. 5 µl of each pool was transferred to a new tube and combined to 4 sample pools for MALDI-TOFTOF MS analyses. The remaining sample amount of the 8 pools was used to perform LTQ-Orbitrap MS. All procedures were carried out with the monocyte lysates from three healthy donors.

3.3.5. Nano-LC separation and MALDI target plate spotting of tryptic peptides

Peptide separation was performed on an Ultimate chromatography system (Dionex - LC Packings, USA) equipped with a Probot MALDI spotting device. 5 µl of the samples were injected by using a Famos autosampler (Dionex - LC Packings) and loaded directly onto a 75 µm x 150 mm reversed-phase column (PepMap 100, 3 µm; Dionex - LC Packings). Peptides were eluted at a flow rate of 300 nl/min by using the following gradient: 0-10 min, 0% solvent B; 10-105 min, 0-50% solvent B; and 105-115 min, 50-100% solvent B. Solvent A contained 0.1% TFA in 95:5 water/ACN , and solvent B contained 0.1% TFA in 20:80 water/ACN . For MALDI analysis, the column effluent was directly mixed with MALDI matrix (3 mg/ml α-cyano-4-hydroxycinnamic acid in 70 % (ACN /0.1 % TFA) at a flow rate of 1.1 µl/min via a µ-Tee fitting. The matrix solution also contained neurotensin at a concentration of 125 pmol/ml (Sigma,

USA) for internal calibration. Fractions were automatically deposited every 10 s onto a MALDI target plate (Applied Biosystems/MDS Sciex, USA) using a Probot microfraction collector. A total of 416 spots were collected from each HPLC run.

3.3.6. MALDI-TOFTOF mass spectrometry

MALDI plates were analyzed on a 4800 MALDI-TOFTOF system (Applied Biosystems) equipped with a Nd:YAG laser operating at 200 Hz. All mass spectra were acquired in positive reflector mode and generated by accumulating data from 800 laser shots. First, MS spectra were recorded from peptide standards, and the default calibration parameters were updated. Second, MS spectra were recorded for all sample spots on the MALDI target plate (416 spots per sample, 4 samples per plate). The MS spectra were recalibrated internally based on the ion signal of neurotensin peptide (Sigma, USA).

The following threshold criteria and settings were used for the acquisition of MS/MS spectra: Mass range: 800 to 4000 Da; minimum signal-to-noise (S/N) for MS/MS acquisition: 100; maximum number of peaks/spot: 8. Peptide CID was performed at a collision energy of 1 kV and a collision gas pressure of approximately 2.5×10^{-6} Torr. During MS/MS data acquisition, a method with a stop condition was used. In this method, a minimum of 1000 shots (20 sub-spectra accumulated from 50 laser shots each) and a maximum of 2000 shots (40 sub-spectra) were allowed for each spectrum. The accumulation of additional laser shots was halted whenever at least 6 ion signals with a S/N of at least 60 were present in the accumulated MS/MS spectrum, in the region above *m/z* 200.

3.3.7. LTQ-Orbitrap measurements

iTRAQ experiments were performed on a hybrid LTQ Orbitrap XL mass spectrometer (Thermo Scientific, Bremen, Germany) coupled to an Eksigent nano LC system (Eksigent Technologies, USA) and analyzed by reversed-phase liquid chromatography nanospray tandem mass spectrometry (nanoLC-MS/MS). Peptides were resuspended in 3% ACN and 0.2% formic acid, loaded from a cooled (10°C) Spark Holland autosampler (Emmen, Netherlands) and separated using an ACN/water solvent system containing 0.2% formic acid with a flow rate of 200 nl/min. Separation of the peptides was performed on a 10 cm long fused silica column (75 µm i.d.; BGB Analytik) in-house packed with 3 µm, 200 Å pore size C_{18} resin

(Michrom BioResources, USA). Elution was achieved using a gradient of 3−48% ACN in 50 min, 48−80% ACN in 3 min and 80% ACN for 7 min.

iTRAQ labeled peptides were analyzed by applying spectral merging of CID and HCD of two consecutive scans from the same precursor. One scan cycle was comprised of a survey full scan MS spectrum from m/z 300 to m/z 2000 acquired in the FT-Orbitrap with a resolution of R= 60‘000 at m/z 400, followed by up to six sequential data- dependent CID and HCD MS/MS scans. CID was done with a target value of 1e4 in the linear trap. Collision energy was set to 35%, Q value to 0.25 and activation time to 30 ms. HCD fragmentation ions including reporter ions were detected in the Orbitrap with a target value of 5e5, and a collision energy of 43%. For all experiments dynamic exclusion was used with one repeat count, 30s repeat duration and 90s exclusion duration. The instrument was calibrated externally according to the manufacturer's instructions. The samples were acquired using internal lock mass calibration on m/z 429.088735 and 445.120025.

3.3.8. Peptide and protein identification and quantification by database searching

Raw spectra were processed with Mascot Distiller 2.2 (Matrix Science, London, UK) and protein identification and quantitation was performed using Mascot Version 2.2.0 (Matrix Science) as the search engine. Mascot generic files were searched against a SwissProt human protein sequence database downloaded from ftp.ebi.ac.uk/pub/databases/SPproteomes (database release February 11, 2009; 117865 protein sequences (with 56722 forward and reverse sequences, respectively, and 259 contaminant sequences).

The following search settings were used for both methods: maximum missed cleavages: 2; maximum number of signals per spectrum: 55. For MALDI-TOFTOF MS the peptide mass tolerance was set to 25 ppm and fragment ion tolerance was 0.3 Da. In contrast, for LTQ-Orbitrap the peptide mass tolerance was 10 ppm and the fragment ion tolerance was set to 0.8 Da. iTRAQ4plex reagent labeling of lysine and of the N-terminal amino group of peptides and methylmethanthiosulfonate (MMTS)-labeled cysteine were specified as fixed modifications, oxidation on methionine as variable modification. For the quantitation of iTRAQ labeled peptides the isotopic correction factor was used as supplied by the manufacturer (Applied Biosystems). iTRAQ ratios of proteins were median normalized and protein ratios were determined as the geometric mean of the peptide ratios. False discovery rates (FDR) were

estimated by searches against a corresponding database containing forward and reversed sequences, according to the method of Kall [15]. Further analysis of proteomics data were performed using MATLAB 7.7.0. software (The MathWorks Inc., Bern, Switzerland).

3.3.9. Flow cytometric analysis

Human-blood derived monocytes were prepared from buffy coats of healthy blood donors (Swiss Red Cross, Schlieren, Switzerland), as described previously [16] and seeded into 12-well tissue culture dishes and stimulated with 2 mg/ml Hb-Hp. At day 7 of culture, cells were harvested by scraping and washed three times with PBS/0.1% BSA. Cells were stained with HLA-DR, CD14, CD86 and CD163 antibodies. Mouse IgG1 κ – APC (BD Pharmingen), Mouse IgG1 κ – PE (BD Pharmingen) and Mouse IgG1 κ – FITC (BD Pharmingen) were used for isotype controls. At least 10'000 events per sample were acquired by FACS*Canto* scan flow cytometer (BD Biosciences, San Jose, USA) using FACS Diva software. Raw data were analyzed using FlowJo 7.2.5. software (Tree Star, USA) and geometric mean fluorescence intensity was normalized to the corresponding isotype control.

3.3.10. Statistics

Proteomics data were analyzed as described above. Confirming and functional data are expressed as mean ± standard error of mean. Significance was calculated by *t*-test or one-way ANOVA. (Graphpad Prism version 4.0.).

3.4. Results and Discussion

We cultured human peripheral blood derived monocytes in Hb-Hp enriched (2 mg/ml) medium to mimic conditions that these cells might encounter within wounded tissues or within an atherosclerotic plaque hemorrhage. In all these conditions massive amounts of Hb can be released from extravasated red blood cells while Hp enters the site either as a plasma-derived protein or from local cellular secretion. In our experiments we used Hb-Hp complexes instead of free Hb to avoid uncontrolled oxidative side reactions that could eventually occur during prolonged cell culture. We performed a shotgun proteomic analysis with iTRAQ based relative quantification to comprehensively characterize the macrophage proteome as well as the more specific Hb-Hp induced changes in protein expression. By combining the benefits of the

commonly used MALDI-TOFTOF for iTRAQ experiments with parallel analyses on an LTQ-Orbitrap XL we could significantly improve the overall yield of identified peptides/proteins. Additionally, this set-up offered the unique possibility of a cross-platform validation of the biologically most relevant results.

3.4.1. Proteomic profiling of monocyte-derived macrophages

In a combined analysis of all the data generated by the two platforms we could identify and relatively quantify a total of 3692 proteins across all conditions and at the level of stringency detailed above. To our knowledge this is the most comprehensive proteome coverage of human monocytes or macrophages reported so far [17-19]. **Figure 2** illustrates the sub-cellular classification of the total detected macrophage proteome using PANTHER classification software *(*www.pantherdb.org/*).* The identified proteins were compared to a reference list (19911 *homo sapiens* genes) in order to statistically determine over-and under-representation of PANTHER classification categories **(Table 2)**. Among 3692 hits, a considerable fraction of 1449 proteins occurred in both, the MALDI-TOFTOF and Orbitrap lists. However, 1047 proteins were exclusively identified with the MALDI-TOFTOF instrument while LTQ-Orbitrap measurements resulted in additional 1593 exclusive protein observations. Earlier studies using 2D gel electrophoresis (2DE) with subsequent LC-MS/MS analysis could represent only a small fraction of the monocyte proteome mostly due to the limited resolution of complex proteomes in the gels [20]. A recent study of Zhang and co-workers [21] revealed 1651 macrophage proteins obtained from shotgun proteomics using iTRAQ with LC-MS/MS analysis. Still, we were able to identify and quantify about three times more proteins using iTRAQ labeling even without a time consuming sub-cellular pre-fractionation but, instead, by combining results from two complementary mass spectrometry technologies.

After isolation from peripheral blood the monocytes were exposed to purified and endotoxin-free Hb-Hp (2 mg/ml) for seven days. Peptides derived from the Hb-Hp exposed cells were labeled with iTRAQ reporter tags 115 and 117, whereas control monocytes were labeled with reporter tags 114 and 116 (see Materials and Methods). The raw MS/MS spectra files obtained by either MALDI-TOFTOF or Orbitrap mass spectrometry were processed by Mascot Distiller and quantitatively analyzed by Mascot searches against a human SwissProt database that contained

the forward and reversed sequences of the human proteome. Two master *XML-files* were generated – one for MALDI-TOFTOF and one for Orbitrap data – that contained the experimental data of all replicate measurements including forward and reverse sequence hits. As a first step to validate the protein identifications, we estimated the theoretical false discovery rate (FDR) as a function of relative Mascot protein ID scores according to the method of Kall [15] and fitted a FDR function cfun(x) = a*exp(b*x) + c*exp(d*x) to each dataset. Based on these calculations we applied a FDR threshold at 5% and only identifications above this cut-off were accepted for further analysis. The FDR for the MALDI-TOFTOF data was below 5% even at the lowest ID score **(Figure 3A)** while LTQ Orbitrap data contained 3039 protein identifications with a protein ID score above the threshold of 49 corresponding to a FDR of 5%. Additionally, we only accepted proteins with at least two unique peptide identifications. In summary, the restrictive protein identification thresholds applied to our data included *1)* at least two peptide identifications per protein *2)* total Mascot ion score > 99% for MALDI-TOFTOF data, and *3)* FDR < 5% for LTQ Orbitrap data.

3.4.2. iTRAQ based protein quantification reveals a distinct macrophage phenotype polarization induced by Hb-Hp exposure

Protein abundance ratios of all identified proteins were calculated based on extracted iTRAQ tag signal intensities. Since the linear range of MALDI-TOFTOF and LTQ-Orbitrap quantifications seems not identical and therefore the range of protein regulations differed in the two datasets, we transformed the protein ratios into $\log_{10}$-values and normalized them according to their median (m): normalized log(10) ratios (y) = (log(10)ratios/std(m)). Following normalization, we performed a *t* test on the $\log_{10}$(Hb-Hp-treatment/control) ratios against the mean value of the $\log_{10}$(control/control) ratios. In summary, proteomics analysis yielded a maximum of 12 treatment/control and 3 control/control ratios. A total of 835 proteins with a *p* value less than 0.005 were considered to be significantly affected by Hb-Hp treatment compared to control ratios. Among these, 99 proteins were commonly identified by both MALDI-TOFTOF and LTQ-Orbitrap. MALDI-TOFTOF measurements detected additional 365 significantly regulated proteins, and by applying a second threshold of > 1.5 fold change 68 proteins were significantly up- and 35 were down-regulated proteins **(Table 1)**. LTQ-Orbitrap analyses yielded 582 additional regulated proteins with 68 significantly up- and 86 down-regulated proteins **(Table 1)**. The correlation

coefficient of the regulated proteins (*p*-value < 0.005) that were identified and quantified by both platforms was 0.94 (99 data points) **(Figure 4D)**.

To obtain more information on the sub-cellular location of proteins represented in our macrophage proteome in relation to the general functional gene ontology (GO) classifications, we generated an enrichment analysis against a GO annotated database, PANTHER classification system. We found significant enrichment of proteins located intracellular (p=6.23E-29) and associated to MHC complexes (p=8.55E-09). Other predominant clusters were associated with cytoskeleton (p=1.13E-18) and cytoplasm localization (p=2.13E-10). In contrast, we found an under-representation of proteins located extracellular (p=5.36E-04) and in the nucleus (5.60E-01) **(see Table 2)**.

In a next step we aimed to determine the functional proteome polarization induced by Hb-Hp by testing the list of either up- or down-regulated proteins against the list of all identified proteins (e.g. the macrophage proteome).

3.4.3. Hb-Hp exposure promotes a macrophage phenotype with high Hb-heme degradation and anti-oxidant capacity

We analyzed the normalized and significantly up-regulated proteins (p < 0.005 and fold change > 1.5) identified with MALDI-TOFTOF and/or LTQ-Orbitrap MS using the PANTHER Classification System. The list of all identified proteins served as a reference list (masterlist). From the 104 up-loaded proteins, 46 were recognized and found to be significantly over-represented (p < 0.005) in categories such as blood circulation (p=1.22E-08), immune system processes (p=1.74E-04), cell adhesion (p=6.81E-04), response mechanisms to stimuli (p=7.38E-04, p=8.28E-04, respectively) and in blood coagulation (p=7.38E-04), represented by the proteins plasminogen activator inhibitor 2 (PAI-2) and fibrinogen. **Table 3** shows the particular biological processes with the number of expected proteins from the list of up-regulated proteins compared to the masterlist.

To our surprise, we found that the down-regulated proteins upon Hb-Hp treatment were mainly related to reduced antigen processing and presentation via human leukocyte antigen (HLA) class 2 (p=6.32E-12) **(see Table 4)**.

Figure 6 highlights the 50 top ranked up-regulated proteins identified with MALDI-TOFTOF and/or LTQ-Orbitrap including HO1, ferritin, fibrinogen α and PAI-2. Additionally, enzymes with anti-oxidative properties to maintain the cellular

homeostasis like thioredoxin reductase 1 (TXNRD1), superoxide dismutase 1 (SOD) and vitamin D binding protein, which contributes to the anti-oxidative potency of vitamin D [22], were found among the top 50 up-regulated proteins in a concerted manner. Furthermore, Hp and several subunits of the Hb molecule appeared to be strongly induced since these compounds had been added to the system as stimulus before. Glutamine synthetase, a key enzyme for the assimilation of ammonium to amino acids bearing anti-oxidative properties, was also among the up-regulated proteins. Additionally, we found NAD(P)H:quinone oxidoreductase, (NQO1) which we previously described as a major cellular defense gene (submitted manuscript), to be up-regulated. In summary, the composition of the significantly up-regulated proteins upon Hb-Hp treatment is characterized by an adaptive response to wounding (CD163; PAI-2; fibrinogen) with subsequent cell-protective and anti-oxidative (HO-1; SOD; TXNRD1) mechanisms to recover the cellular (iron) homeostasis.

Monocytes can differentiate into classically activated inflammatory macrophages (M1) that have a high capacity to secrete inflammatory cytokines and kill invading pathogens [23-24]. At the other end of the continuous macrophage differentiation spectrum an “alternatively” activated macrophage phenotype (M2) has been characterized that is involved in down-regulation of inflammatory processes and wound healing [25]. Yet another monocyte differentiation path leads to the generation of myeloid dendritic cells that are characterized by high-level expression of HLA class 2 and potent antigen presenting function [26]. The polarization of the different macrophage phenotypes is primarily determined by environmental factors. For example, T-cell derived IFN-γ is the principle classic macrophage activator leading to M1 polarization. A more heterogeneous group of mediators that is considered to have mainly anti-inflammatory properties such as IL-4 or glucocorticoids skew macrophage differentiation towards M2 polarization. So far, the Hb-Hp up-regulated protein clusters found in our study are compatible with a more “alternatively” activated macrophage phenotype with high Hb clearance and anti-oxidant capacity that might provide an active role in wound healing. A wounded tissue environment can be considered to be Hb rich and pro-oxidant. Therefore, the principle phenotype of the Hb-Hp induced macrophage described here seems to be biologically meaningful. Also, we found no evidence of inflammatory gene expression that would be compatible with M1 polarization.

3.4.4. Hb-Hp polarized macrophages are characterized by profoundly suppressed HLA–class 2 proteins

PANTHER classification of the down-regulated proteins displayed a highly significant enrichment of negatively regulated proteins associated with antigen processing and presentation by HLA class 2 proteins (p=6.32E-12) **(Table 4)**. Down-regulation of the human leukocyte class 2 isotypes (HLA-DR, HLA-DQ, and HLA-DP) is shown in **Figure 7**. 19 out of 28 HLA class 2 protein identifications detected with MALDI-TOFTOF MS were significantly decreased ($p < 0.005$), none was found to be increased. Even a higher number of significantly down-regulated HLA class 2 proteins could be found in the LTQ Orbitrap derived data (46 downregulated out of 49 total identified; **Figure 9B**). We chose HLA-DRB1 (*accession* # P20039) and HLA-DPB1 (*accession* # Q5SQ73) to further analyze the abundance ratios of their individual constituting peptides across duplicate control and treatment experiments performed with three independent donor monocytes. **Figure 8A** and **B** show the $\log_{10}$ ratios of the peptides matching to HLA-DRB1 or HLA-DPB1 that were found in all three and two donors, respectively. The overall pattern of peptide ratios across all cell culture conditions, biologic replicates and individual donors clearly visualizes the down regulation of the “mother” protein. In contrast to HLA class 2, only one out of the four identified HLA class 1 proteins was found to be significantly suppressed.

3.4.5. Transcriptional down-regulation contributes to HLA class 2 suppression by Hb-Hp

HLA class 2 expression is determined by transcriptional as well as by post-transcriptional/post-translational mechanisms. Posttranslational processes affect cell surface expression, sub-cellular trafficking and lysosomal degradation and represent an important determinant of overall protein abundance. In contrast, the Class II transactivator CIITA controls expression of HLA class 2 at the genetic level and the expression of several genes encoding accessory proteins required for MHCII restricted antigen-presentation, namely the invariant chain (Ii), HLA-DM and HLA-DO [27-28]. CIITA transcription can be selectively activated by IFN-γ, LPS, and IL-4, and is downregulated by IL-10, nitric oxide, and TGF-β [29-30]. By binding to the MHCII enhanceosome the transcription of HLA-class II genes is activated [31].

We have therefore specifically analyzed HLA class 2 mRNA abundance and its regulation by Hb-Hp in an independent dataset of gene array experiments. These

data were derived from a comprehensive gene array experiments of macrophages cultured under control as well as high Hb-Hp conditions that were identical to the conditions of our proteome experiments. The major difference in the experimental set-up of these studies was that the mRNA expression was not examined at day 7 of cell culture but at days 2 and 5, accounting for the different dynamics of the synthesis, degradation and steady-state levels of mRNA and proteins, respectively. The gene array data are available at www.ebi.ac.uk/aerep/login (reviewer account login: Reviewer_E-MEXP-2820, Password: 1279719286410).

Figure 9 shows a summary of mRNA expression levels of HLA class 1 and 2 (in relation to control levels in untreated cells) at days 2 and 5. While the $\log_{10}$ of the treatment-to-control ratio of HLA class 1 expression did not differ from 0 at either time point we found a statistically significant ($p < 0.005$) HLA class 2 mRNA suppression by Hb-Hp treatment. However, although these data suggest a minor, though sustained, transcriptional suppression of HLA class 2 mRNA, the very pronounced decrease in HLA class 2 protein levels **(Figure 9B)** are more likely the result of combined transcriptional/post-translational mechanisms. It might, for example, being speculated that the highly enhanced Hb-Hp endocytosis and breakdown might impact subcellular trafficking and degradation pathways shared between the two proteins.

3.4.6. Immunophenotyping and cell viability assessment support macrophage proteome polarization towards high Hb clearance, increased anti-oxidative capacity and low HLA class 2 expression

To confirm the Hb-Hp induced CD163^{high}/HLA class 2^{low} macrophage phenotype implicated by our proteome analysis we quantified by flow-cytometry the cell surface expression of CD163 and HLA-DR along with the macrophage differentiation marker CD14 and the co-stimulatory molecule CD86. After seven days of differentiation in the presence of Hb-Hp the PBMC derived macrophages displayed a significantly suppressed cell-surface HLA-DR expression while CD163 and CD14 were consistently enhanced in all experiments **(Figure 10)**. Interestingly, cell surface expression of the co-stimulatory molecule CD86 which was not captured in our mass spectrometry exploration was also significantly lower in the Hb-Hp polarized cells. CD86 is essential for efficient antigen presentation [32-33] and along with the profound down-regulation of HLA class 2 the data suggest that Hb-Hp polarized macrophages

might have a reduced capacity to presenting antigens and stimulating specific immune responses. Although speculative, it might be suspected that while the Hb-Hp polarized macrophages support clearance of extracellular Hb, anti-oxidant protection as well as essential wound healing processes, the same cells were tailored to avoid accidental stimulation of immune responses that could potentially target auto-antigens released in injured tissue environments.

Since extracellular Hb can be a potential source of heme derived toxic radicals that could impede macrophage cell survival in our experiments it was essential to prove that the enhanced anti-oxidative protein cluster expression was also functionally reflected by an enhanced viability of Hb-Hp polarized cells compared to control macrophages **(Figure 11B)**.

The findings of our proteome analysis are in agreement with a recent study by Boyle and co-workers [34] that reproduced a potentially atheroprotective macrophage phenotype with high CD163 and low HLA class 2 expression ($CD163^{high}$/HLA class 2^{low}) by culturing peripheral blood monocytes in the presence of Hb-Hp. These $CD163^{high}$/HLA class 2^{low} macrophages were consistently found in atherosclerotic coronary arteries with a particularly high density within areas of intraplaque hemorrhage. Functionally, these macrophages cleared Hb more quickly with less oxidative cell damage and increased cell survival. Therefore, the Hb-Hp driven macrophage polarization described here likely represents a specialized macrophage phenotype with a distinct *in vivo* function in wound healing and atherosclerosis.

3.4.7. Conclusion

Specialized macrophages have a critical role in controlling inflammatory responses induced by any form of tissue damage and at the same time in supporting wound healing. Macrophages are also the cell type that is uniquely capable to remove and detoxify extracellular hemoglobin through the CD163 Hb scavenger receptor pathway. So far, little knowledge was available how this Hb clearance function of macrophages could by itself impact the differentiation of these cells. In a comprehensive proteome exploration – which represents the so far most complete coverage of the macrophage proteome – we found that Hb-Hp exposure polarizes the macrophage phenotype towards increased expression of proteins associated with Hb/heme clearance and anti-oxidative functions. These changes were reflected by an increased viability of macrophages cultured in high Hb-Hp conditions. On the other

hand, Hb-Hp exposure profoundly suppressed HLA class 2 protein expression, putatively via inference with transcriptional as well as post-translational regulatory processes. It is therefore conceivable that the Hb-Hp induced CD163^{high}/HLA class 2^{low} macrophage represents a specialized phenotype tailored to supporting Hb clearance, anti-oxidant protection and wound healing while avoiding presentation of released auto-antigens to the immune system.

Table 1 - *Comparison of the number of proteins identified with MALDI-TOFTOF and LTQ-Orbitrap mass spectrometry*

	Number of proteins			
Dataset	**Total** [a]	**p < 0.005**[b]	**up-regulated (p < 0.005, fold change >1.5)**	**down-regulated (p < 0.005, fold change > 1.5)**
MALDI + Orbitrap*	1370 (37%)	99 (3%)	17	11
MALDI	2203 (60%)	365 (10%)	68	35
Orbitrap	2858 (77%)	582 (16%)	68	86
All identified proteins	3691 (100%)	848 (23%)	104	102

[a] *Protein hits with at least two unique protein identifications and a FDR <5%.* [b] *p < 0.005 indicates significant difference in expression ratio upon Hb-Hp treatment. * Proteins identified in both MALDI-TOFTOF and LTQ-Orbitrap datasets.*

Table 2 - *PANTHER GO compartment classification*

		No. of proteins classfied from masterlist			
Cellular Component	**Homo sapiens genes - (19911)**	**observed**	**expected**	**over/under-represented**	**P - value**
Unclassified	17808	2089	1886.25	+	1.98E-73
intracellular	1192	264	126.26	+	6.23E-29
protein complex	197	82	20.87	+	1.56E-24
cytoskeleton	1003	205	106.24	+	1.13E-18
actin cytoskeleton	415	109	43.96	+	4.11E-17
ribonucleoprotein complex	164	52	17.37	+	1.17E-11
vesicle coat	42	24	4.45	+	7.57E-11
heterotrimeric G-protein complex	43	24	4.55	+	1.21E-10
cytoplasm	146	46	15.46	+	2.13E-10
tubulin complex	25	18	2.65	+	4.99E-10
MHC protein complex	58	25	6.14	+	8.55E-09
proton-transporting ATP synthase complex	20	13	2.12	+	3.83E-07
microtubule	348	61	36.86	+	1.46E-04
extracellular region	505	31	53.49	-	5.36E-04
extracellular matrix	501	31	53.07	-	6.49E-04
cell junction	121	4	12.82	-	4.19E-03
SNARE complex	38	10	4.03	+	8.40E-03
organelle	94	18	9.96	+	1.35E-02
mitochondrion	91	17	9.64	+	1.98E-02
tight junction	34	0	3.6	-	2.72E-02
plasma membrane	131	7	13.88	-	3.34E-02
intermediate filament cytoskeleton	130	21	13.77	+	4.11E-02
gap junction	21	0	2.22	-	1.08E-01
endoplasmic reticulum	2	1	0.21	+	1.91E-01
immunoglobulin complex	32	4	3.39	+	4.39E-01
cytosol	6	1	0.64	+	4.70E-01
nucleus	23	2	2.44	-	5.60E-01
chromosome	1	0	0.11	-	8.99E-01
extracellular space	1	0	0.11	-	8.99E-01
nuclear chromosome	1	0	0.11	-	8.99E-01
nucleolus	1	0	0.11	-	8.99E-01

Table 3 - *Gene Ontology analysis of up-regulated proteins upon Hb-Hp exposure using PANTHER classification system.*

		No. of proteins up-regulated in masterlist			
Biological Process	**masterlist REFLIST (2109)**	**observed**	**expected**	**overrepresented**	**P - value**
Blood circulation	23	9	0.62	+	1.22E-08
Immune system response	348	21	9.41	+	1.74E-04
Cell adhesion	131	11	3.54	+	6.81E-04
Response to external stimulus	40	6	1.08	+	7.38E-04
Blood coagulation	40	6	1.08	+	7.38E-04
Response to stimulus	253	16	6.84	+	8.28E-04
System process	245	15	6.62	+	1.75E-03
Defense response to bacterium	10	3	0.27	+	2.58E-03

Table 4 - *Gene Ontology analysis of down-regulated proteins upon Hb-Hp exposure using PANTHER Classification system.*

		No. of proteins down-regulated in masterlist			
Biological Process	**masterlist REFLIST (2109)**	**observed**	**expected**	**overrepresented**	**P - value**
antigen processing and presentation of peptide or polysaccharide antigen via MHC class II	18	10	0.39	+	6.32E-12
antigen processing and presentation	30	11	0.65	+	4.07E-11
cellular defense response	65	13	1.42	+	8.86E-10
response to stimulus	253	16	5.52	+	5.15E-05
immune system process	348	19	7.59	+	5.85E-05

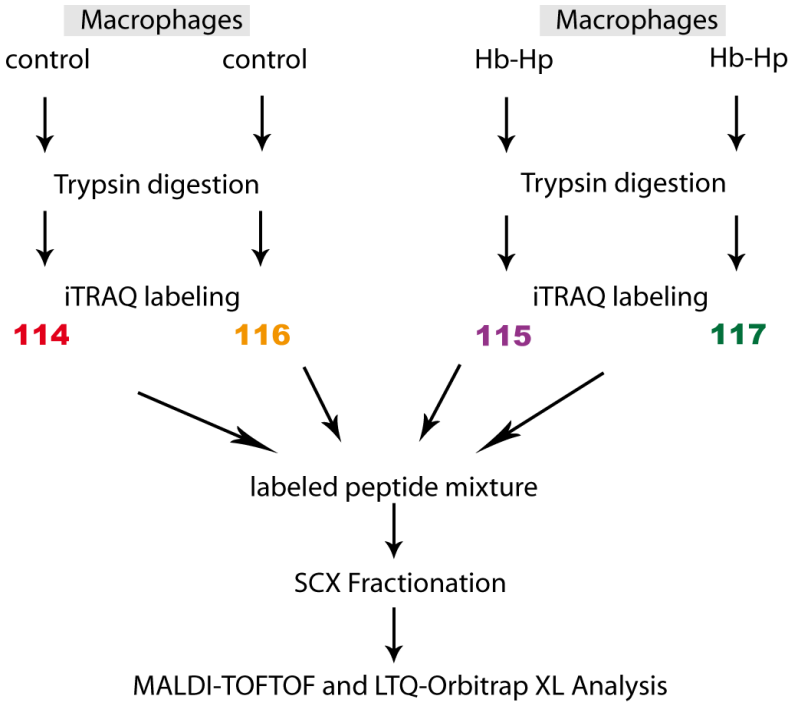

Figure 1 – Experimental setup for the proteome analysis to monitor the effect of macrophages exposed to Hb-Hp. *Human peripheral blood monocytes were incubated for 7 days with purified Hb-Hp (1:1 molar ratio) complexes (2 mg/ml). At day 7 cells were lysed, the nuclei removed by centrifugation and the remaining cellular proteome was digested with trypsin. Following that, control cells were labelled with iTRAQ 114 resp. iTRAQ 116, Hb-Hp treated cells were labeled with iTRAQ 115 resp. iTRAQ 117. Labeled peptides were combined and fractionated by SCX-chromatographie with subsequent MALDI-TOFTOF and LTQ-Orbitrap analysis. Three independent experiments were performed.*

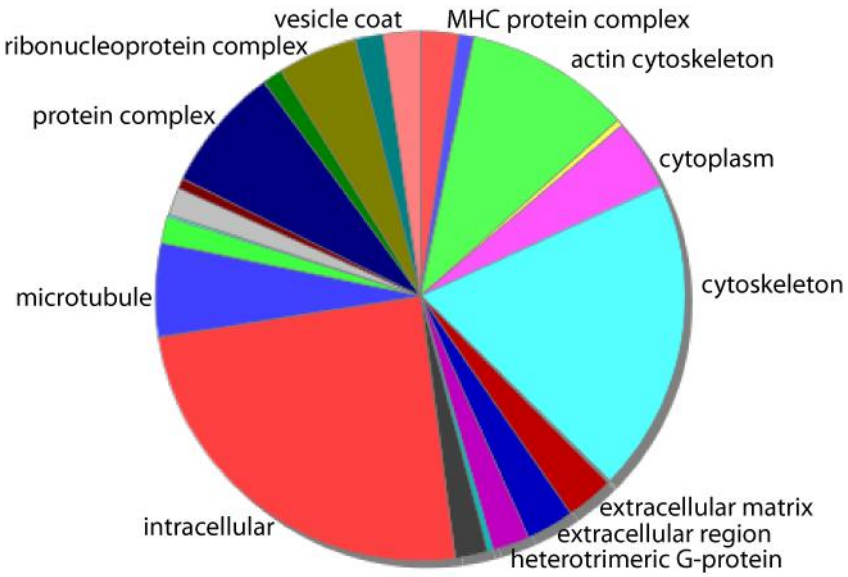

Figure 2 – PANTHER gene ontology compartment classification of the identified macrophage proteome vs the whole human genome. *2109 protein ID's (identifier: gene symbol) were classified according to their compartment localization. The complete list of cellular component classification is shown in* ***Table 2****.*

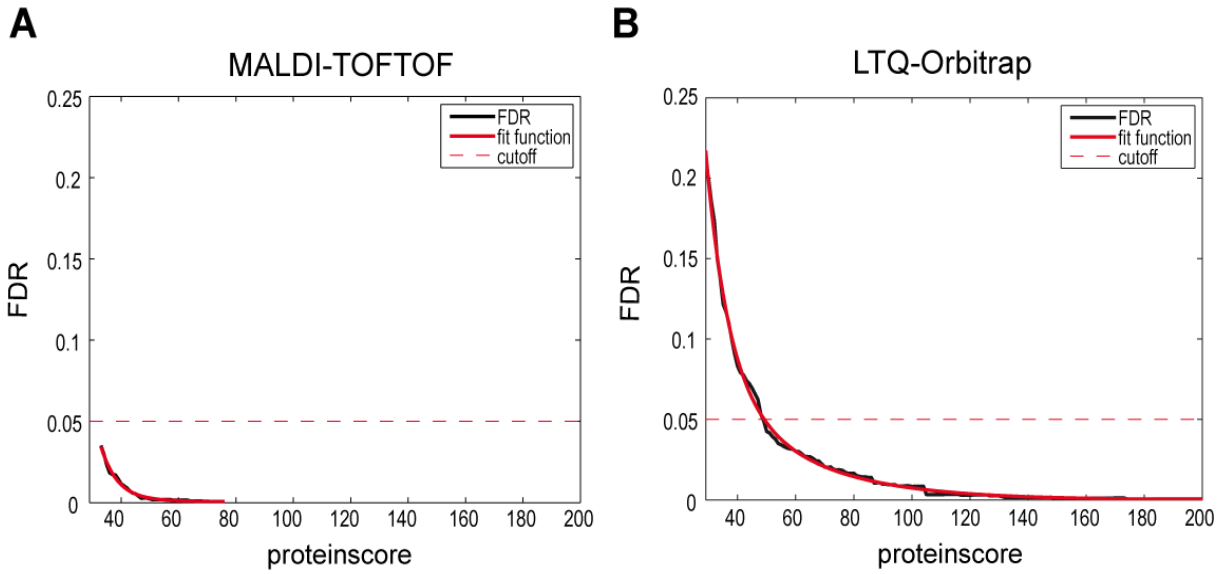

Figure 3 - Theoretical estimated false discovery rate (FDR) is mapped to the protein score (x-axis) of all identified proteins by (A) MALDI-TOFTOF and (B) LTQ-Orbitrap. *The function cfun(x) = a*exp(b*x) + c*exp(d*x) (red line) was fitted to the data curve by MATLAB. The red dotted line indicates the FDR threshold at 5%. All identifications with a FDR < 5% were accepted (minimum two unique peptides).*

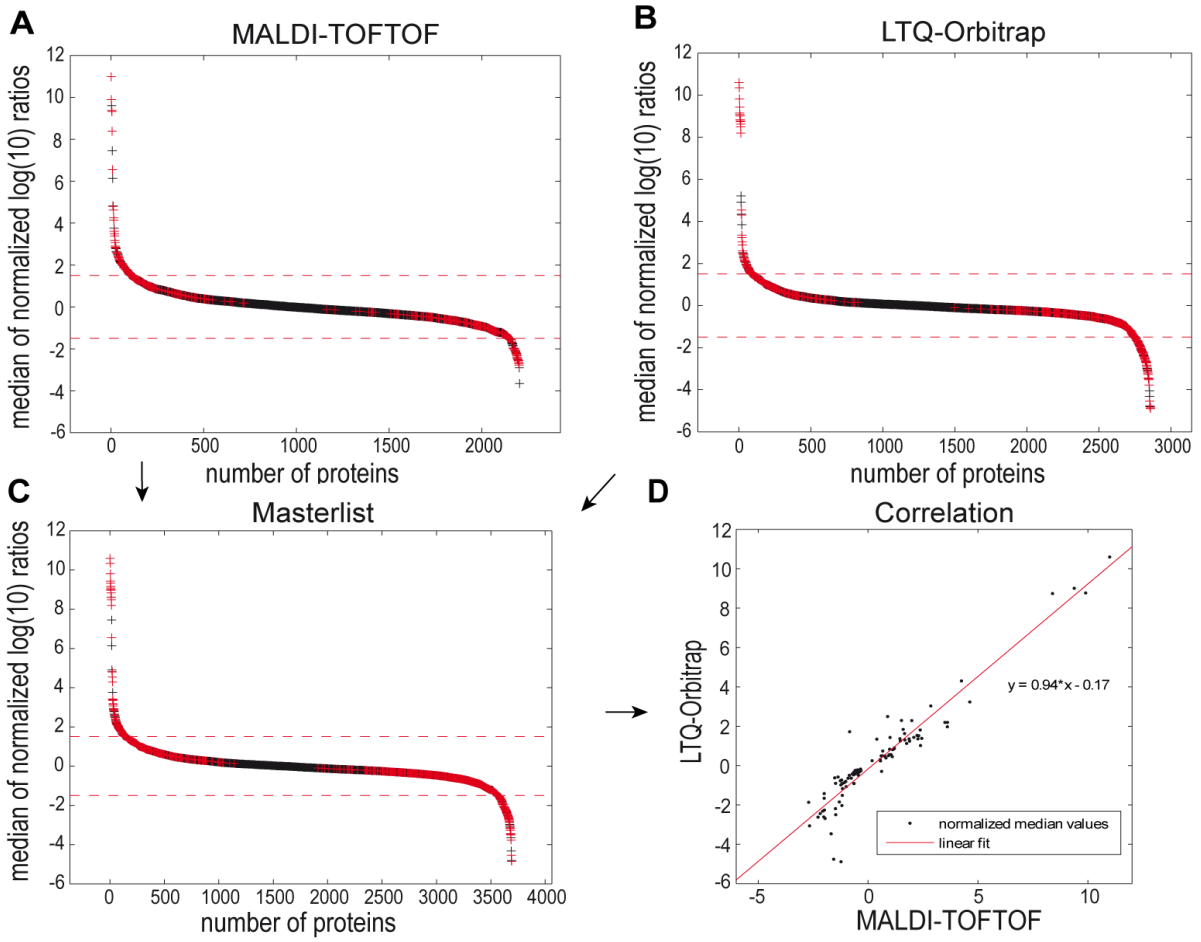

Figure 4 - Global view at pooled proteins from 3 healthy donors *identified by either* ***(A)*** *MALDI-TOFTOF MS (n=2203) or* ***(B)*** *LTQ-Orbitrap MS (n=2858) sorted by their medians. Total identified proteins from both platforms were shown in* ***(C)****. Red crosses indicate significant up- or down-regulated proteins by Hb-Hp (2 mg/ml) treatment (p < 0.005), black crosses indicate unchanged proteins. Red dotted line illustrates the 1.5-fold Standard deviation threshold.* ***(D)*** *illustrates the correlation of significant regulated (p < 0.005) proteins (n=99) identified in both MALDI-TOF and LTQ Orbitrap. The normalized median values for each protein and the linear fit are shown. Only proteins with a FDR < 5% are included.*

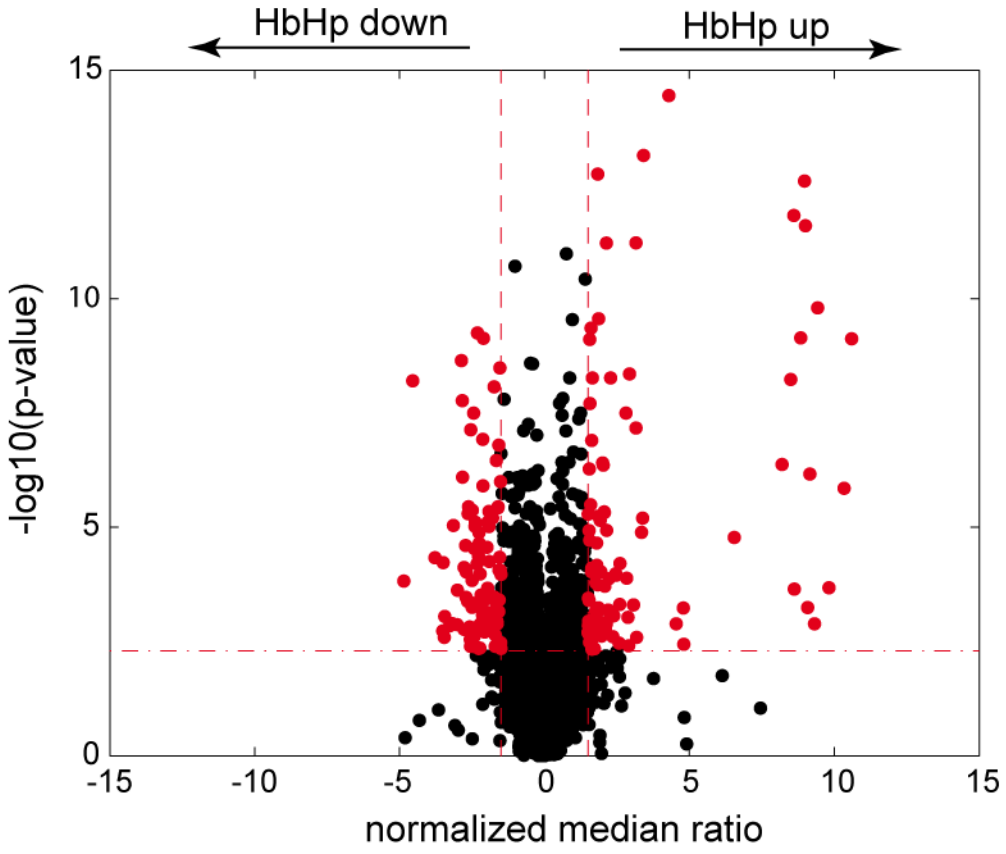

Figure 5 – Volcano-plot of all identified proteins (n=3692). *Red dots (n=205) indicate proteins that met our criteria of displaying > 1.5-fold changes (bordered by dashed line) with p < 0.005 (bordered by dash-dot line). These proteins were further selected for PANTHER classification analyses.*

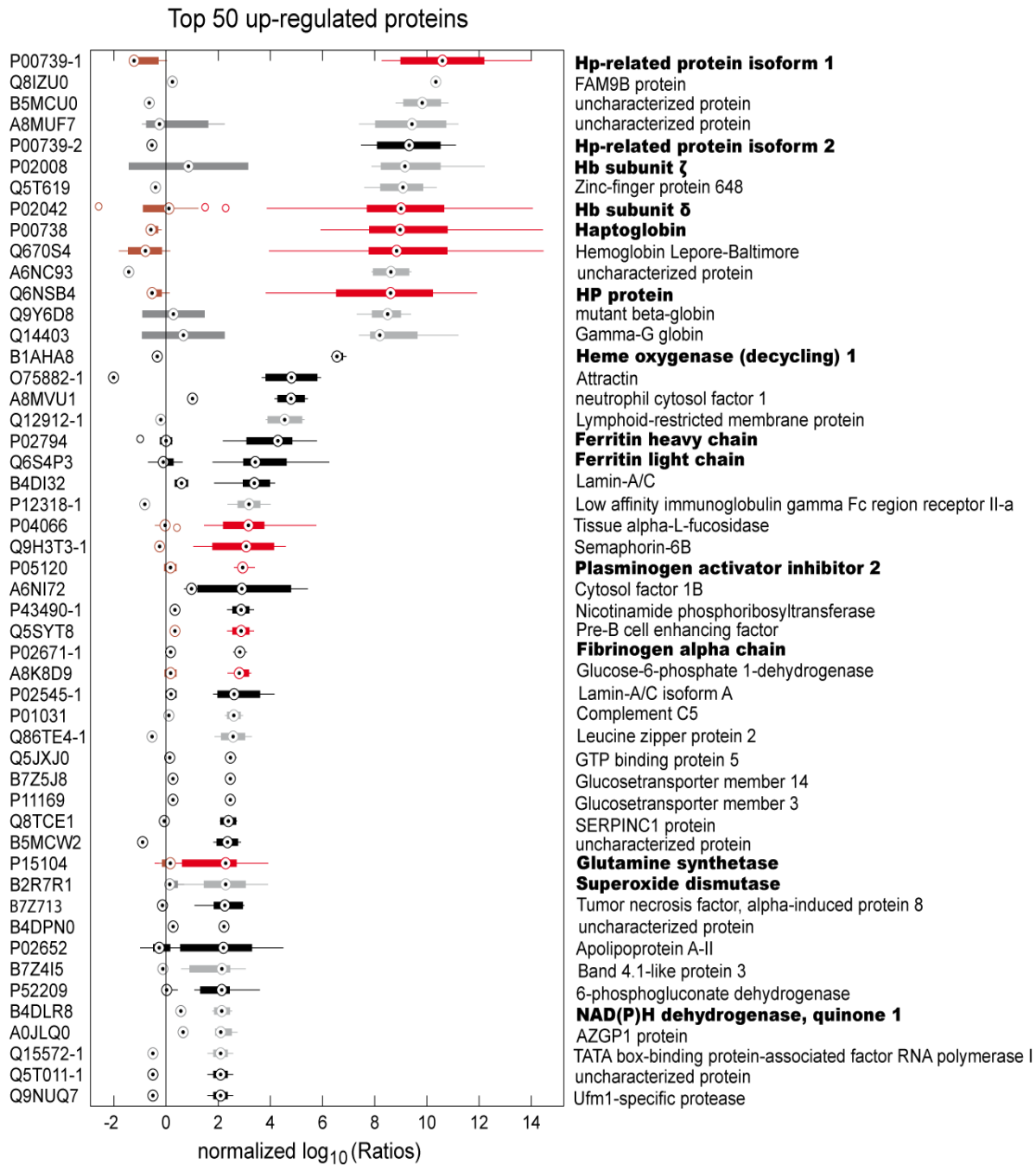

Figure 6 - Top 50 up-regulated proteins identified by MS measurements (p < 0.005). *Right boxes represent Hb-Hp vs control normalized log(10) ratios of identified proteins with both techniques (red), only with MALDI-TOFTOF MS (black), or only with LTQ-Orbitrap MS (grey). Left boxes indicate control vs control normalized log(10) ratios of each identified protein. The interquartile range (25-75%), whiskers and median are shown for each protein. Protein names are indicated on the right y-axis; bold text highlights proteins characteristic in Hb polarized macrophages; accession numbers are shown on the left y-axis.*

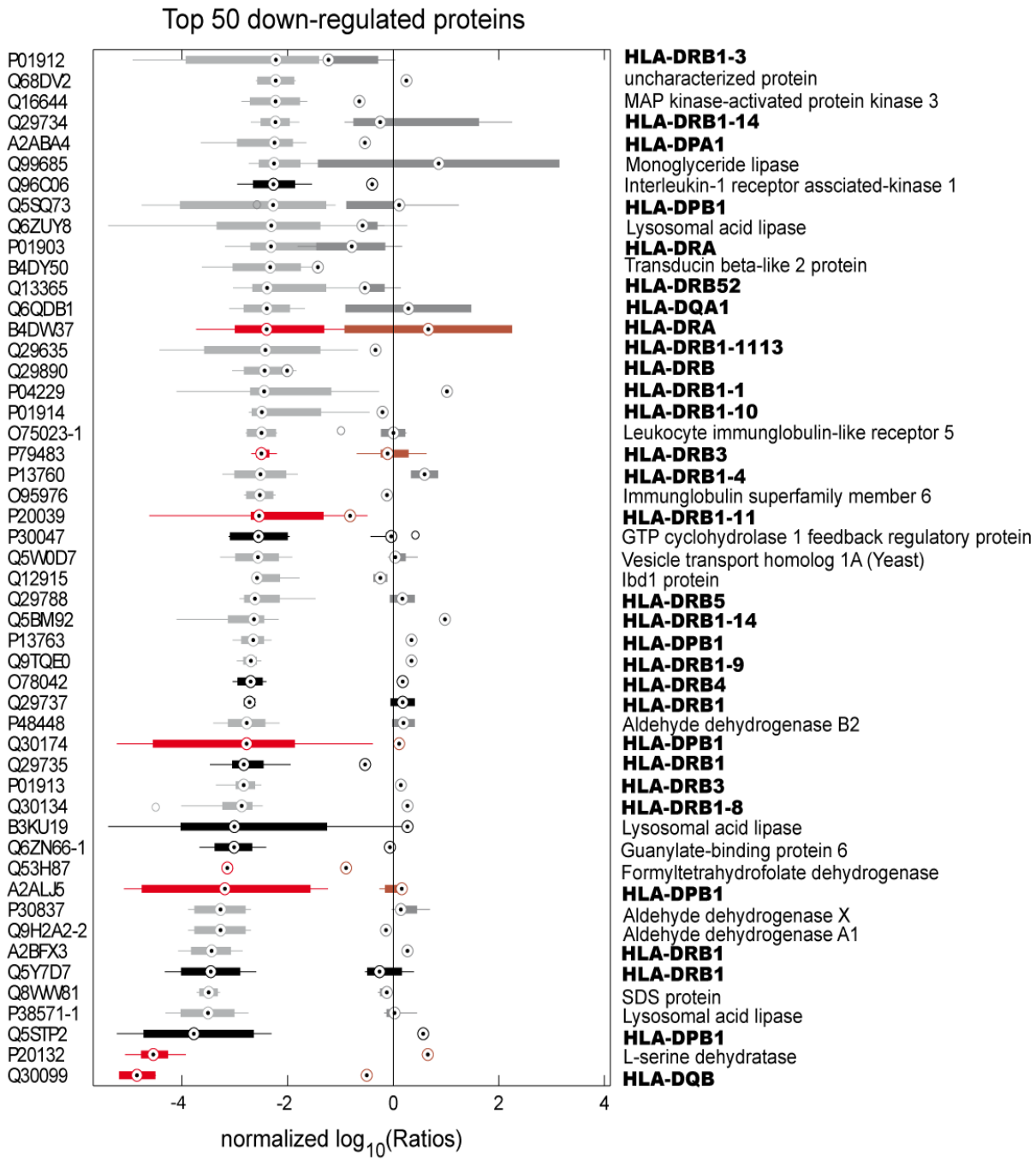

Figure 7 - Top 50 down-regulated proteins identified by MS measurements (p < 0.005). *Left boxes represent Hb-Hp vs control normalized log(10) of identified proteins with both techniques (red), only with MALDI-TOFTOF MS (black), or only with LTQ-Orbitrap MS (grey). Right boxes indicate control vs control normalized log(10) ratios of each identified protein. The interquartile range (25-75%), whisker and median is shown for each protein. Protein names are indicated on the right y-axis, bold text highlights HLA class 2 proteins, accession numbers are shown on the left y-axis. Note the dominant and highly polymorphic HLA-DR molecules.*

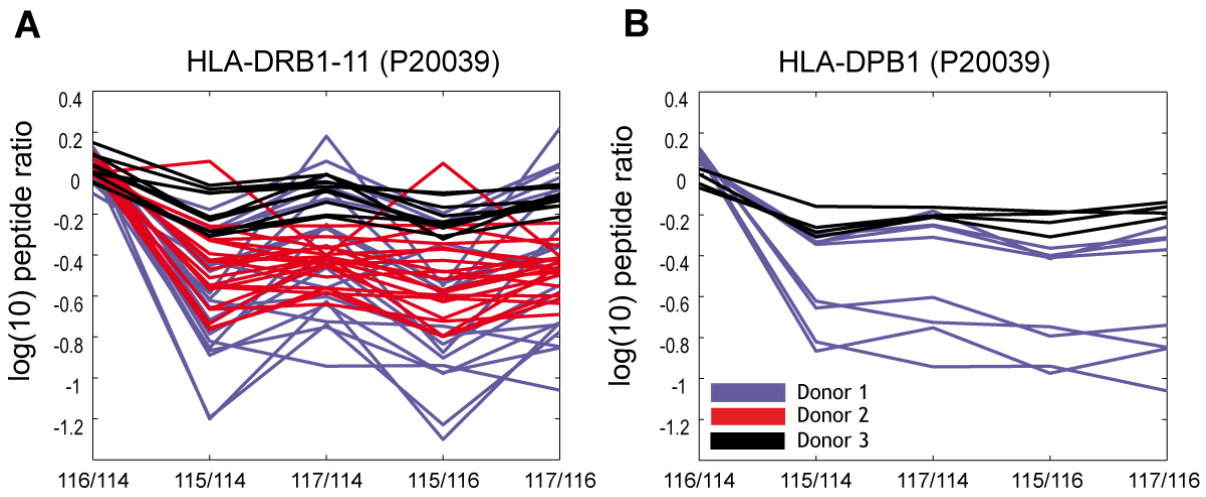

Figure 8 – Individual log (10) ratios of peptides identifying protein HLA-DRB1 (accession # P20039) or HLA-DPB1 (accession # Q5SQ73). *116/114 is indicating the control vs control ratio while 115/114, 117/114, 115/116 and 117/116 represent Hb-Hp vs control ratios. Blue lines refer to peptides identified in macrophages of Donor 1, red lines refer to peptides of Donor 2 macrophages and black lines refer to the ones of Donor 3.*

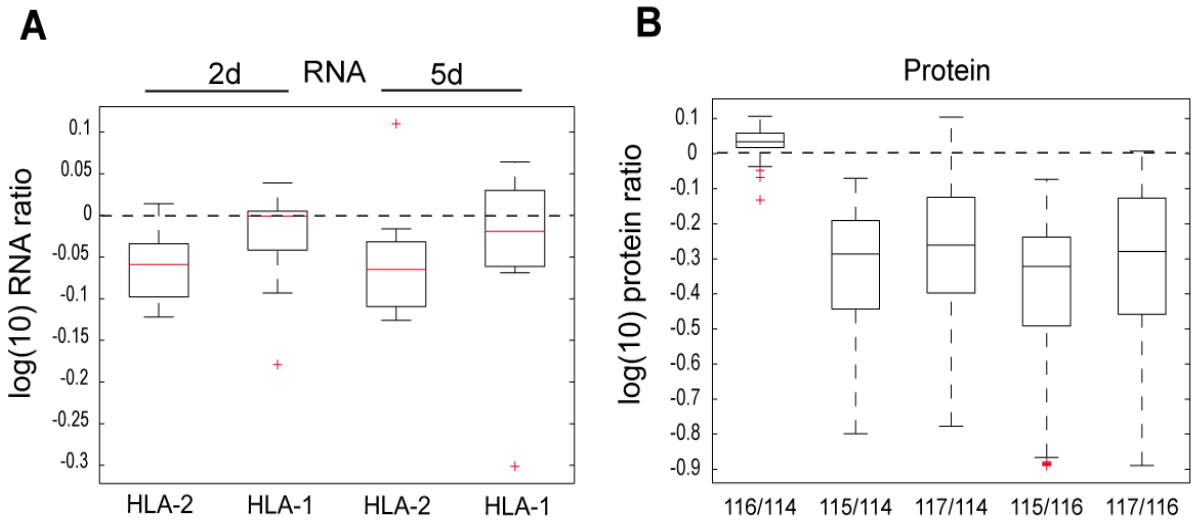

Figure 9 – HLA class 1 and 2 mRNA ratios and significantly (p < 0.005) down-regulated HLA class 2 proteins. *Boxplots for each mRNA or protein ratio including median (red line) and outliers (red crosses) are shown. RNA ratios of HLA class 2 and HLA class 1 genes extracted at days 2 and 5 of incubation with Hb-Hp (2 mg/ml) are shown in* ***(A)****. All quantified HLA-II proteins after 7 days of incubation with Hb-Hp (2 mg/ml) are illustrated in* ***(B)****. 116/114 indicate the control vs control ratio, while 115/114, 117/114, 115/116 and 117/116 refer to Hb-Hp vs control ratios (x-axis). Transcriptomic and proteomic data derive from three independent gene array and three iTRAQ experiments.*

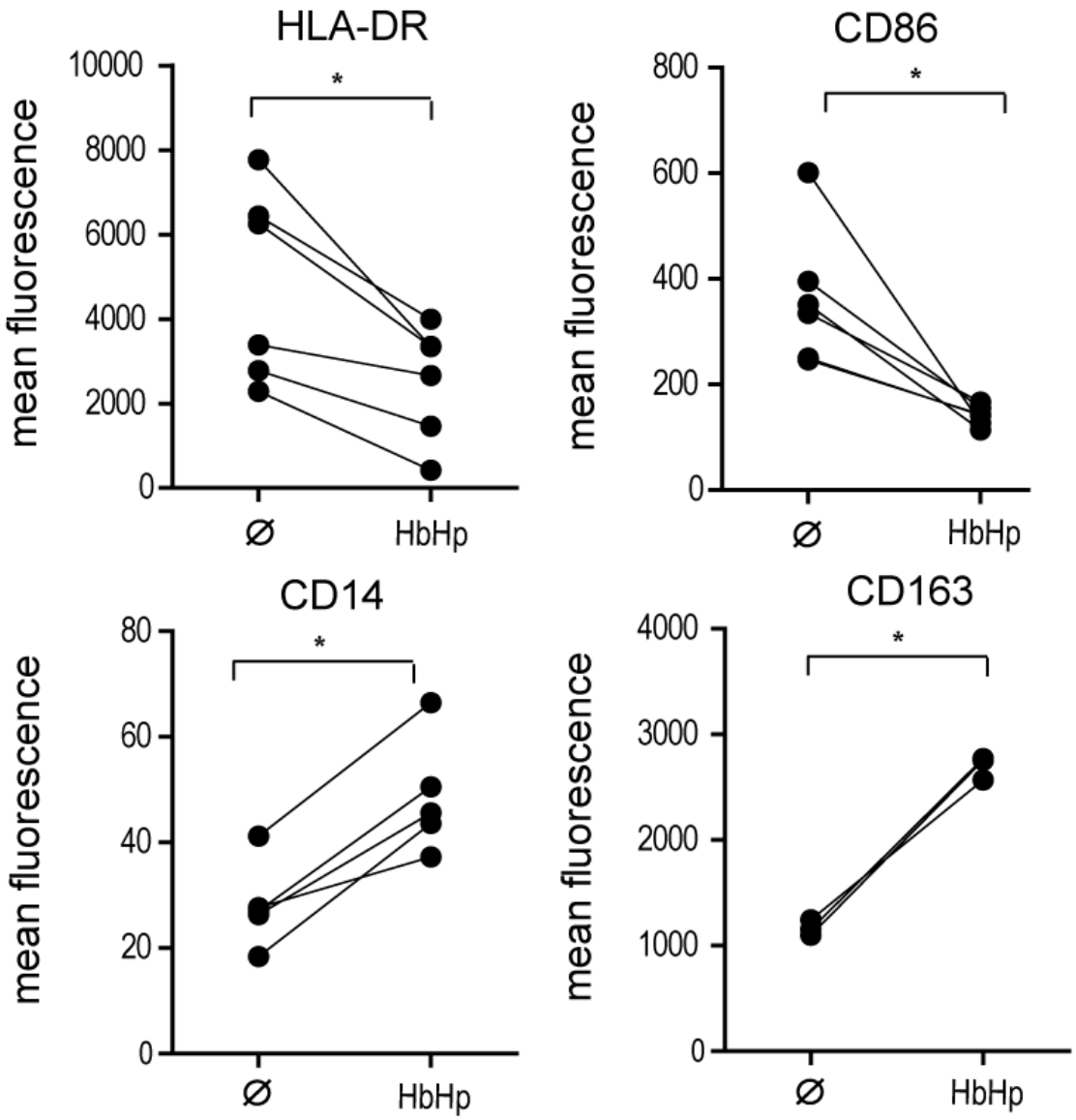

Figure 10 - Flow cytometric analyses of HLA-DR, CD86, CD14 and CD163 expression *of human PBMC derived monocytes from buffy coats incubated with Hb-Hp (2 mg/ml) or untreated for 7 days. Data represent mean fluorescence intensity normalized to an isotype control for at least three independent experiments. The raw FACS data are given in the supplement* ***(Figure S1 – S3)*** *of this chapter * $p < 0.05$*

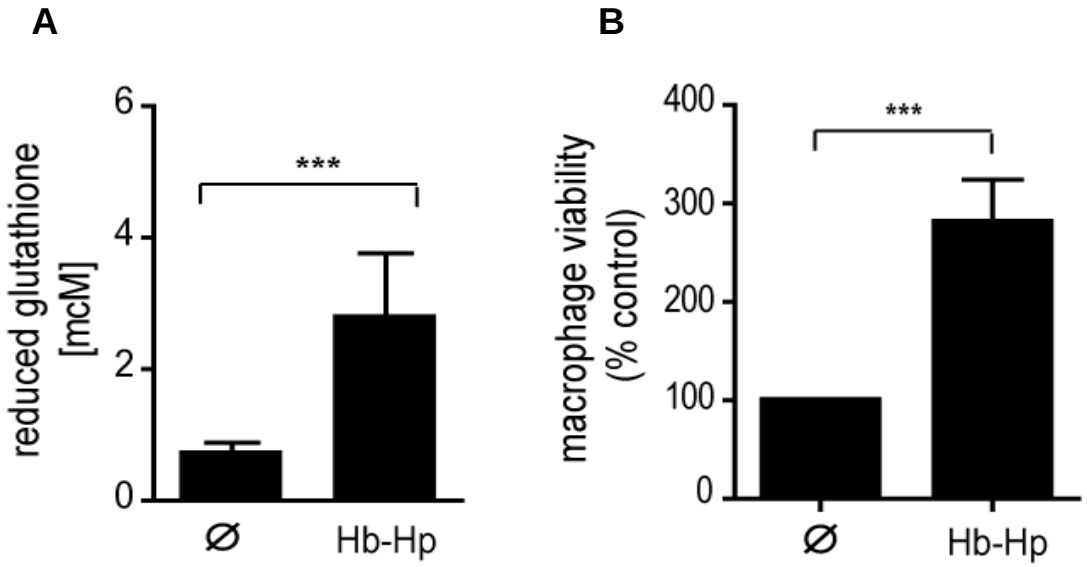

Figure 11 - Anti-oxidant and anti-inflammatory response of monocytes towards Hb-Hp exposure. (A) *Intracellular reduced glutathione (GSH) of PBMC derived monocytes was measured after 5 days of incubation with highly purified Hb-Hp (2 mg/ml). GSH was quantified by applying a GSH standard curve.* ***(B)*** *Viability was measured relative to control cultures (100%) at day 7 after start of culture and incubation with Hb-Hp (2 mg/ml). Values represent means ± SEM of at least three independent experiments. *** p < 0.0005*

3.5. Supplement

Table 1A: TOP 50 down-regulated proteins (1-25) from masterlist after 7 days of Hb-Hp exposure

ACCESSION	NAME	GENE SYMBOL	MEDIAN LOG RATIOS norm	MEDIAN LOG CONTROL RATIOS norm	PVALUE
P00739-1	Lymphocyte antigen OS	HLA-DQ-beta	-4.852775826	0.622730733	0.000150848
Q8IZU0	L-serine dehydratase OS	SDS	-4.543543038	0.150995779	6.23016E-09
B5MCU0	Major histocompatibility complex, class II, DP beta 1 OS	HLA-DPB1	-3.776452937	0.404566887	4.64203E-05
A8MUF7	Isoform 1 of Lysosomal acid lipase/cholesteryl ester hydrolase OS	LIPA	-3.507340763	0.520598812	0.001841509
P00739-2	SDS protein OS		-3.494711545	-0.370540913	5.90555E-05
P02008	MHC class II antigen OS	HLA-DRB1	-3.454613088	0.539286424	0.002556637
Q5T619	Major histocompatibility complex, class II, DR beta 1 (Fragment) OS	HLA-DRB1	-3.440829234	0.429376986	0.00089262
P02042	Aldehyde dehydrogenase X, mitochondrial OS	ALDH1B1	-3.270809495	0.180021407	0.001425084
P00738	Isoform 2 of Aldehyde dehydrogenase family 8 member A1 OS	ALDH8A1	-3.270809495	0.180021407	0.001425084
Q670S4	Major histocompatibility complex, class II, DP beta 1 (Fragment) OS	HLA-DPB1	-3.188702181	0.405748643	0.001277044
A6NC93	Formyltetrahydrofolate dehydrogenase isoform a variant (Fragment) OS		-3.142186369	-0.054226401	9.17164E-06
Q6NSB4	Isoform 1 of Guanylate-binding protein 6 OS	GBP6	-3.014281328	0.51433911	0.001358055
Q9Y6D8	cDNA FLJ39087 fis, clone NT2RP7019273, highly similar to Lysosomal acid lipase/cholesteryl esterhydrolase OS		-3.006058582	0.53721676	0.000236834
Q14403	HLA class II histocompatibility antigen, DRB1-8 beta chain OS	HLA-DRB1	-2.868802815	0.243517553	2.24729E-09
B1AHA8	HLA class II histocompatibility antigen, DRB3-2 beta chain OS	HLA-DRB3	-2.83122657	0.303180622	1.69432E-08
O75882-1	MHC class II HLA beta chain (Fragment) OS	HLA-DRB1	-2.829423266	0.237300768	7.99864E-07
A8MVU1	HLA-DPB1 OS	HLA-DPB1	-2.776426439	0.626732301	7.58496E-05
Q12912-1	Aldehyde dehydrogenase family 3 member B2 OS	ALDH3B2	-2.774634041	0.518427286	0.001714884
P02794	MHC class II antigen (Fragment) OS	HLA-DRB1	-2.720874408	0.172867878	2.50333E-05
Q6S4P3	Major histocompatibility complex class II DR beta 4 OS	HLA-DRB4	-2.701598386	0.438001468	0.000338817
B4DI32	HLA class II histocompatibility antigen, DRB1-9 beta chain OS	HLA-DRB1	-2.693398396	0.291835075	9.48269E-05
B1Q3B4	HLA class II histocompatibility antigen, DP(W2) beta chain OS	HLA-DPB1	-2.650390052	0.268940652	0.000414718
P12318-1	MHC class II antigen (Fragment) OS	HLA-DRB1	-2.637396354	0.353876888	5.03186E-06
P04066	MHC class II HLA-DR2 (Dw12) a-associated glycoprotein beta-chain (Fragment) OS		-2.618854661	0.239742828	3.56369E-06
P09601	Ibd1 protein (Fragment) OS	Ibd1	-2.579075956	-0.217577798	0.001504038

Table 1B: TOP 50 down-regulated proteins (1-25) from masterlist after 7 days of Hb-Hp exposure identified with MALDI-TOFTOF

ACCESSION	MALDI LOG RATIO1 norm	MALDI LOG RATIO2 norm	MALDI LOG RATIO3 norm	MALDI LOG RATIO4 norm	MALDI LOG RATIO5 norm	MALDI LOG RATIO6 norm	MALDI LOG RATIO7 norm	MALDI LOG RATIO8 norm	MALDI LOG RATIO9 norm	MALDI LOG RATIO10 norm	MALDI LOG RATIO11 norm	MALDI LOG RATIO12 norm	MALDI LOG CTRL RATIO1 norm	MALDI LOG CTRL RATIO2 norm	MALDI LOG CTRL RATIO3 norm
P00739-1															
Q8IZU0															
B5MCU0															
A8MUF7															
P00739-2															
P02008															
Q5T619															
P02042															
P00738															
Q670S4	**-1.67351**	**-1.95315**	**-1.23730**	**-1.45877**									**0.19077**		
A6NC93															
Q6NSB4															
Q9Y6D8															
Q14403	**-2.66116**	**-2.66911**	**-2.72519**	**-2.65322**									**0.00000**		
B1AHA8															
O75882-1															
A8MVU1	**-1.42302**	**-2.77385**	**-0.38609**	**-0.46109**									**0.96009**		
Q12912-1	-2.85622	-3.40603	-2.15272	-2.69305									0.51843		
P02794															
Q6S4P3															
B4DI32															
B1Q3B4															
P12318-1															
P04066															
P09601	-2.69305	-2.51285	-2.64530	-1.77542									-0.21758		

Table 1C: TOP 50 down-regulated proteins (1-25) from masterlist after 7 days of Hb-Hp exposure identified with LTQ-Orbitrap

ACCESSION	ORBI LOG RATIO1 norm	ORBI LOG RATIO2 norm	ORBI LOG RATIO3 norm	ORBI LOG RATIO4 norm	ORBI LOG RATIO5 norm	ORBI LOG RATIO6 norm	ORBI LOG RATIO7 norm	ORBI LOG RATIO8 norm	ORBI LOG RATIO9 norm	ORBI LOG RATIO10 norm	ORBI LOG RATIO11 norm	ORBI LOG RATIO12 norm	ORBI LOG CTRL RATIO1 norm	ORBI LOG CTRL RATIO2 norm	ORBI LOG CTRL RATIO3 norm
P00739-1	-4.49747	-5.19319	-4.51237	-5.19319									0.62273		
Q8IZU0	-4.61916	-4.91620	-4.63478	-5.07876	-4.46793	-3.92734	-4.46793	-4.06152					0.18953	0.11246	
B5MCU0	-4.52735	-2.77900	-5.23249	-3.02556	-4.57284	-2.30308	-4.88144	-2.50602					0.62673	0.18240	
A8MUF7	-3.74394	-4.31131	-2.74137	-3.27074									0.52060		
P00739-2	-3.72191	-3.36434	-3.62508	-3.27995									-0.37054		
P02008	-3.71097	-4.32515	-2.59616	-3.19826									0.53929		
Q5T619	-3.58319	-4.07407	-2.84817	-3.29847									0.42938		
P02042	-3.64628	-3.88024	-2.69694	-2.89534									0.18002		
P00738	-3.64628	-3.88024	-2.69694	-2.89534									0.18002		
Q670S4	-4.42425	-5.09748	-4.42425	-5.09748									0.62073		
A6NC93	-3.04231	-3.05917	-3.22520	-3.22520									-0.05423		
Q6NSB4	-3.09324	-3.66766	-2.40581	-2.93532									0.51434		
Q9Y6D8	-4.79655	-3.74394	0.30774	-5.39607	-4.31131	-0.43334	-2.65326	-2.74137	-0.87866	-3.29847	-3.27074	-1.63177	0.53722	0.52060	0.74204
Q14403	-4.01191	-3.08468	-4.49747	-3.38348	-2.47218	-2.79421	-2.94339	-3.05073					0.42072	0.24352	
B1AHA8	-3.00891	-2.49921	-3.35483	-2.71906	-2.56112	-2.66774	-2.94339	-2.95962					0.31453	0.29184	
O75882-1	-3.11909	-2.63887	-3.47143	-2.88741	-1.94544	-2.77143	-2.27803	-2.97594					0.28270	0.19190	
A8MVU1	-4.52735	-2.77900	-5.23249	-3.02556	-4.57284	-2.30308	-4.88144	-2.50602					0.62673	0.18240	
Q12912-1															
P02794	-2.60323	-2.83263	-2.62455	-2.81720									0.17287		
Q6S4P3	-2.54723	-3.04231	-2.39927	-2.85597									0.43800		
B4DI32	-2.49921	-2.71906	-2.66774	-2.95962									0.29184		
B1Q3B4	-2.71166	-3.04231	-2.30308	-2.58912									0.26894		
P12318-1	-3.51151	-2.45877	-4.09937	-2.42554	-2.16826	-2.53342	-2.74137	-2.74886					0.52060	0.18715	
P04066	-2.53342	-2.50602	-2.87164	-2.77143	-1.47233	-2.70429	-1.79151	-2.91126					0.27812	0.20136	
P09601															

Table 2A: TOP 50 down-regulated proteins (26-50) from masterlist after 7 days of Hb-Hp exposure

ACCESSION	NAME	GENE SYMBOL	MEDIAN LOG RATIOS norm	MEDIAN LOG CONTROL RATIOS norm	PVALUE
Q9H3T3-1	Vesicle transport through interaction with t-SNAREs homolog 1A (Yeast) OS	VTI1A	-2.561425671	-0.52781212	0.002826589
P05120	GTP cyclohydrolase 1 feedback regulatory protein OS	GCHFR	-2.551082301	-0.122998681	0.004019117
A6NI72	HLA class II histocompatibility antigen, DRB1-11 beta chain OS	HLA-DRB1	-2.539800928	0.187154963	7.36354E-08
P43490-1	Immunoglobulin superfamily member 6 OS	IGSF6	-2.525994402	-0.542248335	0.000450865
Q5SYT8	HLA class II histocompatibility antigen, DRB1-4 beta chain OS	HLA-DRB1	-2.513033431	0.394584953	0.003939854
P02671-1	HLA class II histocompatibility antigen, DRB3-1 beta chain OS	HLA-DRB3	-2.495821823	0.227206505	0.000145528
A8K8D9	Isoform 1 of Leukocyte immunoglobulin-like receptor subfamily B member 5 OS	LILRB5	-2.493789923	0.012706461	0.000562901
P02545-1	HLA class II histocompatibility antigen, DR-1 beta chain OS		-2.48623285	0.194268658	4.24459E-06
P01031	HLA class II histocompatibility antigen, DRB1-1 beta chain OS	HLA-DRB1	-2.442152799	0.427216309	3.18806E-08
Q86TE4-1	HLA class II DR-beta (HLA-DR B) OS		-2.434416249	0.377009644	0.002509735
Q5JXJ0	HLA-DRB1-1113 protein OS	HLA-DRB1-1113	-2.41997373	0.199000142	2.92198E-05
B7Z5J8	cDNA FLJ51117, highly similar to HLA class II histocompatibility antigen, DRalpha chain OS		-2.396054265	0.38581241	9.57102E-06
P11169	MHC class II antigen (Fragment) OS	HLA-DQA1	-2.394756128	0.529673877	0.004078302
Q8TCE1	DRB52 protein (Fragment) OS	DRB52	-2.387232828	0.252791612	7.67448E-06
B5MCW2	cDNA FLJ55528, highly similar to Transducin beta-like 2 protein OS		-2.33027927	0.304510168	6.32698E-05
P15104	HLA class II histocompatibility antigen, DR alpha chain OS	HLA-DRA	-2.315700136	0.223088605	5.64162E-10
B2R7R1	cDNA FLJ43203 fis, clone FEBRA2008468, highly similar to lysosomal acid lipase/cholesteryl ester hydrolase OS		-2.308702953	0.919303586	0.000526685
B7Z713	MHC class II antigen OS	HLA-DPB1	-2.274239283	0.314656921	4.26714E-05
B4DPN0	Interleukin-1 receptor associated-kinase 1 splice variant c OS	IRAK1	-2.267076439	-0.657851885	0.004467039
P02652	Monoglyceride lipase OS	MGLL	-2.256332	0.156263058	1.30241E-05
B7Z4I5	Major histocompatibility complex, class II, DP alpha 1 (Fragment) OS	HLA-DPA1	-2.24900521	-0.034967943	2.24238E-05
P52209	MHC class II HLA beta chain (Fragment) OS	HLA-DRB1	-2.230306228	0.307739976	0.0013343
B4DLR8	MAP kinase-activated protein kinase 3 OS	MAPKAPK3	-2.228104518	0.259725131	0.004380904
A0JLQ0	Putative uncharacterized protein DKFZp781H1755 OS	DKFZp781H1755	-2.225000139	-0.724456232	0.001583672
Q15572-1	HLA class II histocompatibility antigen, DR-1 beta chain OS	HLA-DRB1	-2.221485708	0.310004044	0.000105396

Table 2B: TOP 50 down-regulated proteins (26-50) from masterlist after 7 days of Hb-Hp exposure identified with MALDI-TOFTOF

ACCESSION	MALDI LOG RATIO1 norm	MALDI LOG RATIO2 norm	MALDI LOG RATIO3 norm	MALDI LOG RATIO4 norm	MALDI LOG RATIO5 norm	MALDI LOG RATIO6 norm	MALDI LOG RATIO7 norm	MALDI LOG RATIO8 norm	MALDI LOG RATIO9 norm	MALDI LOG RATIO10 norm	MALDI LOG RATIO11 norm	MALDI LOG RATIO12 norm	MALDI LOG CTRL RATIO1 norm	MALDI LOG CTRL RATIO2 norm	MALDI LOG CTRL RATIO3 norm
Q9H3T3-1	-3.27551	-2.70106	-2.42179	-1.91301									-0.52781		
P05120															
A6NI72	-2.56689	-1.35826	-2.55138	-1.49482	-2.55138	-0.48955	-2.52822	-0.69937					0.21503	0.18671	
P43490-1	-2.74134	-2.23095	-2.82308	-2.31064									-0.54225		
Q5SYT8															
P02671-1															
A8K8D9	-2.74945	-2.79020	-2.20234	-2.23813									0.01271		
P02545-1	-2.59026	-2.68505	-2.71713	-2.73326									0.15411		
P01031	-2.70106	-1.26579	-2.67707	-1.70510	-2.71713	-0.41406	-2.65322	-0.92011					0.08400	0.48829	
Q86TE4-1															
Q5JXJ0															
B7Z5J8															
P11169	-1.67351	-2.23813	-2.55138	-3.10455									0.52967		
Q8TCE1															
B5MCW2	-2.12463	-2.53593	-1.92635	-3.32166	-1.57399	-2.75757	-1.37582	-3.61963					-0.23099	0.84001	
P15104	-2.36956	-1.59865	-2.73326	-1.76898	-2.73326	-0.92011	-3.18467	-1.16412					0.12538	0.22309	
B2R7R1	-2.42930	0.26713	-3.38714	-1.25437	-2.18810	0.08400	-2.04146	-1.50690					0.91930	1.57319	
B7Z713	-2.26699	-2.64530	-1.93973	-2.28149									0.31466		
B4DPN0															
P02652															
B7Z4I5	-2.72519	-2.22378	-2.27423	-1.93303	-3.63959	-1.86665	-3.18467	-1.64216					0.17452	-0.24445	
P52209															
B4DLR8															
A0JLQ0	-2.59808	-1.90635	-2.54365	-1.84693									-0.72446		
Q15572-1															

Table 2C: TOP 50 down-regulated proteins (26-50) from masterlist after 7 days of Hb-Hp exposure identified with LTQ-Orbitrap

ACCESSION	ORBI LOG RATIO1 norm	ORBI LOG RATIO2 norm	ORBI LOG RATIO3 norm	ORBI LOG RATIO4 norm	ORBI LOG RATIO5 norm	ORBI LOG RATIO6 norm	ORBI LOG RATIO7 norm	ORBI LOG RATIO8 norm	ORBI LOG RATIO9 norm	ORBI LOG RATIO10 norm	ORBI LOG RATIO11 norm	ORBI LOG RATIO12 norm	ORBI LOG CTRL RATIO1 norm	ORBI LOG CTRL RATIO2 norm	ORBI LOG CTRL RATIO3 norm
Q9H3T3-1															
P05120	-3.11909	-3.06765	-2.03452	-1.96191									-0.12300		
A6NI72	-4.02422	-2.41237	-1.28818	-4.61916	-2.63170	-1.48144	-2.98414	-2.58912	-0.51954	-3.56250	-2.75636	-0.72483	0.53100	0.15610	0.18715
P43490-1															
Q5SYT8	-2.77900	-3.23424	-1.80701	-2.24706									0.39458		
P02671-1	-2.68961	-2.49921	-2.20433	-2.49243									0.22721		
A8K8D9															
P02545-1	-2.26560	-1.26293	-2.54032	-1.46779	-2.43215	-0.45156	-2.66774	-0.66779					0.22018	0.19427	
P01031	-3.51151	-2.45877	-1.08107	-4.09937	-2.42554	-1.51358	-2.17423	-2.53342	-0.26636	-2.74137	-2.74886	-0.71129	0.52060	0.18715	0.42722
Q86TE4-1	-2.60323	-3.05073	-1.83306	-2.26560									0.37701		
Q5JXJ0	-3.77734	-2.18623	-1.31369	-4.42425	-2.34752	-1.44970	-3.38348	-2.49243	-0.66779	-4.01191	-2.63170	-0.81812	0.57218	0.12709	0.19900
B7Z5J8	-3.17160	-2.37974	-1.18050	-3.73290	-2.82490	-1.43621	-2.66774	-2.01196	-0.61199	-3.21619	-2.41237	-0.88227	0.49336	0.38581	0.25279
P11169															
Q8TCE1	-2.57508	-2.45877	-1.14026	-3.03392	-2.71166	-1.40060	-1.87529	-2.62455	-0.42427	-2.31570	-2.81720	-0.69112	0.38361	0.19900	0.25279
B5MCW2															
P15104	-2.47891	-2.36036	-1.12038	-2.89534	-2.77143	-1.33946	-1.92908	-2.31570	-0.60227	-2.31570	-2.68230	-0.83224	0.34149	0.34819	0.21079
B2R7R1	-4.79655	-5.39607	-2.65326	-3.29847									0.53722		
B7Z713	-4.09937	-1.26712	-4.76336	-1.27132	-3.97532	-1.21726	-4.61916	-1.09280					0.60061	-0.00256	
B4DPN0	-2.95149	-2.35393	-2.18022	-1.53678									-0.65785		
P02652	-1.12832	-2.24706	-1.54612	-2.26560	-1.96742	-2.73391	-2.36680	-2.71906					0.34596	-0.03343	
B7Z4I5															
P52209	-2.32203	-2.69694	-1.78123	-2.13858									0.30774		
B4DLR8	-2.55416	-2.87164	-1.62694	-1.90205									0.25973		
A0JLQ0															
Q15572-1	-4.25665	-1.95092	-1.32225	-4.93376	-2.32203	-1.48600	-3.60405	-2.12094	-0.49461	-4.27021	-2.45209	-0.66779	0.60666	0.31000	0.15850

Table 3A: TOP 50 up-regulated proteins (1-25) from masterlist after 7 days of Hb-Hp exposure

ACCESSION	NAME	GENE SYMBOL	MEDIAN LOG RATIOS norm	MEDIAN LOG CONTROL RATIOS norm	PVALUE
P00739-1	Isoform 1 of Haptoglobin-related protein OS	HPR	10.59688738	-1.225505984	7.53693E-10
Q8IZU0	Protein FAM9B OS	FAM9B	10.34243665	0.24815879	1.40277E-06
B5MCU0	Putative uncharacterized protein R3HDM2 OS	R3HDM2	9.819450203	-0.641378582	0.000209299
A8MUF7	Putative uncharacterized protein HBE1 OS	HBE1	9.424964392	-0.246585394	1.59089E-10
P00739-2	Isoform 2 of Haptoglobin-related protein OS	HPR	9.319578135	-0.537430802	0.001287874
P02008	Hemoglobin subunit zeta OS	HBZ	9.15552063	0.859472914	6.8718E-07
Q5T619	Zinc finger protein 648 OS	ZNF648	9.08102272	-0.400250556	0.000567473
P02042	Hemoglobin subunit delta OS	HBD	9.005960777	0.111136217	2.54542E-12
P00738	Haptoglobin OS	HP	8.972775485	-0.579731136	2.67747E-13
Q670S4	Hemoglobin Lepore-Baltimore (Fragment) OS		8.839711042	-0.785719104	7.18439E-10
A6NC93	Putative uncharacterized protein ENSP00000346992 (Fragment) OS		8.620328034	-1.427264868	0.00022395
Q6NSB4	HP protein OS	HP	8.606956288	-0.535239955	1.51022E-12
Q9Y6D8	Mutant beta-globin OS	HBB	8.494988851	0.286767456	5.83555E-09
Q14403	Gamma-G globin (Fragment) OS		8.196010627	0.664173541	4.21354E-07
B1AHA8	Heme oxygenase (Decycling) 1 (Fragment) OS	HMOX1	6.550386048	-0.335288407	1.66417E-05
O75882-1	Isoform 1 of Attractin OS	ATRN	4.807601365	-2.007274463	0.003637615
A8MVU1	Putative neutrophil cytosol factor 1C OS	NCF1C	4.793453347	1.017209465	0.000583262
Q12912-1	Isoform 1 of Lymphoid-restricted membrane protein OS	LRMP	4.546192231	-0.201955431	0.001298518
P02794	Ferritin heavy chain OS	FTH1	4.291733615	0.004672308	3.60935E-15
Q6S4P3	Ferritin OS	FTL	3.421461499	-0.105933396	7.33147E-14
B4DI32	cDNA FLJ56081, highly similar to Lamin-A/C OS		3.386576159	0.594331913	6.27842E-06
P12318-1	Isoform 1 of Low affinity immunoglobulin gamma Fc region receptor II-a OS	FCGR2A	3.178190941	-0.816010226	0.002546601
P04066	Tissue alpha-L-fucosidase OS	FUCA1	3.156774268	-0.03561842	6.04514E-12
Q9H3T3-1	Isoform 1 of Semaphorin-6B OS	SEMA6B	3.070553185	-0.244277193	0.000500991
P05120	Plasminogen activator inhibitor 2 OS	SERPINB2	2.935930414	0.172877603	4.43515E-09

Table 3B: TOP 50 up-regulated proteins (1-25) from masterlist after 7 days of Hb-Hp exposure identified with MALDI-TOFTOF

ACCESSION	MALDI LOG RATIO1 norm	MALDI LOG RATIO2 norm	MALDI LOG RATIO3 norm	MALDI LOG RATIO4 norm	MALDI LOG RATIO5 norm	MALDI LOG RATIO6 norm	MALDI LOG RATIO7 norm	MALDI LOG RATIO8 norm	MALDI LOG RATIO9 norm	MALDI LOG RATIO10 norm	MALDI LOG RATIO11 norm	MALDI LOG RATIO12 norm	MALDI LOG CTRL RATIO1 norm	MALDI LOG CTRL RATIO2 norm	MALDI LOG CTRL RATIO3 norm
P00739-1	14.02137	9.00584	12.96776	8.45195									0.02959		
Q8IZU0															
B5MCU0															
A8MUF7															
P00739-2	9.94334	7.47552	11.11030	8.69582									-0.53743		
P02008															
Q5T619															
P02042	14.05747	10.86735	11.15457	7.88669	3.86123	1.49936	13.10263	12.02924	12.11887	6.25959	4.61322	2.28810	0.05897	0.19077	1.24146
P00738	14.44327	10.62838	9.15594	7.43822	13.37230	12.00453	8.38491	8.48135					-0.16874	-0.33988	
Q670S4	14.47121	5.53250	13.68320	3.94573									0.16637		
A6NC93															
Q6NSB4	10.48936	8.27479	7.48788	3.82523	11.92137	8.72086	8.50197	4.07915					-0.26698	0.14182	
Q9Y6D8															
Q14403															
B1AHA8	6.64320	6.91762	6.32025	6.45758									-0.33529		
O75882-1	3.96576	5.94150	3.66739	5.64944									-2.00727		
A8MVU1	5.43705	4.38713	5.19978	4.15787									1.01721		
Q12912-1															
P02794	4.02366	5.25421	2.17785	4.19590	5.21469	3.21729	5.29702	5.78499	2.42919	4.30183	5.75232	3.39815	-0.23099	0.00424	-0.98917
Q6S4P3	3.94740	4.69113	2.80007	4.68832	5.29214	2.51211	4.55999	5.64496	3.90707	5.05155	6.25279	3.54963	-0.68938	-0.07273	0.63323
B4DI32	2.75600	4.18167	1.84805	3.80971	4.17217	3.56979	3.12693	3.20336					0.85044	0.33822	
B1Q3B4															
P12318-1	2.35436	3.13909	3.21729	4.00884									-0.81601		
P04066	5.38850	3.39244	2.60722	5.75888	3.37333	2.23584	4.16423	3.60439	2.94022	4.39917	3.59167	2.49801	-0.42811	0.04641	0.41969
P09601	3.74529	2.83500	3.70298	2.84802	4.71492	3.51828	4.78140	3.46240					-0.09436	0.03801	

Table 3C: TOP 50 up-regulated proteins (1-25) from masterlist after 7 days of Hb-Hp exposure identified with LTQ-Orbitrap

ACCESSION	ORBI LOG RATIO1 norm	ORBI LOG RATIO2 norm	ORBI LOG RATIO3 norm	ORBI LOG RATIO4 norm	ORBI LOG RATIO5 norm	ORBI LOG RATIO6 norm	ORBI LOG RATIO7 norm	ORBI LOG RATIO8 norm	ORBI LOG RATIO9 norm	ORBI LOG RATIO10 norm	ORBI LOG RATIO11 norm	ORBI LOG RATIO12 norm	ORBI LOG CTRL RATIO1 norm	ORBI LOG CTRL RATIO2 norm	ORBI LOG CTRL RATIO3 norm
P00739-1	11.58491	8.26599	12.53440	9.49987	10.94826	8.96214	11.86423	10.24551					-1.31797	-1.22551	
Q8IZU0	10.48905	10.17286	10.49477	10.19583									0.24816		
B5MCU0	10.25074	10.82210	8.79959	9.38816									-0.64138		
A8MUF7	10.95139	7.39906	10.52896	11.04050	7.95526	8.09048	10.09636	7.70231	11.20361	10.20281	8.30154	8.75357	-0.24659	-0.92228	2.25063
P00739-2															
P02008	7.87803	12.21538	9.24831	9.06273	7.99235	11.64549	9.40566	8.48026					-1.42726	3.14621	
Q5T619	8.82540	10.37175	7.59373	9.33664									-0.40025		
P02042	10.46747	7.50604	9.08858	10.30264	8.22402	8.21307	9.42285	7.93394	9.62303	9.34331	8.69559	8.92334	0.16330	-0.88588	-2.58209
P00738	10.95936	8.13257	5.92743	11.48438	8.78961	6.48694	9.88324	8.74999	6.07998	10.47095	9.45803	6.62591	-0.60227	-0.63155	-0.57973
Q670S4	10.91240	7.48415	8.63279	11.23176	8.41414	7.63164	10.26490	8.07027	9.15305	10.65497	9.04663	7.91255	-0.46685	-1.10458	-1.80701
A6NC93	7.87803	9.24831	7.99235	9.40566									-1.42726		
Q6NSB4	11.01461	8.11940	5.92492	11.52005	8.76707	6.47724	9.97135	8.71194	6.02184	10.51886	9.42125	6.56404	-0.53524	-0.53524	-0.57013
Q9Y6D8	7.89692	8.79689	8.74316	7.31263	8.24682	9.39256	9.20962	7.89576					-0.90402	1.47755	
Q14403	7.39906	10.52896	7.95526	8.09048	7.70231	11.20361	8.30154	8.75357					-0.92228	2.25063	
B1AHA8															
O75882-1															
A8MVU1															
Q12912-1	3.82240	3.96758	5.12481	5.31265									-0.20196		
P02794	4.31678	4.74324	2.64524	3.99501	4.65760	2.40670	4.58475	4.85912	2.96626	4.28164	4.81643	2.71416	0.25279	0.00510	0.22954
Q6S4P3	3.11696	3.20081	2.06965	3.28976	3.27846	1.77864	3.25784	3.38932	2.74401	3.45360	3.51049	2.43543	-0.23535	-0.13914	0.28955
B4DI32															
B1Q3B4	3.23201	3.28906	3.40352	3.50402									-0.11764		
P12318-1															
P04066	3.86834	2.15131	1.46030	3.72854	2.22936	1.58145	3.82240	2.11918	1.52159	3.70947	2.24108	1.62645	0.06060	-0.13644	-0.11764
P09601	5.78757	2.26014	0.93698	5.75151	2.04453	0.46583	5.10202	2.29159	1.22786	5.08287	2.11807	0.74395	0.00000	0.15850	0.46370

Table 4A: TOP 50 up-regulated proteins (26-50) from masterlist after 7 days of Hb-Hp exposure

ACCESSION	NAME	GENE SYMBOL	MEDIAN LOG RATIOS norm	MEDIAN LOG CONTROL RATIOS norm	PVALUE
Q9H3T3-1	Isoform 1 of Semaphorin-6B OS	SEMA6B	3.070553185	-0.244277193	0.000500991
P05120	Plasminogen activator inhibitor 2 OS	SERPINB2	2.935930414	0.172877603	4.43515E-09
A6NI72	Putative neutrophil cytosol factor 1B OS	NCF1B	2.904682314	0.980176613	0.003907854
P43490-1	Isoform 1 of Nicotinamide phosphoribosyltransferase OS	NAMPT	2.880662484	0.345958909	0.000939154
Q5SYT8	Novel protein similar to Pre-B cell enhancing factor (PBEF) (Fragment) OS	RP11-92J19.4	2.880662484	0.345958909	0.000939154
P02671-1	Isoform 1 of Fibrinogen alpha chain OS	FGA	2.832446306	0.178586329	0.00013054
A8K8D9	Glucose-6-phosphate 1-dehydrogenase OS		2.808818309	0.178467398	3.16535E-08
P02545-1	Isoform A of Lamin-A/C OS	LMNA	2.607629217	0.193811258	6.23269E-05
P01031	Complement C5 OS	C5	2.598246328	0.112463162	0.00048499
Q86TE4-1	Isoform 1 of Leucine zipper protein 2 OS	LUZP2	2.570977173	-0.532618734	0.003444602
Q5JXJ0	GTP binding protein 5 (Putative) (Fragment) OS	GTPBP5	2.469116214	0.144051778	0.000112193
B7Z5J8	cDNA FLJ56136, highly similar to Solute carrier family 2, facilitated glucosetransporter member 14 OS		2.462908026	0.268940652	0.000103691
P11169	Solute carrier family 2, facilitated glucose transporter member 3 OS	SLC2A3	2.462908026	0.268940652	0.000103691
Q8TCE1	SERPINC1 protein OS	SERPINC1	2.386957994	-0.064109589	0.000867209
B5MCW2	Putative uncharacterized protein RPL3 OS	RPL3	2.357793604	-0.893844283	0.002463707
P15104	Glutamine synthetase OS	GLUL	2.289339567	0.163298576	0.000698336
B2R7R1	Superoxide dismutase OS	SOD2	2.28457437	0.144051778	5.40676E-09
B7Z713	cDNA FLJ58699, highly similar to Homo sapiens tumor necrosis factor, alpha-induced protein 8 (TNFAIP8), mRNA OS		2.254978725	-0.136439009	0.000763551
B4DPN0	cDNA FLJ51265, moderately similar to Beta-2-glycoprotein 1 (Beta-2-glycoprotein I) OS		2.219994911	0.271109915	0.000133107
P02652	Apolipoprotein A-II OS	APOA2	2.201207421	-0.258125291	0.00064633
B7Z4I5	cDNA FLJ58675, highly similar to Band 4.1-like protein 3 OS		2.141734813	-0.120319079	1.16608E-05
P52209	6-phosphogluconate dehydrogenase, decarboxylating OS	PGD	2.136068931	0.025549062	6.08218E-12
B4DLR8	cDNA FLJ50573, highly similar to H. sapiens NAD(P)H dehydrogenase, quinone 1 (NQO1), transcript variant 3, mRNA OS		2.135025098	0.568087056	0.001272386
A0JLQ0	AZGP1 protein (Fragment) OS	AZGP1	2.100528365	0.654569157	0.001659301
Q15572-1	Isoform 1 of TATA box-binding protein-associated factor RNA polymerase I subunit C OS	TAF1C	2.094564616	-0.500818117	0.001922775

Table 4B: TOP 50 up-regulated proteins (26-50) from masterlist after 7 days of Hb-Hp exposure identified with MALDI-TOFTOF

ACCESSION	MALDI LOG RATIO1 norm	MALDI LOG RATIO2 norm	MALDI LOG RATIO3 norm	MALDI LOG RATIO4 norm	MALDI LOG RATIO5 norm	MALDI LOG RATIO6 norm	MALDI LOG RATIO7 norm	MALDI LOG RATIO8 norm	MALDI LOG RATIO9 norm	MALDI LOG RATIO10 norm	MALDI LOG RATIO11 norm	MALDI LOG RATIO12 norm	MALDI LOG CTRL RATIO1 norm	MALDI LOG CTRL RATIO2 norm	MALDI LOG CTRL RATIO3 norm
Q9H3T3-1	3.70475	1.04714	3.78545	1.47247	4.50608	2.08028	4.59315	2.43636					-0.11175	-0.37681	
P05120	2.75600	2.78689	2.91682	2.95504									-0.06411		
A6NI72	5.43705	1.65150	4.38713	0.75922	5.19978	1.64862	4.15787	0.68768					1.01721	0.94314	
P43490-1															
Q5SYT8															
P02671-1	3.10046	2.88901	2.77589	2.57036									0.17859		
A8K8D9	2.80007	2.71594	2.81757	2.35923	3.24502	3.11473	3.26864	2.68902					-0.05121	0.40814	
P02545-1	4.15627	3.71536	3.49230	3.05736									0.40814		
P01031															
Q86TE4-1	1.86174	2.36166	2.78029	3.28822									-0.53262		
Q5JXJ0															
B7Z5J8															
P11169															
Q8TCE1	2.06987	2.09842	2.67550	2.71146									-0.06411		
B5MCW2	1.81223	2.64832	2.06727	2.87395									-0.89384		
P15104	2.64150	-0.43281	2.33973	-0.12047	3.91382	0.49207	3.62068	0.73432					0.26713	-0.26247	
B2R7R1	2.87180	3.90876	1.14865	2.44113	3.75755	0.50339	1.37544	3.49416	1.52905	0.80858	3.37142	0.81208	0.36944	0.09646	0.69489
B7Z713															
B4DPN0	2.39073	2.08806	2.35193	2.05422									0.27111		
P02652	4.19116	3.76629	4.50168	4.08239									0.39271		
B7Z4I5	2.11133	0.58546	2.36895	0.70568	2.79568	0.87812	3.05942	0.92954					-0.28963	-0.07273	
P52209	2.33239	3.21729	2.44113	2.44590	3.19738	2.03851	1.15511	3.59349	2.50976	1.13244	3.47363	2.03851	-0.17316	0.09231	0.45031
B4DLR8															
A0JLQ0															
Q15572-1															

Table 4C: TOP 50 up-regulated proteins (26-50) from masterlist after 7 days of Hb-Hp exposure identified with LTQ-Orbitrap

ACCESSION	ORBI LOG RATIO1 norm	ORBI LOG RATIO2 norm	ORBI LOG RATIO3 norm	ORBI LOG RATIO4 norm	ORBI LOG RATIO5 norm	ORBI LOG RATIO6 norm	ORBI LOG RATIO7 norm	ORBI LOG RATIO8 norm	ORBI LOG RATIO9 norm	ORBI LOG RATIO10 norm	ORBI LOG RATIO11 norm	ORBI LOG RATIO12 norm	ORBI LOG CTRL RATIO1 norm	ORBI LOG CTRL RATIO2 norm	ORBI LOG CTRL RATIO3 norm
Q9H3T3-1															
P05120	3.07743	2.60960	3.40622	2.98062									0.40986		
A6NI72															
P43490-1	2.74750	2.34419	3.37504	3.01382									0.34596		
Q5SYT8	2.74750	2.34419	3.37504	3.01382									0.34596		
P02671-1															
A8K8D9															
P02545-1	2.15790	2.12141	1.80777	1.81406									-0.02052		
P01031	2.95262	2.77093	2.42556	2.26119									0.11246		
Q86TE4-1															
Q5JXJ0	2.70177	2.48807	2.45016	2.25380									0.14405		
B7Z5J8	2.60316	2.27591	2.60592	2.32266									0.26894		
P11169	2.60316	2.27591	2.60592	2.32266									0.26894		
Q8TCE1															
B5MCW2															
P15104	2.23895	2.00986	2.77783	2.60039									0.16330		
B2R7R1	1.98648	3.15514	1.94505	2.95422	2.14359	2.58371	2.11807	2.42556					-0.02826	0.14405	
B7Z713	2.95020	3.00122	2.59854	1.82784	1.91142	1.08990							-0.13644		
B4DPN0															
P02652	1.75047	2.26435	-0.88227	2.13806	2.27171	-0.35288	1.43565	2.77438	-0.99289	1.83533	2.82393	-0.49461	-0.45156	-0.06469	-0.53209
B7Z4I5	2.10913	2.17214	2.40571	2.51112									-0.12032		
P52209	1.39157	2.32678	1.19926	1.36476	2.39772	1.08489	1.27638	2.23363	1.47325	1.27638	2.34827	1.35124	-0.04121	-0.12837	0.11246
B4DLR8	2.53776	1.91263	2.35742	1.77610									0.56809		
A0JLQ0	2.31028	1.88834	2.73702	1.89078									0.65457		
Q15572-1	2.14690	2.57720	1.59380	2.04223									-0.50082		

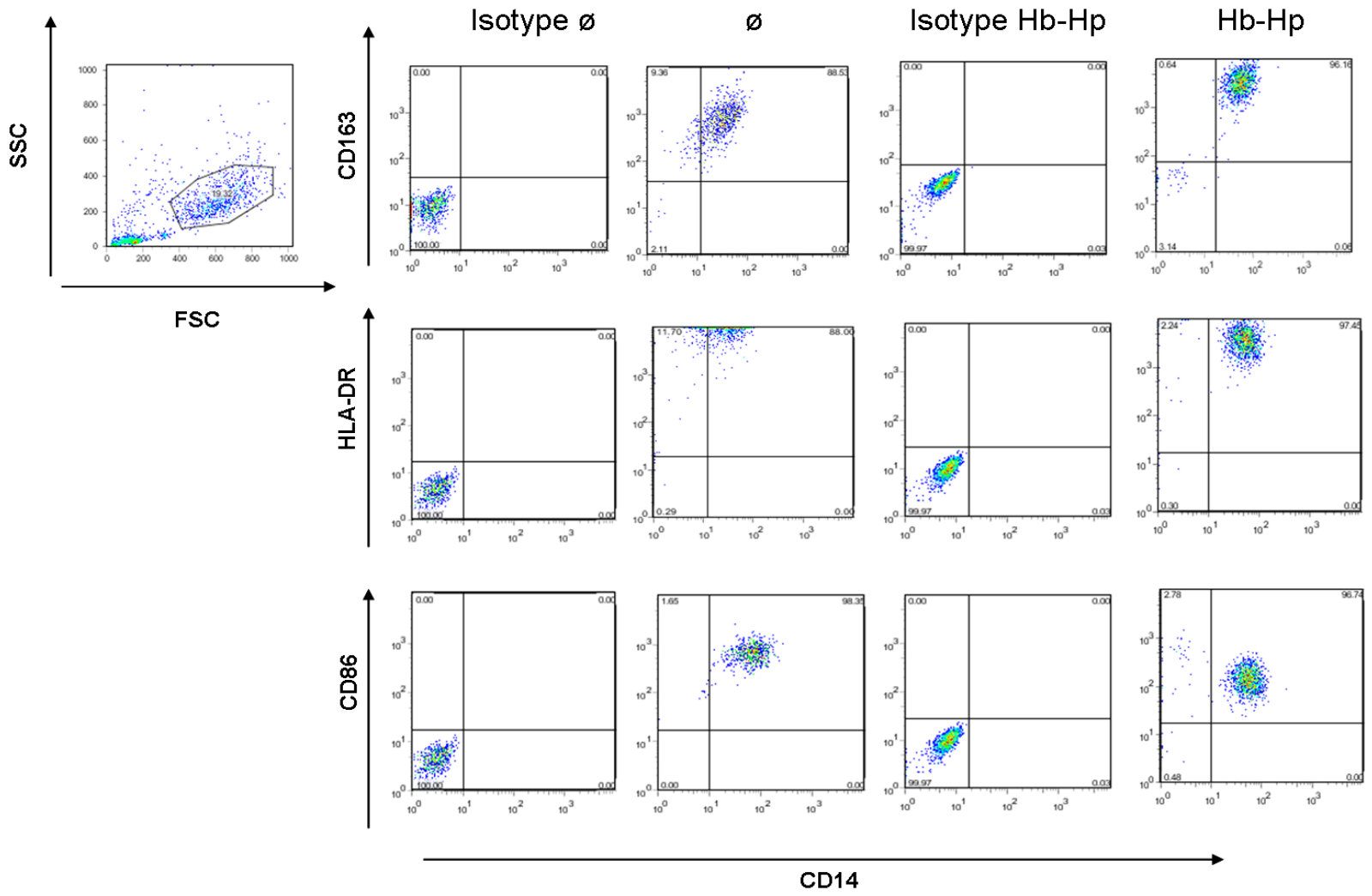

Figure S1 – Flow cytometric analysis of indicated cell surface markers of human macrophages after 7 days of Hb-Hp (2 mg/ml) exposure or untreated control macrophages. *Shown are raw data of one representative experiment. X-axis and y-axis represent fluorescence intensity of indicated markers.*

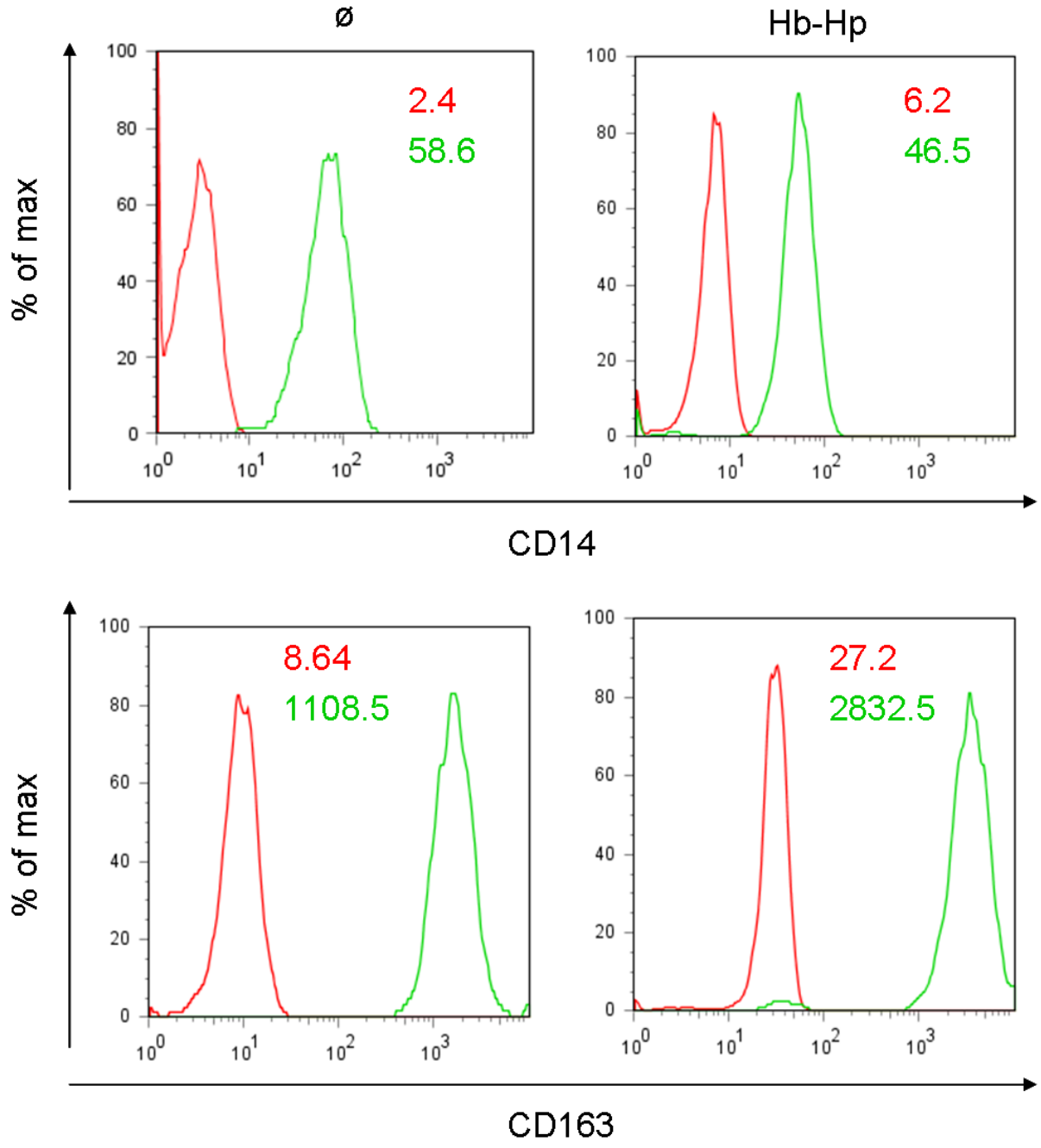

Figure S2 – Flow cytometric analysis of indicated cell surface markers of human macrophages after 7 days of Hb-Hp (2 mg/ml) exposure or untreated control macrophages. *Shown are histograms with geometric means. Red: isotype control, green: sample. X-axis represents fluorescence intensity of indicated markers.*

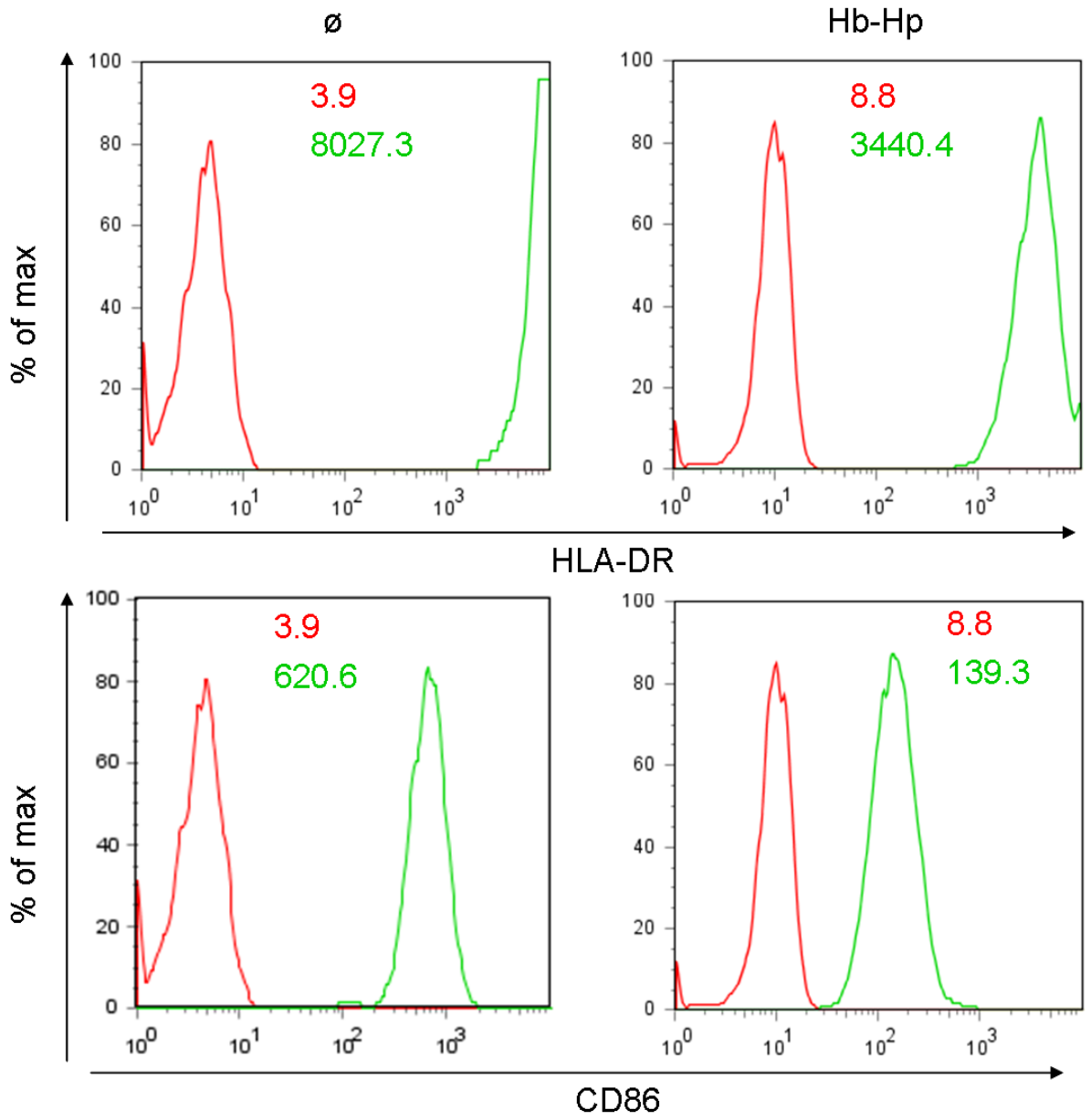

Figure S3 – Flow cytometric analysis of indicated cell surface markers of human macrophages after 7 days of Hb-Hp (2 mg/ml) exposure or untreated control macrophages. *Shown are histograms with geometric means. Red: isotype control, green: sample. X-axis represents fluorescence intensity of indicated markers.*

3.6. References

1. Alayash AI. Oxygen therapeutics: can we tame hemoglobin? Nat Rev Drug Discov. 2004;3:152-159.

2. Reeder BJ, Svistunenko DA, Cooper CE, Wilson MT. The radical and redox chemistry of myoglobin and hemoglobin: from in vitro studies to human pathology. Antioxid Redox Signal. 2004;6:954-966.

3. Widmer CC, Pereira CP, Gehrig P, et al. Hemoglobin can attenuate hydrogen peroxide-induced oxidative stress by acting as an antioxidative peroxidase. Antioxid Redox Signal. 2010;12:185-198.

4. Newman ES, Rice-Evans CA, Davies MJ. Identification of initiating agents in myoglobin-induced lipid peroxidation. Biochem Biophys Res Commun. 1991;179:1414-1419.

5. Levy AP, Asleh R, Blum S, et al. Haptoglobin: basic and clinical aspects. Antioxid Redox Signal. 2010;12:293-304.

6. Kato GJ. Haptoglobin halts hemoglobin's havoc. J Clin Invest. 2009;119:2140-2142.

7. Boretti FS, Buehler PW, D'Agnillo F, et al. Sequestration of extracellular hemoglobin within a haptoglobin complex decreases its hypertensive and oxidative effects in dogs and guinea pigs. J Clin Invest. 2009;119:2271-2280.

8. Buehler PW, Abraham B, Vallelian F, et al. Haptoglobin preserves the CD163 hemoglobin scavenger pathway by shielding hemoglobin from peroxidative modification. Blood. 2009;113:2578-2586.

9. Theilgaard-Monch K, Jacobsen LC, Nielsen MJ, et al. Haptoglobin is synthesized during granulocyte differentiation, stored in specific granules, and released by neutrophils in response to activation. Blood. 2006;108:353-361.

10. Nielsen MJ, Moller HJ, Moestrup SK. Hemoglobin and heme scavenger receptors. Antioxid Redox Signal. 2010;12:261-273.

11. Kristiansen M, Graversen JH, Jacobsen C, et al. Identification of the hemoglobin scavenger receptor. Nature. 2001;409:198-201.

12. Schaer CA, Schoedon G, Imhof A, Kurrer MO, Schaer DJ. Constitutive endocytosis of CD163 mediates hemoglobin-heme uptake and determines the noninflammatory and protective transcriptional response of macrophages to hemoglobin. Circ Res. 2006;99:943-950.

13. Tacke F, Randolph GJ. Migratory fate and differentiation of blood monocyte subsets. Immunobiology. 2006;211:609-618.

14. Mosser DM, Edwards JP. Exploring the full spectrum of macrophage activation. Nat Rev Immunol. 2008;8:958-969.

15. Kall L, Storey JD, MacCoss MJ, Noble WS. Assigning significance to peptides identified by tandem mass spectrometry using decoy databases. J Proteome Res. 2008;7:29-34.

16. Schaer DJ, Schaer CA, Buehler PW, et al. CD163 is the macrophage scavenger receptor for native and chemically modified hemoglobins in the absence of haptoglobin. Blood. 2006;107:373-380.

17. Shui W, Gilmore SA, Sheu L, Liu J, Keasling JD, Bertozzi CR. Quantitative proteomic profiling of host-pathogen interactions: the macrophage response to Mycobacterium tuberculosis lipids. J Proteome Res. 2009;8:282-289.

18. Zhao C, Zhang H, Wong WC, et al. Identification of novel functional differences in monocyte subsets using proteomic and transcriptomic methods. J Proteome Res. 2009;8:4028-4038.

19. Polati R, Castagna A, Bossi A, et al. High resolution preparation of monocyte-derived macrophages (MDM) protein fractions for clinical proteomics. Proteome Sci. 2009;7:4.

20. Kadiu I, Wang T, Schlautman JD, et al. HIV-1 transforms the monocyte plasma membrane proteome. Cell Immunol. 2009;258:44-58.

21. Zhang H, Zhao C, Li X, et al. Study of monocyte membrane proteome perturbation during lipopolysaccharide-induced tolerance using iTRAQ-based quantitative proteomic approach. Proteomics. 2010.

22. Wiseman H. Vitamin D is a membrane antioxidant. Ability to inhibit iron-dependent lipid peroxidation in liposomes compared to cholesterol, ergosterol and tamoxifen and relevance to anticancer action. FEBS Lett. 1993;326:285-288.

23. O'Shea JJ, Murray PJ. Cytokine signaling modules in inflammatory responses. Immunity. 2008;28:477-487.

24. Gordon S. The macrophage: past, present and future. Eur J Immunol. 2007;37 Suppl 1:S9-17.

25. Kreider T, Anthony RM, Urban JF, Jr., Gause WC. Alternatively activated macrophages in helminth infections. Curr Opin Immunol. 2007;19:448-453.

26. Banchereau J, Steinman RM. Dendritic cells and the control of immunity. Nature. 1998;392:245-252.

27. Westerheide SD, Louis-Plence P, Ping D, He XF, Boss JM. HLA-DMA and HLA-DMB gene expression functions through the conserved S-X-Y region. J Immunol. 1997;158:4812-4821.

28. Taxman DJ, Cressman DE, Ting JP. Identification of class II transcriptional activator-induced genes by representational difference analysis: discoordinate regulation of the DN alpha/DO beta heterodimer. J Immunol. 2000;165:1410-1416.

29. Harton JA, Ting JP. Class II transactivator: mastering the art of major histocompatibility complex expression. Mol Cell Biol. 2000;20:6185-6194.

30. Reith W, Mach B. The bare lymphocyte syndrome and the regulation of MHC expression. Annu Rev Immunol. 2001;19:331-373.

31. Boss JM, Jensen PE. Transcriptional regulation of the MHC class II antigen presentation pathway. Curr Opin Immunol. 2003;15:105-111.

32. Carlsen HS, Yamanaka T, Scott H, Rugtveit J, Brandtzaeg P. The proportion of CD40+ mucosal macrophages is increased in inflammatory bowel disease whereas CD40 ligand (CD154)+ T cells are relatively decreased, suggesting differential modulation of these costimulatory molecules in human gut lamina propria. Inflamm Bowel Dis. 2006;12:1013-1024.

33. Hara J, Ohtani H, Matsumoto T, et al. Expression of costimulatory molecules B7-1 and B7-2 in macrophages and granulomas of Crohn's disease: demonstration of cell-to-cell contact with T lymphocytes. Lab Invest. 1997;77:175-184.

34. Boyle JJ, Harrington HA, Piper E, et al. Coronary intraplaque hemorrhage evokes a novel atheroprotective macrophage phenotype. Am J Pathol. 2009;174:1097-1108.

4. Transcriptomic profiling of macrophages exposed to hemoglobin

4.1. Abstract

Tissue injury and hemolysis can initiate oxidative stress mediated by heme toxicity leading to inflammation. Macrophages display the unique ability to clear hemoglobin (Hb) and are therefore essential for wound healing. The cellular response of macrophages to heme involves the oxidative stress responsive transcription factor Nuclear Factor E2-related factor (Nrf-2) pathway resulting in the activation of antioxidant responsive element (ARE) – containing genes. To investigate the response of macrophages towards Hb-Hp complexes we applied global transcriptomic and proteomic strategies and found IL-8 to be the most induced gene. We could show that IL-8 expression correlates with Nrf-2 activation and confirmed the up-regulation of a characteristic set of anti-oxidant genes. In contrast, we could proof the absence of NF-κB-driven pro-inflammatory mediators such as TNF-α and IL-1β. Pre-treatment of macrophages with the glucocorticoid dexamethasone followed by Hb-Hp exposure resulted in significant IL-8 induction supporting a new role for IL-8 apart from its pro-inflammatory actions. Furthermore, we detected a link between enhanced erythropoiesis and increased oxidative stress by the highly induced kit ligand suggesting an induced “stress-erythropoiesis” upon increased heme availability. In summary, our data suggest a highly specialized macrophage subset with benefits in hemolysis, wound healing and inflammation.

4.2. Introduction

Release of free Hb in case of red blood cell (RBC) destruction or hemolysis is critical due to the toxic nature of free Hb that can easily act as a peroxidase in the presence of superoxide radicals generated by inflammatory cells with very high oxidizing potential [1-2]. Immediate binding of Hb to circulating acute phase plasma protein Haptoglobin (Hp) reduces Hb induced oxidative stress by preventing oxidation of Hb [3-4]. Macrophages exhibit the unique characteristic of expressing the scavenger receptor CD163 on their surface that is the only known receptor for Hb-Hp and Hb binding and removal by subsequent internalization and recycling [5-6]. The cellular response of macrophages to this highly reactive heme stimulus results in the significant activation of detoxifying genes that are regulated by the conserved oxidative response transcription factor Nuclear Factor E2-related factor (Nrf-2). The antioxidant response element (ARE) is a DNA element located at the regulatory regions of phase II detoxification enzymes and proteins, such as heme oxygenase 1 (HO-1), glutathione-S-transferases (GST), NAD(P)H:quinone oxidoreductase-1 (NQO1) and ferritin, that contribute to the cellular antioxidant defense systems [7-8].

In pathologic conditions, such as hemolysis, atherosclerosis, infection, inflammation and wound healing tissue macrophages play a crucial role. Not only by removal of Hb(-Hp) but also by recognizing and phagocytosing of potential pathogens they actively promote tissue repair mediated by the release of bioactive compounds that stimulate cell proliferation and attract more leukocytes to the damaged tissue [9]. Due to their huge spectrum of activity, macrophages exhibit several sub-populations. A recent study suggests a new grouping of macrophage populations based on three homeostatic activities – host defense, wound healing and immune regulation [10].

We discovered significant characteristics of the macrophage phenotype polarization cultured in Hb-rich environment to mimic conditions within wounded tissues and atherosclerotic plaques. The long-term effect of Hb resulted in significant suppression of HLA class 2 molecules most likely in order to reduce self-antigen presentation. We investigated the genome of macrophages differentiated under the influence of Hb-Hp. Applying whole genome arrays we found that Hb-Hp-treated macrophages are characterized by remarkable expression and secretion of high amounts of IL-8 with a

complete lack of pro-inflammatory mediators, such as IL-1β, TNF-α and IL-6. Interestingly, those macrophages did not express the anti-inflammatory cytokine IL-10 that was reported to be produced upon Hb-Hp stimulation before [11].

4.3. Methods

4.3.1. Cell culture and experimental conditions

Human monocytes were prepared from buffy coats of healthy blood donors (Blutspendedienst, Schlieren, Switzerland) by a strictly standardised protocol. Briefly, after Ficoll gradient separation (Ficoll-Paque^{TM} PLUS, Amersham Biosciences) and three washes with Mg^{2+}/Ca^{2+} -free phosphate buffered saline (PBS; GIBCO Europe), cells were suspended in Iscove's modified Dulbecco's medium (IMDM; GIBCO Europe) supplemented with 10% heat-inactivated pooled human serum (complete medium) to prevent activation and seeded at a density of 10^7 cells/ml in 6-well tissue culture plates (Falcon Oxnard, USA). During 2 h under standard cell culture conditions (37°C, 5% CO2) in a SteriCult tissue culture incubator (Fisher Scientific, USA) monocytes adhered to the tissue culture plates. Afterwards, the cells were washed 3-4 times with Gey's balanced salt solution (Sigma) to remove nonadherent cells and the remaining monocytes were stimulated with 2 mg/ml Hb/Hp or Hb. Endotoxin free Hb was obtained from Hemosol (Ontario, Canada). Hp (mixed phenotype) was from Sigma (Buchs, Switzerland). Monocytes derived macrophages were kept in complete medium for 2 days respective 5 days for mRNA expression analysis using RT-PCR and Agilent whole genome 4 x 44 K arrays. For protein expression analysis culture time was prolonged to 7 days.

For glucocorticoid priming, monocytes were incubated for 36 h with dexamethasone (Sigma) at a concentration of 2.5×10^{-7} M. After this priming period, 500 µg/ml purified Hb-Hp (1:1 molar ratio) was added. Following incubation for an additional 0, 8, or 18 h, RNA was extracted and samples were analyzed with Agilent whole genome 44K arrays using a competitive two-color hybridization protocol.

4.3.2. Reverse Transcription and Quantitative Real Time (RT)-PCR

Total RNA was purified with the RNeasy mini kit according to the manufacturer's instructions (Qiagen, Basel, Switzerland). The method is based on the originally designed procedure of Chomczynski & Sacchi [12]. RNA used for microarray analysis

was treated with a DNase I digestion step (Qiagen). RNA was quantified spectrophotometrically using Nanodrop ND-1000 spectrophotometer (NanoDrop Technologies, USA). Taqman RT-PCR reagents (Applied Biosystems, Life Technologies Corp., USA) were used for the generation of cDNA for all samples on a Mastercycler gradient (Vaudaux-Eppendorf, Schoenenbuch, Schwitzerland). cDNA samples were amplified using SYBR Green master mix reagent (Applied Biosystems) and sequence-specific primer pairs with a 7500 Fast Real-Time PCR System (Applied Biosystems). Melting curve analysis was performed after each PCR experiment to control for specificity of amplification reactions and to exclude excessive primer-dimer formation. Temperature cycling profiles were as follows: 10 min at 95°C, 45 cycles of 15 sec at 95°C, 10 sec at 67–55°C, and 13 sec at 72°C. Gene specific quantitative data were normalized for Hypoxanthine phosphoribosyltransferase (HPRT) RNA abundance in the respective sample and are expressed as fold-expression in relation to the non-treated control. Primers were carefully designed to give a product of 150–200 bp using OligoPerfect™ Designer (Invitrogen) and were synthesized by Microsynth Laboratory (Balgach, Schweiz) (see **Table 1**).

4.3.3. Quantification of secreted proteins

The inflammatory cytokine TNF-α was quantified in undiluted supernatants of monocytes collected 30 min, 2 h, 4 h, 6 h, 24 h and 48 h after applying the stimulus (Hb-Hp 2 mg/ml). IL-8 was quantified in supernatants of monocytes collected after 4 h, 24 h, 48 h and 5 days of exposure to Hb-Hp. IL-1β was measured in undiluted supernatants of Hb-Hp treated monocytes after 12 h, 48 h, 3 days and 4 days of incubation. For IL-8 measurements supernatants were diluted 1:1000 in complete medium. Each cytokine was measured individually using Bio-Plex Pro Magnetic Human Cytokine SinglePlex assays on the Bio-Plex 100 platform according to the manufacturer's instructions (Bio-Rad, USA). Complete medium was used as blank for supernatant measurements. Data were analyzed on the Bio-Plex fluorescence reader using Bio-Plex Manager software 4.1.1. (Bio-Rad).

4.3.4. Isolation of globin from heme

Human hemoglobin was diluted in phosphate buffer (100mM, pH 7.4) to a final concentration of 10 mg/ml, acidified to a pH of 1-2 using 37% HCl (Merck) and extracted with butanone (Sigma). The heme-containing butanone layer was separated from the globin-containing aqueous layer by centrifugation (16'000 x g for 10 min) and cleaned-up using PD-10 Desalting columns (GE Healthcare). Thus, the eluted globin-containing solution was sterile filtered for monocyte stimulation.

4.3.5. Western blot analysis

Monocytes grown on 6-well tissue culture plates were harvested using 300 µl/well CelLytic-M reagent (Sigma) supplemented with Complete Mini Protease Inhibitor (Roche Diagnostics). Lysate supernatant was separated by SDS/PAGE with 20 ug total protein load using a 4-15% gradient Tris-HCl gel (Criterion, Bio-Rad) and transferred to a nitrocellulose membrane (Amersham Biosciences, USA) using a wet transfer apparatus (Bio-Rad Power Pac). After blocking of unspecific binding sites, membranes were incubated with the specific antibody **(Table 2)** in PBS /0.1% Tween 20 /10% goat serum resp. 5% milk (GIBCO, Europe) for at least 1 h at room temperature and probed with horseradish peroxidase-conjugated anti-rabbit IgG (resp. anti-goat IgG) (Amersham Biosciences) at a dilution of 1:10'000. Bands were visualized using Amersham ECL detection kit according to manufacturer's

instructions and analyzed on a Chemi Doc XRS system with Quantity One 1-D Analysis software (Bio-Rad).

4.3.6. Nuclear extracts

Nuclear extracts were prepared using a nuclear extract kit (Active Motif, USA) according to the manufacturer's protocol. Monocytes grown on 12-well tissue culture dishes for 4, 24 and 48 h were washed and collected by scraping with ice-cold PBS in the presence of phosphatase inhibitors. After centrifugation, cells were resuspended in hypotonic buffer and treated with detergent to promote the leakage of cytoplasmic fraction into the supernatant. The remaining nuclear proteins were solubilized in lysis buffer containing a protease inhibitor cocktail. To determine the protein concentration of the nuclear fractions, samples were diluted 1:100 in reaction buffer (Invitrogen) and measured in a Qubit^{TM} Quantitation reader (Invitrogen).

4.3.7. Transcription factor analysis

Nuclear extracts of monocytes were prepared as described. Nuclear Nrf-2 or NF-κB p65 binding activity was determined by using TransAM transcriptional factor assaying kits according to the manufacturer's instructions (Active Motif, USA). This is an ELISA-based quantitative assay of Nrf-2 or NF-κB p65 binding activity using antibodies directed against Nrf-2 or NF-κB p65 subunit.

4.3.8. Gene array experiments

Gene expression profiling was performed by competitive dual-color hybridization of complementary RNA probes of treated and untreated cells on human 4 x 44 K 60-meroligonucleotide microarray chips (Agilent Technologies, USA) according to manufacturer's instructions. For quality control and to quantify samples, each purified RNA sample (1 µl) was analyzed on RNA 6000 Nanochip (Bioanalyzer 2100 instrument, 2100 Expert software, Agilent Technologies). High quality total RNA had an 18/28 S ribosomal RNA ratio > 1.5. Total RNA was frozen in aliquots at -80°C. cRNA probes were then synthesized from 200ng aliquots of total RNA using low input fluorescence linear amplification kit protocol and spiked with control targets (Agilent Technologies). Cyanine-3-dCTP (Cy3, control cells) or cyanine-5-dCTP (Cy5, treated cells) labeled cRNA probes were purified on RNAeasy mini spin columns (Qiagen) and spectrophotometrically quantified (NanoDrop Technologies,

USA). Equal quantities of Cy3- and Cy5-labeled probes (825 µg each) were mixed and incubated in fragmentation buffer in the dark for 30 min at 60°C. After fragmentation, control and respective treatment samples were hybridized on whole human genome (4 x 44 K) oligonucleotide microarrays (Agilent Technologies) for 17 h at 65°C in a hybridization oven (Agilent Technologies) under rotation of 10 rpm. After washing twice in GE washing buffer (Agilent Technologies) for 1 min, microarray slides were carefully placed in acetonitrile (ACN) for 30 sec and dried. Slides were scanned using a dual-laser microarray scanner and analyzed with Feature Extraction software (Agilent Technologies). Data mining was achieved using the Rosetta Resolver Gene Expression Data Analysis System Version 7.2 (Rosetta Biosoftware, USA). Further data analysis was performed using Matlab 7.9 (The MathWorks Inc., Bern, Switzerland). Genes regulated ≥ 1.5 fold were set as specifically regulated. Functional clustering of regulated genes was investigated using GeneGo Metacore software (GeneGo, USA).

4.3.9. Sample treatment for iTRAQ analyses

Human-blood derived monocytes were prepared from 3 healthy donors, as described before and cultured in IMDM (GIBCO, Europe), supplemented with 10% heat-inactivated, pooled human serum from 8 healthy donors. For each tested condition (media alone or 2 mg/ml Hb-Hp) samples were prepared in 3 biological replicates as mentioned above, whereas each replicate was divided into two portions for experimental replicates. At day 7 of culture total cellular protein was extracted from human-blood derived macrophages, grown in 24-well plates. Supernatant was removed and cells were harvested by scraping using 100 µl CelLytic-M reagent (Sigma) supplemented with Complete Mini Protease Inhibitor (Roche Diagnostics). After three freeze-thaw cycles and sonication with a Branson Sonifier 250, cellular debris was removed by centrifugation at 16’000 x g for 10 min. Protein concentration of each sample was determined using a protein Bradford assay (Bio-Rad, USA). Samples normalized to 60 µg of protein were precipitated by adding 1 volume of trichloroacetic acid (TCA) to 4 volumes of protein solution to a final concentration of 10-12% w/v TCA and incubated at 4°C for 10 min. After centrifugation at 16’000 x g supernatant was removed, pellets were washed three times with ice-cold acetone and dried in a heat block at 95°C for 10 min.

4.3.10. iTRAQ labeling

Pellets were reconstituted in 20 µl of dissolution buffer and 1 µl of denaturant according to the protocol of the iTRAQ manufacturer (Applied Biosystems, USA). Additionally, we added 4 µl of 6 M freshly prepared urea to the pellets. Disulfide bonds were reduced by adding 2 µl of reducing agent and blocked by treatment with 1 µl of cysteine blocking reagent. A total of 60 µg of protein was digested overnight at 37°C with trypsin (Promega, USA) in the ratio 1:10, trypsin to protein. Peptides were covalently modified for two hours with an isobaric tag reagent according to the following scheme: iTRAQ 114 (control macrophages), iTRAQ 115 (Hb-Hp treated macrophages), iTRAQ 116 (control macrophages) and iTRAQ 117 (Hb-Hp treated macrophages). After combining the iTRAQ reagent labeled peptides, the reaction was stopped by adding 10 µl of phosphoric acid (pH 2-3).

4.3.11. SCX fractionation

The labeled peptides were fractionated by strong cation exchange liquid chromatography (SCX) using a Polysulfoethyl A 2.1 mm x 200 mm, 5 µm, 300 Å column (PolyLC, USA). Solvent A was 10 mM potassium phosphate, 25% acetonitrile (ACN), pH 2.7, and solvent B was 10 mM potassium phosphate, 350 mM potassium chloride, 25% ACN, pH 2.7. The iTRAQ labeled peptides were diluted in a ratio 1:4 in solvent A and applied to the SCX column. Chromatography was performed at a flow rate of 0.3 ml/min according to the following gradient: 0-10 min 0% solvent B; 10-60 min 0-100% solvent B; 60-65 min 100% solvent B; 65-90 min 0-100% solvent A. For each HPLC run, 24 out of 27 fractions were collected and partially evaporated to remove ACN in a vacuum concentrator. The collected fractions were re-dissolved in 5% ACN, 0.1% trifluoroacetic acid (TFA), combined to 8 pools (each pool contained 3 fractions) and desalted with Sep Pak C_{18} cartridges (Waters, USA). The 8 labeled sample pools were dried in a vacuum concentrator and reconstituted in 10 µl of 3% (v/v) ACN /0.2% formic acid. 5 µl of each pool was transferred to a new tube and combined to 4 sample pools for MALDI-TOFTOF MS analyses.

4.3.12. Nano-LC separation and MALDI target plate spotting of tryptic peptides

Peptide separation was performed on an Ultimate chromatography system (Dionex - LC Packings, USA) equipped with a Probot MALDI spotting device. A volume of 5 µl of each sample was injected by using a Famos autosampler (Dionex - LC Packings) and loaded directly onto a 75 µm x 150 mm reversed-phase column (PepMap 100, 3 µm; Dionex - LC Packings). Peptides were eluted at a flow rate of 300 nl/min by using the following gradient: 0-10 min, 0% solvent B; 10-105 min, 0-50% solvent B; and 105-115 min, 50-100% solvent B. Solvent A contained 0.1% TFA in 95:5 water/ACN , and solvent B contained 0.1% TFA in 20:80 water/ACN . For MALDI analysis, the column effluent was directly mixed with MALDI matrix solution (3 mg/ml α-cyano-4-hydroxycinnamic acid in 70 % (ACN /0.1 % TFA) at a flow rate of 1.1 µl/min via a µ-Tee fitting. The matrix solution also contained neurotensin at a concentration of 125 pmol/ml (Sigma, USA) for internal calibration. Fractions were automatically deposited every 10 s onto a MALDI target plate (Applied Biosystems/MDS Sciex, USA) using a Probot microfraction collector. A total of 416 spots were collected from each HPLC run.

4.3.13. MALDI-TOFTOF mass spectrometry

MALDI plates were analyzed on a 4800 MALDI-TOFTOF system (Applied Biosystems) equipped with a Nd:YAG laser operating at 200 Hz. All mass spectra were acquired in positive reflector mode and generated by accumulating data from 800 laser shots. First, MS spectra were recorded from peptide standards, and the default calibration parameters were updated. Second, MS spectra were recorded for all sample spots on the MALDI target plate (416 spots per sample, 4 samples per plate). The MS spectra were recalibrated internally based on the ion signal of neurotensin peptide (Sigma).

The following threshold criteria and settings were used for the acquisition of MS/MS spectra: Mass range: 800 to 4000 Da; minimum signal-to-noise (S/N) for MS/MS acquisition: 100; maximum number of peaks/spot: 8. Peptide CID was performed at a collision energy of 1 kV and a collision gas pressure of approximately 2.5 x 10^{-6} Torr. During MS/MS data acquisition, a method with a stop condition was used. In this method, a minimum of 1000 shots (20 sub-spectra accumulated from 50 laser shots each) and a maximum of 2000 shots (40 sub-spectra) were allowed for each

spectrum. The accumulation of additional laser shots was halted whenever at least 6 ion signals with an S/N of at least 60 were present in the accumulated MS/MS spectrum, in the region above *m/z* 200.

4.3.14. Peptide and protein identification and quantification by database searching

Raw spectra were processed with Mascot Distiller 2.2 (Matrix Science, London, UK) and protein identification and quantitation was performed using Mascot Version 2.2.0 (Matrix Science) as search engine. Mascot generic files were searched against a SwissProt human protein sequence database that was downloaded from ftp.ebi.ac.uk/pub/databases/SPproteomes (database release February 11, 2009; 117865 protein sequences (with 56722 forward and reverse sequences, respectively, and 259 contaminant sequences). The following search parameters were used: trypsin digestion, maximum missed cleavages: 2; maximum number of signals per spectrum: 55, peptide mass tolerance: 25 ppm and fragment ion tolerance: 0.3 Da. Further, iTRAQ4plex reagent labeling of lysine and of the N-terminal amino group of peptides and methylmethanethiosulfate-labeled (MMTS) modifications of cysteine were specified as fixed modifications, oxidation on methionine as variable modification. For the quantitation of iTRAQ labeled peptides the isotopic correction factor was used as supplied by the manufacturer (Applied Biosystems). iTRAQ ratios of proteins were median normalized and protein ratios were determined as the geometric mean of the peptide ratios. False discovery rates (FDR) were estimated by searches against a corresponding database containing forward and reversed sequences, according to the method of Kall (as described in chapter 3). Further analysis of proteomics data were performed using MATLAB 7.7.0. software (The MathWorks Inc., Bern, Switzerland).

4.4. Results

4.4.1. Differential gene expression in Hb-Hp treated macrophages

We performed gene array experiments of human peripheral blood monocyte-derived macrophages exposed for 2 and 5 days to Hb-Hp (2 mg/ml). Transcriptional profiles of identical experimental settings from three independent donors were analysed with Rosetta Biosoftware. After 2 days 451 genes were regulated ≥ 1.5-fold ($p \leq 0.01$) in these macrophages. Of the 451 genes significantly affected by 2 days of Hb-Hp

incubation, 153 were also significantly regulated after 5 days of Hb-Hp exposure (see supplemental data). Additionally, 775 genes affected by Hb-Hp treatment after 5 days were detected **(Figure 1)**. We assumed the 153 consistently regulated genes at both time points to be of biological significance and investigated them further. First, we applied a correlation analysis of genes commonly regulated at both time points. Thus, we determined which functional categories are over-represented among the up-regulated genes with a given statistical significance ($p < 0.01$; fold change > 1.5) using Metacore software. Genes were classified according to Metacore biological processes and in particular, significantly up-regulated genes were over-represented in categories related to cell adhesion, chemotaxis and responses to oxidative stress. Further, we found genes over-represented in the blood coagulation process and iron transport **(Figure 2)**. The complete set of genes is accessible at www.ebi.ac.uk/aerep/login (reviewer account login: Reviewer_E-MEXP-2820; Password: 1279719286410).

4.4.2. Confirmation of the microarray results by RT-PCR and western blot

In order to confirm the transcriptional expression pattern obtained from the microarray analysis we performed RT-PCR of selected genes related to chemotaxis (IL-8), anti-oxidative response (HO-1, SLC7A11), blood coagulation (PAI-2) and iron (heme) transport (ABCB6). Further, we chose to confirm the increased expression of the cholesterol transporter ABCG1 and the erythropoiesis stimulating kit ligand (KITLG) **(Figure 3)**. The regulation of IL-8 **(Figure 4B)**, HO-1, PAI-2 and xCT but also CD163 (data not shown) was confirmed at the protein level. Among the significantly regulated genes upon Hb-Hp exposure, we found that also NAD(P)H:quinone oxidoreductase (NQO1) and malic enzyme (ME1) contribute to the group of anti-oxidative genes.

4.4.3. Consistent IL-8 secretion drives leukocyte chemotaxis to injured tissue

IL-8, a cytokine with a recently detected NRF2 binding locus, was consistently enhanced by Hb-Hp treatment, both at 2 and 5 days. First, we investigated the secretion of IL-8 by Bio-Plex analysis in the macrophage supernatant at several time points after Hb-Hp treatment **(Figure 4A)**. At the earliest time point at 4 h, we could not observe any induced IL-8 secretion compared to untreated cells. With increasing time, at 24 h we detected a moderate but already significantly enhanced IL-8

secretion upon Hb-Hp stimulation. After 5 days of Hb-Hp exposure we observed a massive IL-8 secretion (up to 80 ng/ml). **Figure 4B** illustrates quantitative assessment of IL-8 within and outside the cell. At day 7 and 10 the major part of IL-8 was already secreted and not sequestered within the cell. In order to confirm the heme group being responsible for the IL-8 induction we isolated globin from hemoglobin and monitored IL-8 secretion using different concentrations of Hb-Hp and globin. **Figure 4C** shows that only a concentration of 2 mg/ml Hb-Hp causes a significant IL-8 secretion while globin failed to induce release of significant amounts of IL-8 at 2 mg/ml. Based on these findings we could justify the application of relatively high amounts of Hb-Hp and proof the activation of IL-8 most probably independent of the globin group. Since IL-8 under Hb-Hp exposure might be activated by Nrf-2 we investigated the activity of this transcription factor and observed an increasing activation with time **(Figure 4D)**. We assume that Hb-driven Nrf-2 activation leads to selective IL-8 secretion and enhanced leukocyte influx to the damaged tissue sites.

4.4.4. Hb-Hp exposed macrophages display an augmented Nrf-2 activation and selectively secrete IL-8

To further proof the exclusive role of IL-8 in a simulated wound scenario by exposure to high amounts of Hb-Hp we investigated the transcriptional expression and subsequent secretion of nuclear factor - κB (NF-κB) driven cytokines such as IL-1β, TNF-α and lL-6 as shown in **Figure 5**. After 2 days of Hb-Hp treatment neither IL-6 **(A)** nor IL-1β **(B)** was increased at mRNA level. IL-1β was not secreted either **(D)**. We monitored TNF-α levels starting at 30 min after Hb-Hp exposure up to 48h and could not observe any secretion. In contrast, monocytes stimulated with 100 ng/ml LPS showed an early secretion of TNF-α **(C)** with reaching a maximum at 4 h (~10ng/ml) as expected. Consequently, we did not observe any NF-κB (p65) activation (data not shown) in macrophages exposed to Hb-Hp compared to control cells.

We also monitored the effects of dexamethasone, a glucocorticoid for treatment of autoimmune hemolytic anemia, on macrophages. Using gene array analysis we observed that glucocorticoid priming (36h, $2.5x10^{-7}$M) and subsequent Hb-Hp exposure (8-16 h, 500 µg/ml) shifts the monocte differentiation towards a phenotype with highly efficient Hb clearance as shown in **Figure 6**. Moreover, these

macrophages showed a higher induction of IL-8 (fold change of 7.5) compared to macrophages exposed to glucocorticoid alone. Macrophages only treated with Hb-Hp for 8-16 h showed a moderate induction of IL-8 (fold change of 3.0). We observed an even higher expression of IL-8 in macrophages exposed to Hb-Hp (2 mg/ml) for 2 days (fold change of 10.6) or 5 days (fold change of 4.6) (data not shown). We conclude that glucocorticoid treatment could stimulate the monocyte anti-oxidant pathways during hemolysis.

4.4.5. Correlation analysis of macrophage transcriptome and proteome after Hb-Hp exposure

We recently investigated the composition of the macrophage proteome after long-term Hb-Hp using *state-of-the-art* proteome approaches (see chapter 3). As we could demonstrate, many proteins were significantly affected by Hb-Hp leading to the development of a characteristic anti-oxidative, Hb-clearing phenotype with decreased immune activating capacity by mainly reduced HLA class 2 expression. It seems obvious to compare the transcriptional profile of these macrophages at day 2 and 5 with the proteome of macrophages exposed to Hb-Hp for 7 days. To investigate how mRNA expression levels matched to protein expression levels we applied correlation analysis of the genes and proteins that exhibited a *p*-value less than 0.01 **(Figure 7)**. The correlation coefficient *per se* was expected to be suboptimal because of the large time interval between transcriptome and proteome analysis. Nevertheless, correlation analysis showed that HO-1 and PAI-2 were significantly induced at both mRNA and protein level.

Table 1 - *Oligonucleotides used for detection of indicated genes with RT-PCR*

Primer	**5'** **3'**	**5'** **3'**
HO-1	AGGGTGATAGAAGAGGCCAAGACT	TTCCACCGGACAAAGTTCATGGC
IL-8	AGACAGCAGAGCACACAAGC	AGTGTTCCTTCCGGTGGT
SLC7A11	GGCAGTGACCTTTTCTGAGC	TCATTGTCAAAGGGTGCAAA
ABCG1	CTGGTGAACAACCCTCCAGT	ATCTGCTGGGTTGTGGTAGG
PAI-2	GTTCATGCAGCAGATCCAGA	CGCAGACTTCTCACCAAACA
KitL	ATTCAAGAGCCCAGAACCC	CTGCTACTGCTGTCATTCC
HPRT	CCAGTCAACAAG	CACAATCAAGAC

Table 2 - *Antibodies used for western blot analysis*

Antibody	**Organism**	**Host**	**Dilution**	**Manufacturer**
IL-8	human	rabbit	1:1000	Peprotech
α-tubulin	human	mouse	1:5000	Abcam

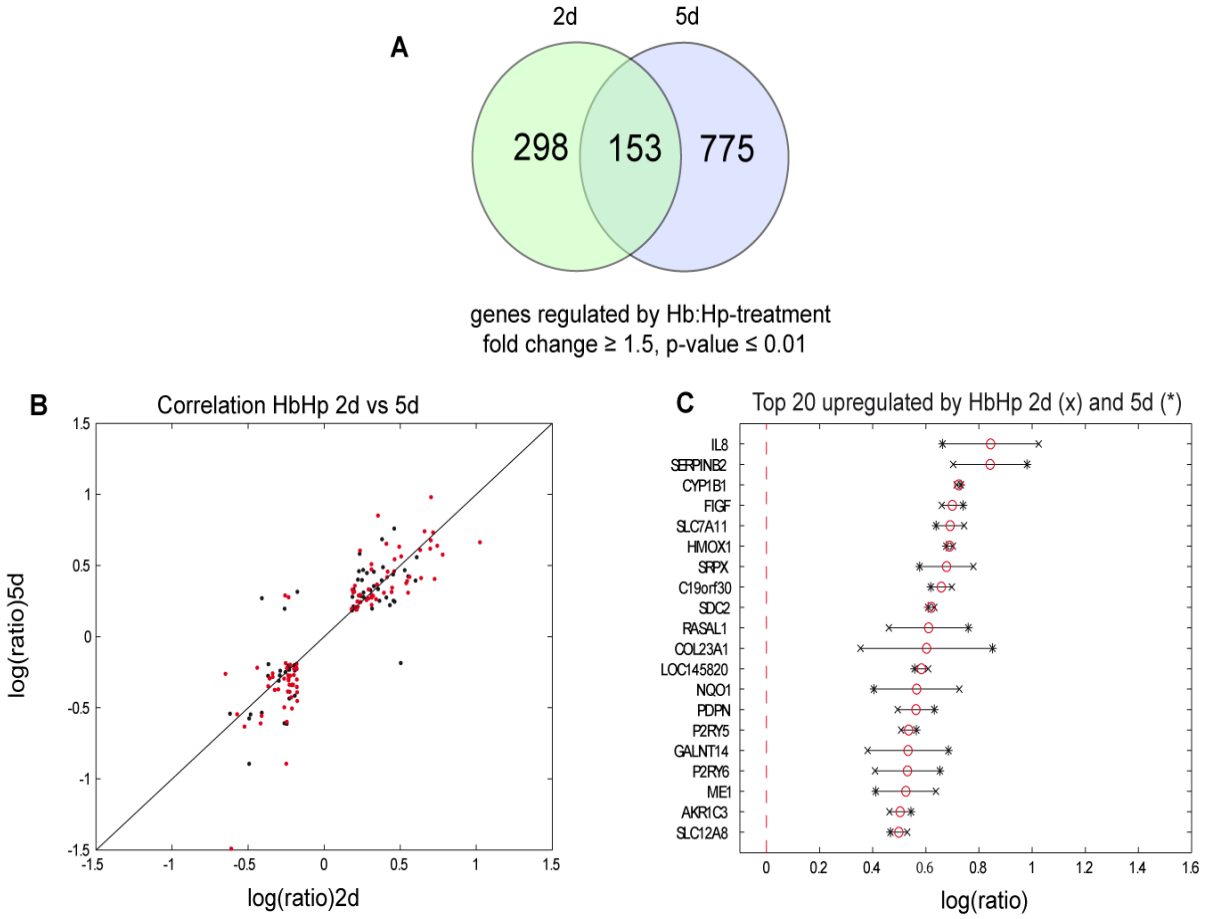

Figure 1 - Genes consistently regulated in macrophages exposed to Hb-Hp. (A) *Venn diagram of significantly regulated genes (p ≤ 0.01 and fold change ≥ 1.5) at day 2 and 5 after Hb-Hp exposure. A complete list of the 153 genes, including ratios and p values, is provided in* ***Supplementary Table 1 - 6****. **(B)** Correlation of significantly regulated genes (p ≤ 0.01 and fold change ≥ 1.5) 2 days and 5 days after Hb-Hp exposure. Red indicates genes with a p ≤ 0.0001. **(C)** Illustration of the top 20 up-regulated genes (p ≤ 0.0001 and fold change ≥ 1.5). Red circles represent the means between the log(ratio) of day 2(x) and day 5(*). Primary sequence cluster name of selected genes are indicated at the left y-axis. Data represent three independent experiments.*

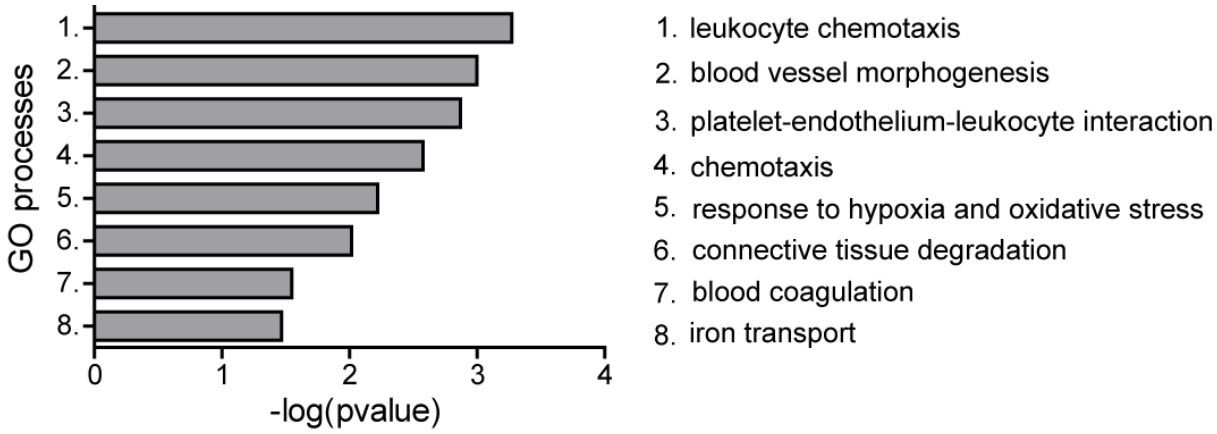

Figure 2 – Functional clustering of genes up-regulated by Hb-Hp exposure. *Genes showing a fold change of at least 1.5 at both time points, day 2 and day 5, were selected and characterized according to their GO biological process in the GeneGo Metacore software and compared to the classification of all present genes in the array in order to find which functional categories were over-represented ($p < 0.01$).*

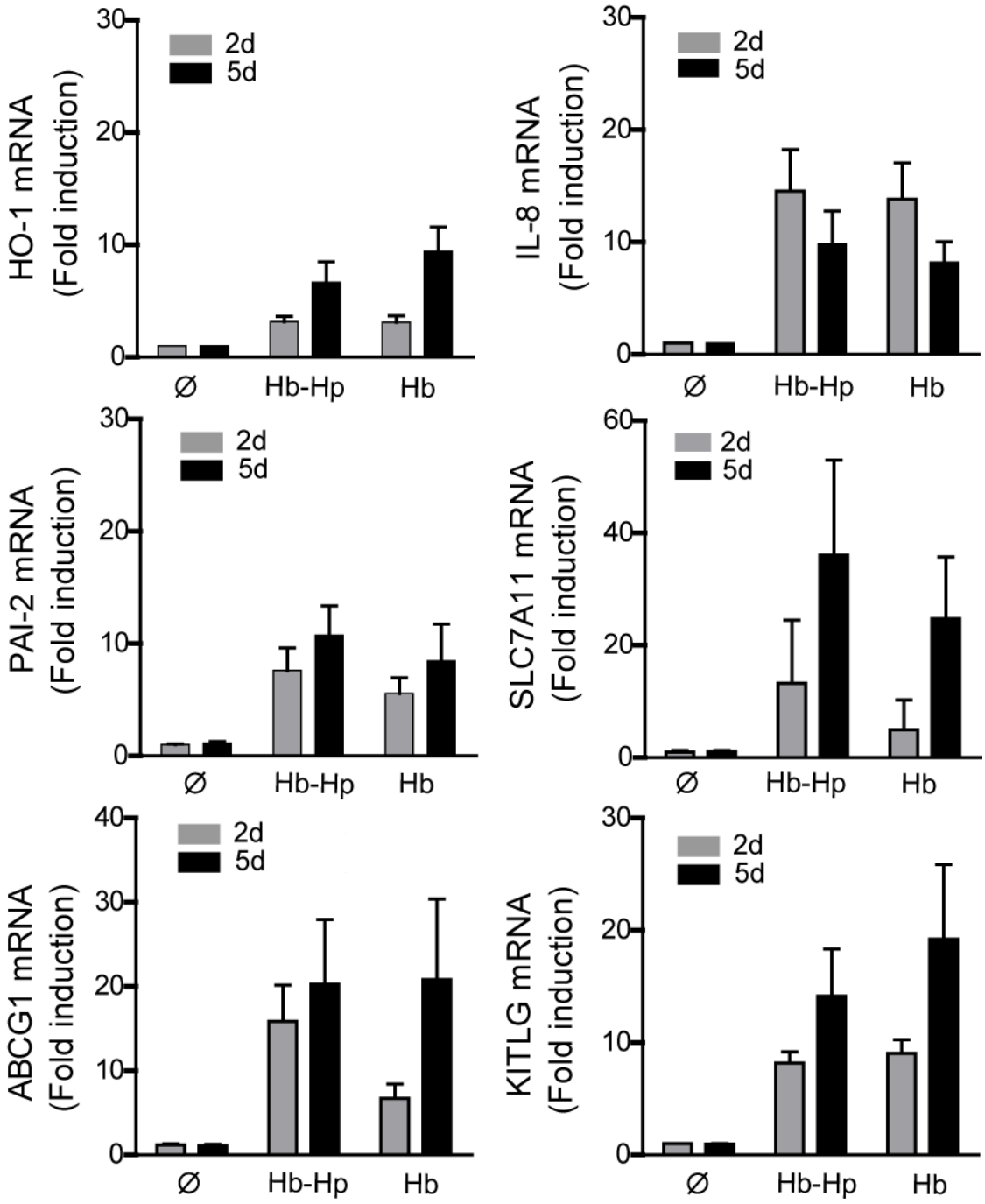

Figure 3 – RNA changes of selected genes responsive to Hb-Hp. *Induction of mRNA levels of selected target genes after incubation with either Hb-Hp or Hb (2 mg/ml each) for 2 days (grey bars) respective 5 days (black bars). Data represent means ± SEM from at least three independent measurements.*

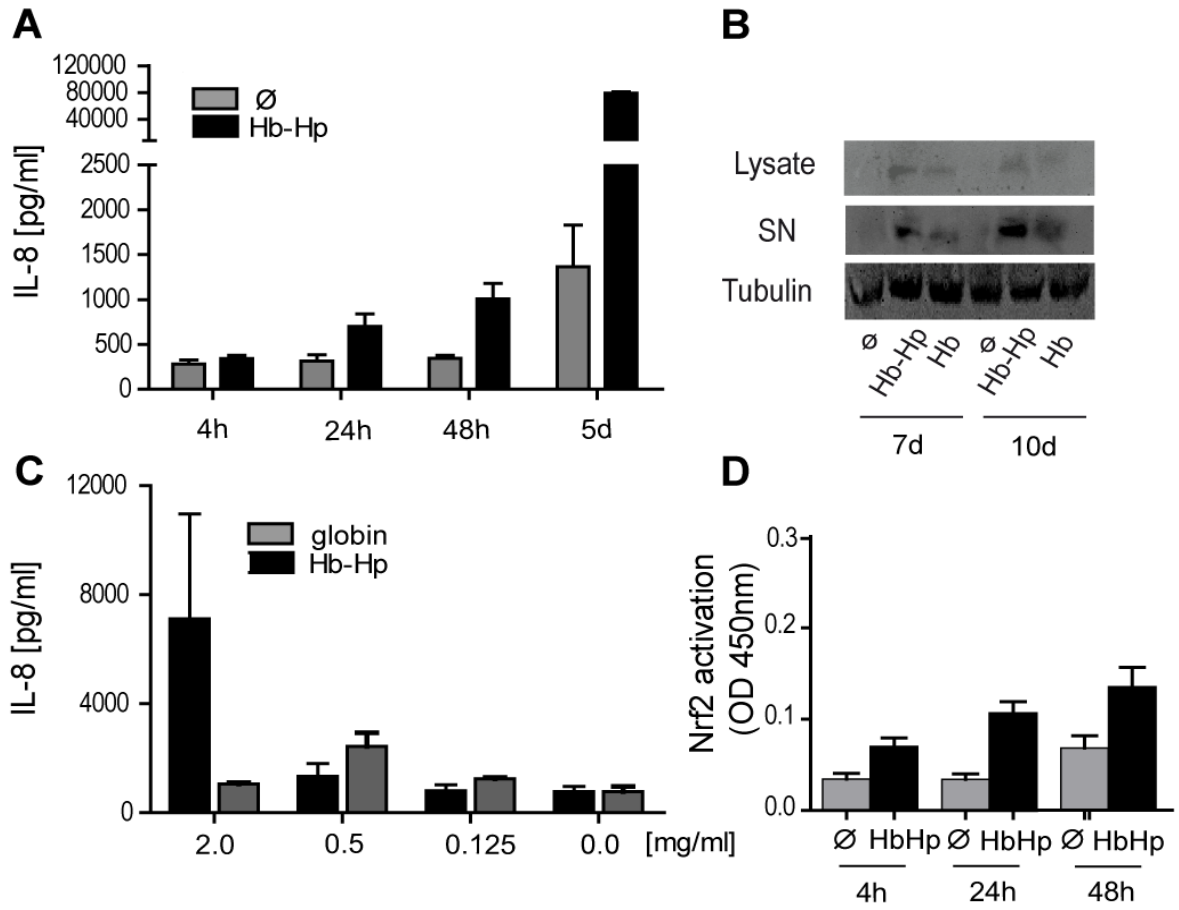

Figure 4 – Macrophages exposed to Hb-Hp display an augmented Nrf-2 activation and selectively secrete IL-8. (A) *IL-8 secretion upon Hb-Hp exposure (2 mg/ml) at different time points using Bio-Plex human cytokine singleplex assay.* ***(B)*** *Confirmation of secreted IL-8 in lysates and supernatants of Hb-Hp or Hb (2 mg/ml each) treated macrophages after 7 days respective 10 days. SN = supernatant.* ***(C)*** *Measurement of IL-8 in Hb-Hp or globin treated macrophage supernatant at different concentrations after 2 days using Bio-Plex human cytokine singleplex assay.* ***(D)*** *Nrf2 activity (OD450) in nuclear extracts of macrophages measured after incubation with Hb-Hp (2 mg/ml) at several time points. Data are means ± SEM from at least three independent measurements.*

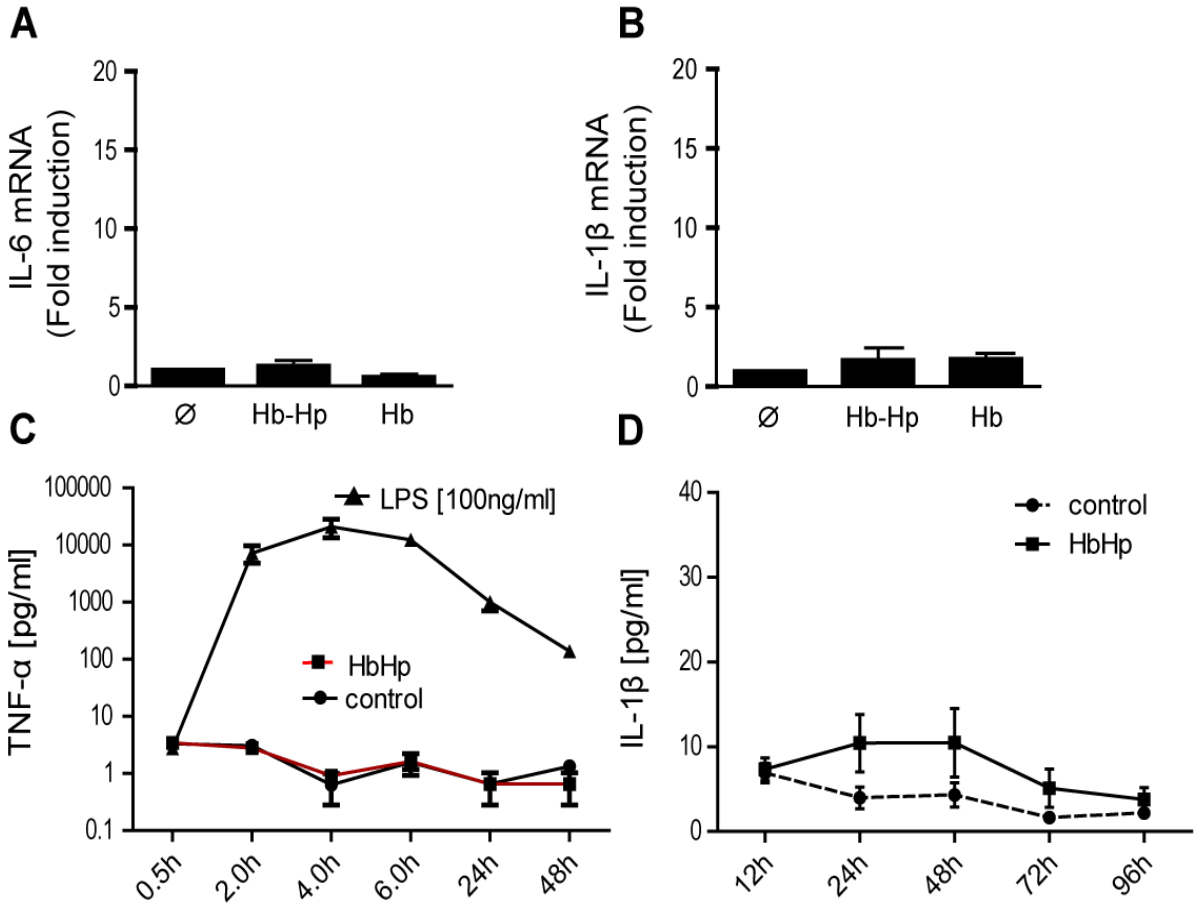

Figure 5 – Confirmation of the non-inflammatory response of Hb-Hp exposed macrophages. *Measurement of mRNA levels of IL-6* ***(A)*** *and IL-1β* ***(B)*** *after 2 days of incubation with Hb-Hp or Hb (2 mg/ml each).* ***(C)*** *TNF-α secretion in supernatants of macrophages stimulated with Hb-Hp or LPS (100 ng/ml) measured at several time points as indicated.* ***(D)*** *IL-1β secretion in supernatants of macrophages exposed to Hb-Hp for indicated time points. Shown are means ± SEM from at least three independent measurements.*

Figure 6 - Effects of the glucocorticoid dexamethasone and Hb-Hp on monocyte gene expression. *The table shows 47 genes significantly co-regulated by dexamethasone priming and Hb-Hp exposure, and were induced >1.5-fold in dexamethasone-primed cells. The graph on the right shows the corresponding gene expression changes (log ratio; mean ± error, n=4) induced by Hb-Hp (500 µg/ml) in either dexamethasone ($2.5x10^{-7}$ M) pre-treated (red) or non-treated (black) monocytes. Note that almost all genes on this list exhibit greater induction or suppression in monocytes pre-treated with dexamethasone pathway.*

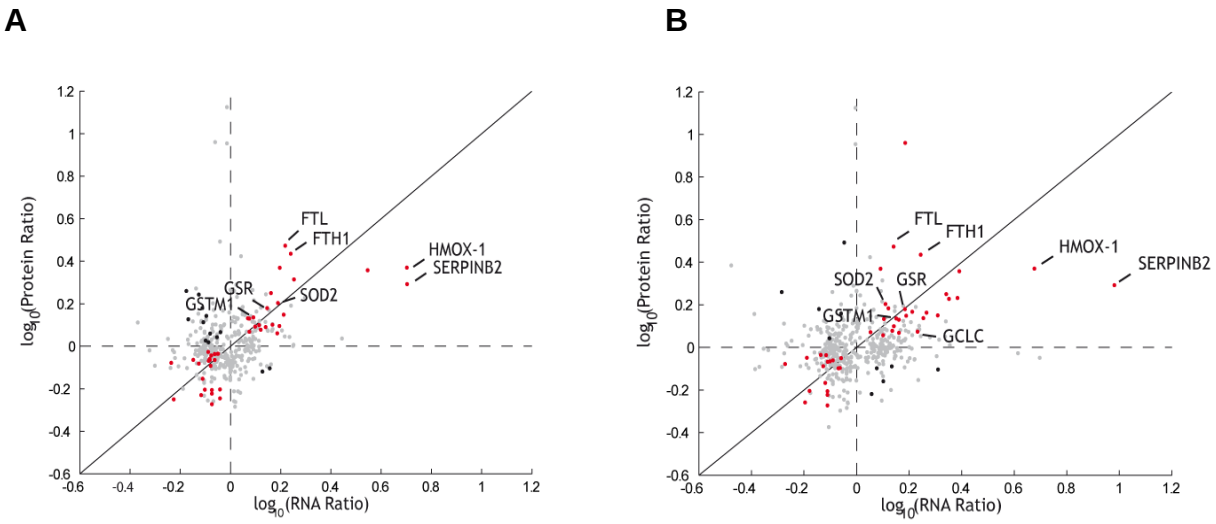

***Figure 7 – Correlation analysis of the macrophage transcriptome and proteome**. **(A)** Log(10) ratio of genes identified at day 2 correlated to their log(10) ratio of protein identified with MALDI-TOFTOF at day 7. **(B)** Log(10) ration of genes identified at day 5 correlated to their log(10) ratio of protein identified with MALDI-TOFTOF at day 7. Macrophages were exposed to 2 mg/ml Hb-Hp for indicated times. Red dots represent correlation of transcripts with their corresponding proteins, black dots indicate anti-correlation of genes and protein data, while grey dots represent no change in expression. (GCLC = Glutamate-cysteine ligase; GSR = Glutathione reductase; GSTM1 = Glutathione-S-transferase M1; FTH1 = Ferritin heavy chain; FTL = Ferritin light chain; SOD2 = Superoxide dismutase 2; SERPINB2 = PAI-2 = Plasminogen activator inhibitor 2). Data represent mean of three independent experiments.*

4.5. Discussion

Macrophages display a huge variety in their phenotypes depending on the particular microenvironment in specific tissues. In case of tissue injury, they are known to be the most important mediators for wound healing which follows a predictable sequence of events [13-15]. Nevertheless, adequate knowledge about this highly specialized macrophage phenotype is still missing. In the current study we could contribute to the understanding of macrophages involved in tissue repair by following findings: *1)* Enhanced Hb uptake capacity by increased scavenger receptor CD163 expression with subsequent HO-1 induction and anti-oxidant homeostasis after administration of excess Hb-Hp. *2)* Selectively stimulated secretion of the leukocyte chemo-attractant IL-8 and inhibited pro-inflammatory activity indicating a protective and non-inflammatory phenotype with the ability to recruit other cells to the site of injury.

Gene arrays provide a powerful tool to explore the differences among expression levels of less abundant but highly active genes, such as cytokines. We could show that macrophages respond to Hb-Hp with a specialized Hb-clearing, anti-oxidant, and tissue repair promoting pathway. Recently, we applied proteomic strategies to discover the complex macrophage proteome but also to investigate the most abundant regulated proteins affected by Hb-Hp treatment. To our surprise, these macrophages displayed a remarkable suppression of antigen presentation by HLA class 2 molecules. Further, these macrophages showed high levels of ferritin which contributes to the Hb degradating and iron recycling activity. To monitor the changes in gene expression and the consistently expression of biological most important regulated genes we focused on the macrophage genotype after 2 and 5 days of Hb-Hp exposure. Nevertheless, a comparison between transcriptome and proteome could be expected to be rather complementary than correlative in the herein presented time frame. Correlation analysis returning a higher correlation coefficient is often due to more narrow time subsets allowing less space for post-translational modifications.

Erythropoiesis is regulated by a number of growth factors, among which kit ligand plays a non-redundant function [16]. Kit ligand has been claimed to cause proliferation

but not differentiation of hematopoietic cells [17-18] and has been reported to support the maintenance of primitive hematopoietic progenitor cells [18]. Acute anemia induces a systemic response characterized by a rapid mobilization and differentiation of erythroid progenitors [19]. In this case the expansion and differentiation of a specialized population of stress erythroid progenitors is known to play an important role during recovery from acute anemia. Kit ligand has been shown to greatly expand the progeny of these stress erythroid progenitors and led to the suggestion that kit ligand/kit signalling may play a role in stress-erythropioesis [20]. Macrophages treated with Hb-Hp showed a high induction of kit ligand linking Hb- clearance of macrophages to enhanced erythropioesis during hemolysis putatively due to increased availability of recycled iron. Although we found high levels of kit ligand mRNA in macrophages exposed to Hb-Hp for 2 and 5 days we did not observe kit ligand in the macrophage proteome after 7 days of Hb-Hp treatment. We assume that there are yet unknown mediators that inhibit the translation of kit ligand mRNA into protein during iron homeostasis. Also, post-translational modifications (PTMs) might have an influence on the protein expression of kit ligand.

The SLC7A11 gene that we found highly induced upon Hb-Hp exposure **(Figure 1C and Figure 3)**, encodes the heterodimeric plasma membrane cystine/glutamate exchanger which mediates the entry of cystine into the cell by simultanous efflux of glutamate [21-22]. Inside the cell, cystine is rapidly reduced to cysteine, the rate limiting substrate for the synthesis of reduced glutathione (GSH), that plays an important role in the cell's defense against oxidative stress [23]. Treatment of macrophages with Hb-Hp showed a high xCT mRNA level compared with untreated macrophages and led us to the assumption that this antiporter is an important marker during monocyte differentiation under Hb-Hp exposure. xCT-overexpressing cells become highly resistant to oxidative stress, particulary upon GSH depletion. Thus, the regulated expression of SLC7A11 contributes to the anti-oxidative activity of macrophages during hemolysis and tissue repair. Also, strong evidence for the anti-oxidative character of Hb-Hp exposed macrophages is the highly induced heme transporter ABCB6 that mediates heme-iron influx from the cytoplasm into the mitochondria and promotes mitochondrial metal homeostasis under oxidative stress [24].

Hb-Hp uptake by macrophages over the period of 2-7 days induced PAI-2 (also SERPINB2) mRNA and protein levels. PAI-2 is considered to be a stress protein and one of the most up-regulated proteins of activated macrophages [25-26]. Further, it is proposed to exhibit roles in the regulation of inflammation and wound healing [26]. Locally secreted PAI-2 in tissues could limit extracellular proteolysis during tissue remodelling, such as it appears during wound healing. These findings contribute to the defined macrophage phenotype.

By analysing the list of transcripts that were enhanced by Hb-Hp treatment we detected an over-representation of genes regulated by the transcription factor Nrf-2 that binds to the anti-oxidant response element (ARE). We could show that anti-oxidant genes such as HO-1, NQO1 and GCLM are highly regulated by Nrf-2. In the present study we could show that the cytokine IL-8, which was recently found to exhibit an ARE binding site, is also likely to be regulated by Nrf-2. In particular, Nrf-2 is suggested to increase the half-life of IL-8 mRNA. We monitored IL-8 secretion and found significant amounts of this cytokine in the supernatant of Hb-Hp treated macrophages. Following, we investigated Nrf-2 activation upon Hb-Hp treatment in these macrophages and found it to be significantly activated. To further investigate the selective activation of Nrf-2 we analysed levels of typical NF-κB driven pro-inflammatory cytokines such as IL-1β, TNF-α and IL-6. As expected, we could not detect any induced expression of inflammatory cytokines and accordingly levels of NF-κB remained at the basal activity compared to control macrophages. It is known that a constitutive expression of NF-κB in monocyte-derived macrophages is essential to maintain mitochondrial homeostasis and increase cell survival [27]. Further, HO-1 derived CO was reported to require NF-κB activity in order to protect against apoptosis of endothelial cells [28].

HO-1 has been demonstrated to be a down-stream effector of IL-10 [29] and Hb-Hp complexes in turn trigger the induction of IL-10 and HO-1 [11]. Interestingly, our Hb-Hp exposed macrophages lacked the expression of IL-10 but showed a high induction of anti-oxidative enzymes such as HO-1. We speculated that former observed IL-10 induction upon Hb-Hp uptake was most probably due to endotoxin-contaminated Hb. Since we use purified endotoxin-free Hb in our experimental setup we could exclude any contaminations and accordingly LPS-induced IL-10 expression. Also, we found

GTP cyclohydrolase 1, an enzyme mediating the biosynthesis of neopterin derivates in human macrophages, to be significantly down-regulated upon Hb-Hp exposure. Neopterin levels in human body fluids serve as a common innate immune system and macrophage activation marker [30], and in turn suggest a deactivation of the macrophages in our experiments. These findings support our theory that Hb-Hp exposed macrophages develop a non-inflammatory phenotype highly dependent on the anti-oxidative effects of HO-1 and its by-products.

A limitation of the study is the *in vitro* culture of pure macrophages cannot reflect the complex situation in wounded tissues. Nevertheless, we were interested in investigating the direct effect of Hb-Hp complexes in a standardised system of macrophages with the unique ability to clear and detoxify these complexes in a wound. Further studies could explore the impact of Hb-Hp polarized macrophages on other cell types such as T-cells, neutrophils and endothelial cells.

In conclusion, Hb-Hp challenged macrophages displayed a protective geno- and phenotype shift characterized by enhanced anti-oxidative response linked to increased iron-homeostasis. Further, these macrophages did not express any pro-inflammatory mediators in order to create a non-inflammatory milieu e.g. in wounds to promote tissue repair. Also, by selective release of IL-8 they could consult other leukocytes and flag the area of damage. The findings in the present study support the idea of a highly specialized Hb-Hp induced macrophage sub-population in hemolysis, wound healing or inflammation. Further, this phenotype switch could be supportingly induced by the application of glucocorticoids in the case of hemolysis.

4.6. Supplement

Table 1: Genes significantly regulated ($p \leq 0.01$ and fold change ≥ 1.5) at 2 days and 5 days after Hb-Hp exposure.

Description	Primary Sequence Cluster Name	log(Ratio) 2d*	Pvalue 2d	log(Ratio) 5d*	Pvalue 5d
Full length insert cDNA clone ZE12B03	Hs.418279	1.036	0.00001024	0.695	0.003
Interleukin 8	IL8	1.025	2.147E-08	0.663	4.515E-30
Sushi-repeat-containing protein, X-linked	SRPX	0.779	0	0.577	0.00007605
Solute carrier family 7, (cationic amino acid transporter, y+ system) member 11	SLC7A11	0.744	8.933E-22	0.639	2.063E-08
NAD(P)H dehydrogenase, quinone 1	NQO1	0.726	0	0.405	6.933E-10
Cytochrome P450, family 1, subfamily B, polypeptide 1	CYP1B1	0.716	0	0.732	9.664E-23
Serpin peptidase inhibitor, clade B (ovalbumin), member 2	SERPINB2	0.703	7.302E-15	0.981	1.74E-37
Heme oxygenase (decycling) 1	HMOX1	0.702	0	0.677	0.00002496
Chromosome 19 open reading frame 30	C19orf30	0.698	6.464E-11	0.619	1.005E-07
C-fos induced growth factor (vascular endothelial growth factor D)	FIGF	0.660	0.000006483	0.740	1.516E-15
Malic enzyme 1, NADP(+)-dependent, cytosolic	ME1	0.638	0	0.412	9.705E-12
Syndecan 2 (heparan sulfate proteoglycan 1, cell surface-associated, fibroglycan)	SDC2	0.632	0	0.609	0.00003165
hypothetical protein LOC145820	LOC145820	0.609	0.0000506	0.558	0.002
Cysteinyl leukotriene receptor 2	CYSLTR2	0.601	0.0000049	0.394	0.0001771
hypothetical protein FLJ20489	FLJ20489	0.562	0	0.420	3.657E-43
Neuromedin U	NMU	0.553	0.0000973	0.424	0.001
Pirin (iron-binding nuclear protein)	PIR	0.552	5.825E-37	0.309	8.614E-11
Fucosidase, alpha-L- 1, tissue	FUCA1	0.546	7.391E-08	0.391	7.429E-13
Tumor necrosis factor (ligand) superfamily, member 14	TNFSF14	0.540	4.61E-13	0.376	4.322E-10
Solute carrier family 12 (potassium/chloride transporters), member 8	SLC12A8	0.530	0.003	0.467	0.009
Purinergic receptor P2Y, G-protein coupled, 5	P2RY5	0.507	2.469E-38	0.564	5.534E-40
Meprin A, alpha (PABA peptide hydrolase)	MEP1A	0.504	0.005	-0.185	0.002
Podoplanin	PDPN	0.494	8.976E-12	0.632	3.475E-19
ATP-binding cassette, sub-family A (ABC1), member 1	ABCA1	0.464	2.061E-13	0.246	0.0001719
Aldo-keto reductase family 1, member C3 (3-alpha hydroxysteroid dehydrogenase, type II)	AKR1C3	0.463	0.00002708	0.544	0
RAS protein activator like 1 (GAP1 like)	RASAL1	0.461	0.0007207	0.760	9.236E-41
Chemokine (C-X-C motif) ligand 3	CXCL3	0.460	9.206E-18	0.459	3.13E-09
Ameloblastin (enamel matrix protein)	AMBN	0.456	0.007	0.253	0.0007211
Endothelin receptor type B	EDNRB	0.454	1.085E-13	0.438	0.0009832

* log(Ratio) was calculated from fold changes of gene expression using the ratio function of Rosetta Biosoftware. Data are from three independent experiments ($p \leq 0.01$).

Table 2: Genes significantly regulated ($p \leq 0.01$ and fold change ≥ 1.5) at 2 days and 5 days after Hb-Hp exposure.

Description	Primary Sequence Cluster Name	log(Ratio) 2d*	Pvalue 2d	log(Ratio) 5d*	Pvalue 5d
Laminin, gamma 1 (formerly LAMB2)	LAMC1	0.447	1.536E-32	0.344	2.258E-16
ATP-binding cassette, sub-family B (MDR/TAP), member 6	ABCB6	0.444	0	0.314	1.621E-38
Intelectin 1 (galactofuranose binding)	ITLN1	0.432	0.0005376	0.221	0.008
MRNA; cDNA DKFZp686B14224 (from clone DKFZp686B14224)	Hs.634057	0.431	0	0.338	2.689E-18
(clone 1NIB-4) normalized cDNA library sequence	Hs.224794	0.420	0.0003348	0.338	5.046E-36
Hypothetical protein DKFZp566N034	TMEM163	0.418	1.204E-40	0.457	2.406E-11
Chemokine (C-X-C motif) ligand 2	CXCL2	0.414	2.829E-11	0.418	7.955E-24
Pyrimidinergic receptor P2Y, G-protein coupled, 6	P2RY6	0.409	6.24E-09	0.653	1.628E-09
CD163 molecule-like 1	CD163L1	0.409	5.776E-14	0.275	0.0001659
Proprotein convertase subtilisin/kexin type 6	PCSK6	0.393	5.59E-39	0.308	3.159E-20
Collagen, type V, alpha 2	COL5A2	0.387	0.008	0.488	7.311E-09
UDP-N-acetyl-alpha-D-galactosamine:polypeptide N-acetylgalactosaminyltransferase 14 (GalNAc-T14)	GALNT14	0.381	0.01	0.685	0
Xylosyltransferase I	XYLT1	0.379	0.009	0.396	0.0007003
Transmembrane and tetratricopeptide repeat containing 1	TMTC1	0.364	0.00009015	0.252	0.000828
Homo sapiens, clone IMAGE:3618365, mRNA	Hs.434957	0.357	0.006	0.177	0.00001433
Chromosome 14 open reading frame 162	C14orf162	0.355	0.0004847	0.334	0.0001288
Collagen, type XXIII, alpha 1	COL23A1	0.354	2.62E-29	0.851	0
Tetratricopeptide repeat domain 9	TTC9	0.348	1.751E-09	0.366	1.886E-14
Zinc finger protein 366	ZNF366	0.341	0.00009755	0.263	1.491E-08
Intercellular adhesion molecule 5, telencephalin	ICAM5	0.327	0.0006515	0.355	6.203E-08
Epithelial membrane protein 2	EMP2	0.327	1.526E-09	0.456	0.0002402
Elongation factor, RNA polymerase II, 2	ELL2	0.322	6.44E-21	0.287	2.129E-14
Chromosome 5 open reading frame 20	C5orf20	0.315	0.007	0.197	0.003
Chromosome 9 open reading frame 30	C9orf30	0.312	7.101E-37	0.223	0
Sulfiredoxin 1 homolog (S. cerevisiae)	SRXN1	0.312	5.849E-09	0.275	1.329E-17
Claudin 23	CLDN23	0.311	2.545E-26	0.294	2.701E-12
G protein-coupled receptor 35	GPR35	0.311	5.692E-09	0.510	4.267E-17
SH3 and PX domains 2A	SH3PXD2A	0.311	2.501E-14	0.473	8.391E-14
Transcribed locus, strongly similar to XP_370665.1 PREDICTED: similar to DnaJ (Hsp40) homolog, subfamily B, member 6 isoform a; heat shock protein J2	Hs.504270	0.308	0.0002835	0.226	4.067E-08
Transcribed locus	Hs.643844	0.306	0.003	0.369	2.963E-07

* log(Ratio) was calculated from fold changes of gene expression using the ratio function of Rosetta Biosoftware. Data are from three independent experiments ($p \leq 0.01$).

Table 3: Genes significantly regulated ($p \leq 0.01$ and fold change ≥ 1.5) at 2 days and 5 days after Hb-Hp exposure.

Description	Primary Sequence Cluster Name	log(Ratio) 2d*	Pvalue 2d	log(Ratio) 5d*	Pvalue 5d
Sphingomyelin phosphodiesterase, acid-like 3A	SMPDL3A	0.304	0.001	0.328	6.297E-15
CRLF1 associated cytokine-like factor 1	CLCF1	0.292	5.815E-22	0.332	7.018E-17
Glutamate-cysteine ligase, modifier subunit	GCLM	0.291	2.365E-24	0.268	3.294E-09
CD226 molecule	CD226	0.281	0.001	0.447	0.002
Glutathione S-transferase M3 (brain)	GSTM3	0.279	7.463E-21	0.257	4.299E-07
CDNA FLJ41489 fis, clone BRTHA2004582	Hs.446388	0.267	0.0002321	0.204	0.001
Von Willebrand factor	VWF	0.259	0.008	0.310	0
Tripartite motif-containing 16	TRIM16	0.259	0.0003023	0.278	5.555E-24
G protein-coupled receptor 68	GPR68	0.257	0.0002085	0.469	0.005
Frequenin homolog (Drosophila)	FREQ	0.249	0.000756	0.398	3.057E-21
Ferritin, heavy polypeptide 1	FTH1	0.240	5.277E-09	0.244	2.019E-41
Myosin binding protein H	MYBPH	0.240	0.000003092	0.286	0.005
Stabilin 1	STAB1	0.236	0.000001097	0.605	0
TRAF2 and NCK interacting kinase	TNIK	0.236	2.085E-08	0.293	3.134E-16
Solute carrier family 7 (cationic amino acid transporter, y+ system), member 8	SLC7A8	0.235	0.0000731	0.243	0.0003104
Transmembrane protein 45B	TMEM45B	0.234	0.002	0.583	2.585E-10
Hypothetical protein LOC283824	LOC283824	0.229	3.78E-15	0.460	0.004
Regulator of chromosome condensation (RCC1) and BTB (POZ) domain containing protein 2	RCBTB2	0.227	1.539E-21	0.290	9.982E-16
Poliovirus receptor-related 4	PVRL4	0.222	0.005	0.401	0.0004936
V-maf musculoaponeurotic fibrosarcoma oncogene homolog F (avian)	MAFF	0.222	2.269E-13	0.209	6.47E-09
Spermine oxidase	SMOX	0.218	1.028E-08	0.247	7.313E-13
Basic helix-loop-helix domain containing, class B, 3	BHLHB3	0.214	6.694E-13	0.190	0.002
Transaldolase 1	TALDO1	0.212	5.099E-14	0.189	5.852E-10
Integrin, alpha E (antigen CD103, human mucosal lymphocyte antigen 1; alpha polypeptide)	ITGAE	0.206	7.098E-14	0.209	1.354E-07
Phosphofructokinase, platelet	PFKP	0.202	2.155E-11	0.358	2.979E-26
Zinc finger protein 746	ZNF746	0.201	9.721E-18	0.198	0.0003449
Microsomal glutathione S-transferase 1	MGST1	0.198	1.966E-24	0.315	1.185E-18
CDNA FLJ38345 fis, clone FCBBF3028671	Hs.380705	0.197	0.0005705	0.467	1.053E-26
Kruppel-like factor 9	KLF9	0.194	5.885E-07	0.330	0.004
Forkhead box C2 (MFH-1, mesenchyme forkhead 1)	FOXC2	0.192	0.01	0.212	0.003

* log(Ratio) was calculated from fold changes of gene expression using the ratio function of Rosetta Biosoftware. Data are from three independent experiments ($p \leq 0.01$).

Table 4: Genes significantly regulated ($p \leq 0.01$ and fold change ≥ 1.5) at 2 days and 5 days after Hb-Hp exposure.

Description	Primary Sequence Cluster Name	log(Ratio) 2d*	Pvalue 2d	log(Ratio) 5d*	Pvalue 5d
Cat eye syndrome chromosome region, candidate 6	CECR6	0.191	4.854E-09	0.311	4.395E-29
Homo sapiens, clone IMAGE:5404753, mRNA	Hs.621233	0.187	0.001	0.208	0.002
ADP-ribosylation factor-like 4C	ARL4C	0.186	0.0003068	0.280	1.262E-07
Cyclin-dependent kinase inhibitor 1C (p57, Kip2)	CDKN1C	0.185	5.032E-11	0.330	4.141E-19
Splicing factor 3a, subunit 2, 66kDa	SF3A2	0.183	0.001	0.183	0.0008051
CD58 molecule	CD58	0.181	2.631E-19	0.195	2.211E-17
Transcribed locus	Hs.621904	0.181	0.002	0.186	0.000007795
Dedicator of cytokinesis 10	DOCK10	-0.176	0.001	0.315	6.891E-14
Deoxyribonuclease I-like 3	DNASE1L3	-0.177	0.000000282	-0.452	1.892E-07
Chromosome 5 open reading frame 13	C5orf13	-0.178	0.000009968	-0.391	0
HLA-B associated transcript 3	ACRBP	-0.179	3.22E-08	-0.301	1.249E-08
Growth factor receptor-bound protein 10	GRB10	-0.179	1.017E-07	-0.354	0.000002994
Discoidin, CUB and LCCL domain containing 1	DCBLD1	-0.180	0.00004725	-0.228	2.388E-22
Potassium voltage-gated channel, shaker-related subfamily, beta member 1	KCNAB1	-0.181	6.353E-11	-0.191	6.045E-12
Activating transcription factor 4 (tax-responsive enhancer element B67)	ATF4	-0.182	3.62E-08	-0.219	5.746E-15
Serine palmitoyltransferase, long chain base subunit 2-like (aminotransferase 2)	SPTLC2L	-0.193	0.0001201	-0.415	0.006
Protein S (alpha)	PROS1	-0.193	0.005	-0.238	9.963E-10
Kenae	CCDC125	-0.194	0.0004643	-0.199	0.0001131
Pleckstrin homology domain containing, family F (with FYVE domain) member 2	PLEKHF2	-0.197	0.0001478	-0.203	3.851E-09
Anaphase promoting complex subunit 7	ANAPC7	-0.198	9.007E-21	-0.227	4.555E-24
Endothelial differentiation, lysophosphatidic acid G-protein-coupled receptor, 7	EDG7	-0.199	2.635E-10	-0.269	0.000001522
SH3 multiple domains 4	SH3MD4	-0.204	5.473E-12	-0.338	9.881E-19
Solute carrier organic anion transporter family, member 4C1	SLCO4C1	-0.209	0.002	-0.337	0.00002972
Paraneoplastic antigen like 6A	PNMA6A	-0.211	0.0000109	-0.506	1.495E-18
Immunoglobulin superfamily, member 4	CADM1	-0.212	6.563E-09	-0.341	0.00005789
Solute carrier family 16 (monocarboxylic acid transporters), member 7	SLC16A7	-0.216	0.00003754	-0.427	6.251E-37
Myosin, light polypeptide kinase	MYLK	-0.223	0.000004242	-0.198	3.132E-07
Poly(A) binding protein, cytoplasmic 4 (inducible form)	PABPC4	-0.224	3.332E-22	-0.275	6.186E-16
Hepatocyte growth factor (hepapoietin A; scatter factor)	HGF	-0.227	0.000001185	-0.388	2.88E-19
CD22 molecule	CD22	-0.228	2.946E-37	-0.338	7.293E-40

* log(Ratio) was calculated from fold changes of gene expression using the ratio function of Rosetta Biosoftware. Data are from three independent experiments ($p \leq 0.01$).

Table 5: Genes significantly regulated ($p \leq 0.01$ and fold change ≥ 1.5) at 2 days and 5 days after Hb-Hp exposure.

Description	Primary Sequence Cluster Name	log(Ratio) 2d*	Pvalue 2d	log(Ratio) 5d*	Pvalue 5d
Transforming growth factor, alpha	TGFA	-0.229	0.005	-0.435	0.0004643
G protein-coupled receptor 92	GPR92	-0.230	0.0002423	-0.233	4.283E-11
Calcium binding protein 39	CAB39	-0.230	0.001	-0.207	0.005
CD1a molecule	CD1A	-0.234	2.172E-11	-0.295	3.406E-15
Pleckstrin homology-like domain, family A, member 3	PHLDA3	-0.234	4.48E-13	0.277	2.396E-13
Transient receptor potential cation channel, subfamily V, member 4	TRPV4	-0.234	0.00003455	-0.307	1.133E-19
Annexin A6	ANXA6	-0.236	2.403E-16	-0.272	0.000007439
RAS-related on chromosome 22	RASL10A	-0.236	0.00002197	-0.204	0.0001026
Transcribed locus	Hs.435992	-0.238	0.001	-0.377	0.002
Stathmin 1/oncoprotein 18	STMN1	-0.239	0.000003264	-0.386	0
Orosomucoid 1	ORM1	-0.245	0.000000113	-0.221	8.642E-08
hypothetical LOC646278	LOC646278	-0.245	0.00002158	-0.599	1.902E-12
Chemokine (C-X-C motif) ligand 10	CXCL10	-0.246	0.002	-0.613	4.539E-08
Apolipoprotein B mRNA editing enzyme, catalytic polypeptide-like 3A	APOBEC3A	-0.249	4.157E-11	-0.893	3.425E-19
Homo sapiens, clone IMAGE:4344826, mRNA	Hs.597585	-0.251	0.000002983	-0.237	0.000002038
Glycolipid transfer protein	GLTP	-0.253	1.799E-13	-0.186	4.901E-14
similar to methylenetetrahydrofolate dehydrogenase (NADP+ dependent) 1-like	LOC644311	-0.254	0.0001551	-0.250	0.003
Tumor necrosis factor receptor superfamily, member 11a, NFKB activator	TNFRSF11A	-0.257	5.229E-07	0.290	5.613E-07
G protein-coupled receptor 30	GPR30	-0.260	0.0002644	0.196	0.008
adipocyte-specific adhesion molecule	ASAM	-0.261	0.01	-0.609	1.258E-07
Baculoviral IAP repeat-containing 7 (livin)	BIRC7	-0.262	4.36E-15	-0.497	2.562E-20
Toll-like receptor 7	TLR7	-0.263	9.055E-08	-0.295	6.697E-09
CDNA: FLJ22734 fis, clone HUV00109	Hs.306842	-0.272	0.0006461	-0.177	0.008
Uveal autoantigen with coiled-coil domains and ankyrin repeats	UACA	-0.289	1.995E-07	-0.240	0.001
Heterogeneous nuclear ribonucleoprotein A1	FAM59A	-0.292	0.0009016	-0.272	0.000004413
Jun dimerization protein p21SNFT	SNFT	-0.298	0.003	-0.310	2.195E-15
Guanine nucleotide binding protein (G protein), gamma 2	GNG2	-0.301	0.000001878	-0.370	1.384E-07
Sterile alpha motif domain containing 13	SAMD13	-0.325	0.000001804	-0.374	5.215E-29
Tribbles homolog 3 (Drosophila)	TRIB3	-0.338	7.693E-37	-0.284	1.954E-16
Interleukin 18 (interferon-gamma-inducing factor)	IL18	-0.339	1.925E-25	-0.258	1.199E-23

* log(Ratio) was calculated from fold changes of gene expression using the ratio function of Rosetta Biosoftware. Data are from three independent experiments ($p \leq 0.01$).

Table 6: Genes significantly regulated ($p \leq 0.01$ and fold change ≥ 1.5) at 2 days and 5 days after Hb-Hp exposure.

Description	Primary Sequence Cluster Name	log(Ratio) 2d*	Pvalue 2d	log(Ratio) 5d*	Pvalue 5d
Beta-1,3-N-acetylgalactosaminyltransferase 1 (globoside blood group)	B3GALNT1	-0.359	0.00000156	-0.294	0.000000841
DnaJ (Hsp40) homolog, subfamily C, member 12	DNAJC12	-0.366	0.0002363	-0.193	0.0001681
Hypothetical protein FLJ22746	FAM124B	-0.368	0.00001427	-0.349	2.51E-17
Retinol binding protein 4, plasma	RBP4	-0.369	0.0004895	-0.276	1.078E-22
CD1e molecule	CD1E	-0.409	0.00002999	0.270	0.002
Peroxisome proliferative activated receptor, gamma, coactivator 1, alpha	PPARGC1A	-0.410	2.543E-15	-0.535	0.002
Mannose receptor, C type 2	MRC2	-0.411	1.145E-12	-0.556	1.975E-14
Murine retrovirus integration site 1 homolog	MRVI1	-0.418	2.58E-15	-0.610	0.000001292
ST6 (alpha-N-acetyl-neuraminyl-2,3-beta-galactosyl-1,3)-N-acetylgalactosaminide alpha-2,6-sialyltransferase 3	ST6GALNAC3	-0.440	0.000001589	-0.219	3.294E-12
Eyes absent homolog 2 (Drosophila)	EYA2	-0.484	0.0003614	-0.547	1.193E-27
G protein-coupled receptor 85	GPR85	-0.493	0.0001025	-0.894	8.906E-09
Otoancorin	OTOA	-0.493	0.0007108	-0.575	0.000494
Phosphoglycerate dehydrogenase	PHGDH	-0.524	1.158E-07	-0.632	4.47E-12
Aldehyde dehydrogenase 1 family, member L2	ALDH1L2	-0.572	1.908E-07	-0.546	2.097E-11
Cadherin 1, type 1, E-cadherin (epithelial)	CDH1	-0.611	2.228E-08	-1.491	0
Leucine rich repeat containing 39	LRRC39	-0.619	4.813E-12	-0.542	0.002
prostaglandin D2 synthase, hematopoietic	PGDS	-0.649	1.196E-07	-0.261	1.399E-13

* log(Ratio) was calculated from fold changes of gene expression using the ratio function of Rosetta Biosoftware. Data are from three independent experiments ($p \leq 0.01$).

4.7. References

1. Reeder BJ, Svistunenko DA, Cooper CE, Wilson MT. The radical and redox chemistry of myoglobin and hemoglobin: from in vitro studies to human pathology. Antioxid Redox Signal. 2004;6:954-966.

2. Kapralov A, Vlasova, II, Feng W, et al. Peroxidase activity of hemoglobin-haptoglobin complexes: covalent aggregation and oxidative stress in plasma and macrophages. J Biol Chem. 2009;284:30395-30407.

3. Gutteridge JM. The antioxidant activity of haptoglobin towards hemoglobin-stimulated lipid peroxidation. Biochim Biophys Acta. 1987;917:219-223.

4. Buehler PW, Abraham B, Vallelian F, et al. Haptoglobin preserves the CD163 hemoglobin scavenger pathway by shielding hemoglobin from peroxidative modification. Blood. 2009;113:2578-2586.

5. Kristiansen M, Graversen JH, Jacobsen C, et al. Identification of the hemoglobin scavenger receptor. Nature. 2001;409:198-201.

6. Asleh R, Guetta J, Kalet-Litman S, Miller-Lotan R, Levy AP. Haptoglobin genotype- and diabetes-dependent differences in iron-mediated oxidative stress in vitro and in vivo. Circ Res. 2005;96:435-441.

7. Chen XL, Kunsch C. Induction of cytoprotective genes through Nrf2/antioxidant response element pathway: a new therapeutic approach for the treatment of inflammatory diseases. Curr Pharm Des. 2004;10:879-891.

8. Ishii T, Itoh K, Takahashi S, et al. Transcription factor Nrf2 coordinately regulates a group of oxidative stress-inducible genes in macrophages. J Biol Chem. 2000;275:16023-16029.

9. DiPietro LA. Wound healing: the role of the macrophage and other immune cells. Shock. 1995;4:233-240.

10. Mosser DM, Edwards JP. Exploring the full spectrum of macrophage activation. Nat Rev Immunol. 2008;8:958-969.

11. Philippidis P, Mason JC, Evans BJ, et al. Hemoglobin scavenger receptor CD163 mediates interleukin-10 release and heme oxygenase-1 synthesis: antiinflammatory monocyte-macrophage responses in vitro, in resolving skin blisters in vivo, and after cardiopulmonary bypass surgery. Circ Res. 2004;94:119-126.

12. Chomczynski P, Sacchi N. Single-step method of RNA isolation by acid guanidinium thiocyanate-phenol-chloroform extraction. Anal Biochem. 1987;162:156-159.

13. Bertone AL. Principles of wound healing. Vet Clin North Am Equine Pract. 1989;5:449-463.

14. Kirsner RS, Eaglstein WH. The wound healing process. Dermatol Clin. 1993;11:629-640.

15. Singer AJ, Clark RA. Cutaneous wound healing. N Engl J Med. 1999;341:738-746.

16. Ashman LK. The biology of stem cell factor and its receptor C-kit. Int J Biochem Cell Biol. 1999;31:1037-1051.

17. Tanaka R, Koike K, Imai T, et al. Stem cell factor enhances proliferation, but not maturation, of murine megakaryocytic progenitors in serum-free culture. Blood. 1992;80:1743-1749.

18. Miura N, Okada S, Zsebo KM, Miura Y, Suda T. Rat stem cell factor and IL-6 preferentially support the proliferation of c-kit-positive murine hemopoietic cells rather than their differentiation. Exp Hematol. 1993;21:143-149.

19. Lenox LE, Perry JM, Paulson RF. BMP4 and Madh5 regulate the erythroid response to acute anemia. Blood. 2005;105:2741-2748.

20. Perry JM, Harandi OF, Paulson RF. BMP4, SCF, and hypoxia cooperatively regulate the expansion of murine stress erythroid progenitors. Blood. 2007;109:4494-4502.

21. Sato H, Tamba M, Kuriyama-Matsumura K, Okuno S, Bannai S. Molecular cloning and expression of human xCT, the light chain of amino acid transport system xc. Antioxid Redox Signal. 2000;2:665-671.

22. Kim JY, Kanai Y, Chairoungdua A, et al. Human cystine/glutamate transporter: cDNA cloning and upregulation by oxidative stress in glioma cells. Biochim Biophys Acta. 2001;1512:335-344.

23. Gatti L, Zunino F. Overview of tumor cell chemoresistance mechanisms. Methods Mol Med. 2005;111:127-148.

24. Glavinas H, Krajcsi P, Cserepes J, Sarkadi B. The role of ABC transporters in drug resistance, metabolism and toxicity. Curr Drug Deliv. 2004;1:27-42.

25. Kruithof EK, Baker MS, Bunn CL. Biological and clinical aspects of plasminogen activator inhibitor type 2. Blood. 1995;86:4007-4024.

26. Medcalf RL, Stasinopoulos SJ. The undecided serpin. The ins and outs of plasminogen activator inhibitor type 2. FEBS J. 2005;272:4858-4867.

27. Pagliari LJ, Perlman H, Liu H, Pope RM. Macrophages require constitutive NF-kappaB activation to maintain A1 expression and mitochondrial homeostasis. Mol Cell Biol. 2000;20:8855-8865.

28. Brouard S, Berberat PO, Tobiasch E, Seldon MP, Bach FH, Soares MP. Heme oxygenase-1-derived carbon monoxide requires the activation of transcription factor NF-

kappa B to protect endothelial cells from tumor necrosis factor-alpha-mediated apoptosis. J Biol Chem. 2002;277:17950-17961.

29. Ricchetti GA, Williams LM, Foxwell BM. Heme oxygenase 1 expression induced by IL-10 requires STAT-3 and phosphoinositol-3 kinase and is inhibited by lipopolysaccharide. J Leukoc Biol. 2004;76:719-726.

30. Murr C, Widner B, Wirleitner B, Fuchs D. Neopterin as a marker for immune system activation. Curr Drug Metab. 2002;3:175-187.

5. Conclusions and Outlook

In diseases causing hemolysis massive amounts of free Hb are released into the circulation. Due to the toxic nature of Hb it is immediately captured by Hp and forms an irreversible complex. The only known receptor for the Hb-Hp complex is CD163, a member of the SRCR family, which is exclusively expressed on monocytes and tissue macrophages. By means of immunofluorescence and uptake assays, it could be shown that besides the critical SRCR domains 4-6, also the domain 8 plays a non-redundant role in Hb-Hp binding and uptake. Once internalized, the degradation of the Hb-Hp complex is mediated by HO-1 with subsequent release of anti-oxidant byproducts, namely CO, iron and bilirubin.

A lot of attention has been paid to the Hb-induced HO-1 pathway within the macrophages. Nevertheless, the idea that Hb-Hp itself could generate a specific macrophage phenotype was not known yet. Macrophages display a huge diversity of phenotypes and capabilities depending in part on the signals from the immediate microenvironment. With means of comprehensive transcriptome and proteome profiling of Hb-Hp exposed macrophages a new and highly specified phenotype with a particular role in wound healing and an enhanced Hb-clearance and anti-oxidative capacity could be identified as summarized in the scheme. Intracellular degradation of Hb and heme activates the Nrf-2/ARE pathway with subsequent enhanced expression of antioxidative enzymes, such as HO-1 and NQO1. The main and newly identified characteristics of these Hb-Hp polarized macrophages are as follows: *i)* increased and selective expression and secretion of IL-8 in order to attract leukocytes to the injured tissue *ii)* complete lack of pro-inflammatory mediators such as TNF-α, IL-1β and IL-6 and *iii)* significant suppression of all detected HLA class 2 molecules and co-stimulatory molecules, in particular CD86. To date, the exact mechanism leading to HLA class 2 suppression during extraordinary Hb-Hp exposure remains unknown. Nevertheless, it might arise from posttranslational modifications (PTMs) that are able to modify CIITA activity and genes encoding HLA class 2 proteins. Additionally, it could be shown that pre-treatment of macrophages with glucocorticoids, such as dexamethasone, and subsequent exposure to Hb-Hp even intensified the anti-oxidative activity of this particular phenotype by increased Hb-Hp clearing and iron-recycling capacity. In conclusion, this work adds new important elements to the understanding of macrophages involved in Hb-Hp clearance and

catabolic detoxification such as in hemolysis and wound healing and might define new targets for therapeutic intervention in hemolytic diseases.

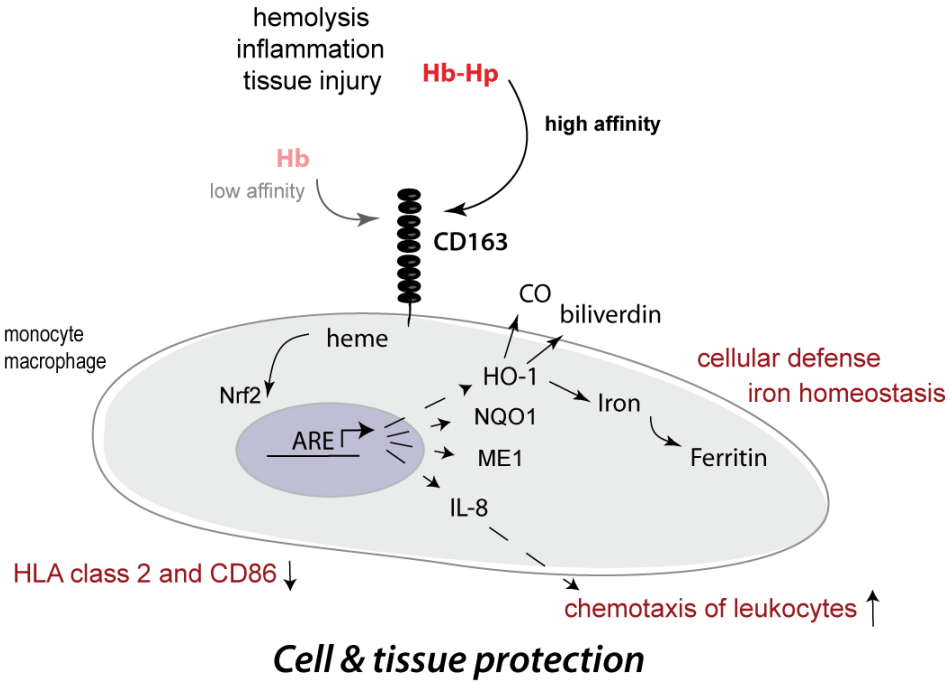

Scheme – Illustration of the global changes in macrophages induced by Hb-Hp exposure. *The long-term exposure to Hb-Hp results in the activation of the Nrf-2/ARE pathway and enhances the expression of anti-oxidative genes (HO-1, NQO1, ME1). Additionally, the by-products (CO, biliverdin, iron) of HO-1 activity have anti-oxidative properties and contribute to the cellular defense mechanisms. IL-8 expression is highly induced by Hb-Hp and serves as a chemoattractant for additional leukocytes. Further, Hb-Hp polarizes macrophages towards potent suppression of HLA class 2 molecules and the co-stimulatory molecule CD86. Together, all mechanisms lead to cell and tissue protection during hemolysis.*

These results build a basis for further investigations on CD163 pseudo-receptors binding to Hb-Hp by means of SPR measurements in order to get more insights into CD163 conformation and function. Moreover, the herein indicated significant and consistent down-regulation of HLA class 2 receptors in human macrophages upon Hb-Hp exposure could stimulate research on shared intracellular trafficking and degradation pathways of Hb-Hp complexes and HLA class 2 molecules, respectively. Furthermore, this thesis revealed a putative link between Nrf-2 activation and IL-8 secretion. Based on these findings, one could over-express and/or silence Nrf-2 using lentiviral systems in order to monitor the impact on IL-8 expression following mutated Nrf-2 activity.

6. Acknowledgements

I am grateful to Prof. Dr. Gabriele Schoedon for providing me the opportunity to do my PhD in her laboratory, for guiding and supervising my work.

A special thank goes to PD Dr. Dominik Schaer, who supervised and guided my work, for his interesting discussions, ideas and his help during my entire dissertation.

I sincerely thank Prof. Dr. Adriano Fontana for taking the responsibility to advise this dissertation academically and for offering excellent criticism during my PhD meetings. For being part of my thesis committee and many valuable suggestions I would like to thank Prof. Dr. Burkhard Becher.

I'm deeply grateful to Elena Dürst who helped me with the analysis of my huge amount of data.

Many thanks go to the FGCZ staff, in particular to Bernd Roschitzki, Jonas Grossmann and Peter Gehrig, for their excellent support, competence and discussions concerning my proteomic project.

I would like to thank Mårten Schneider, who shared his knowledge about FACS analysis with me and the interesting scientific discussions.

Many thanks go to the past and present lab members, especially to the ones who always shared a laugh with me and became friends.

To my precious family and friends: thanks for your strong will and love that kept me going.

7. Curriculum vitae

Family name: Kämpfer
First name: Theresa
Date of Birth: 27th of November 1982
Nationality: German

Education

1993 – 2001
Highschool in Jena

2001 –2006
Diploma at the Friedrich-Schiller University of Jena; Final Exams: Microbiology, Medical Microbiology and Immunology. Diploma thesis: **„Experimentelle Autoimmune Enzephalomyelitis und *Bystander* Aktivierung von T-Zellen in C57BL/6 Mäusen“** in the laboratory of Clinical Immunology under the supervision of Prof. Kamradt, University Hospital Jena, University of Jena.

2006 – 2010
PhD Dissertation at the University of Zurich, PhD Thesis: **“Hemoglobin Catabolism in Human Macrophages and Inflammation”** in the Inflammation Research Unit, Division of Internal Medicine, University Hospital of Zurich, under the supervision of Prof. Dr. Gabriele Schoedon and PD Dr. Dominik Schaer.